Spring 5-31-1976

Separations of multicomponent mixtures via thermal parametric pumping

John Daniel Stokes
New Jersey Institute of Technology

Copyright Warning & Restrictions

The copyright law of the United States (Title 17, United States Code) governs the making of photocopies or other reproductions of copyrighted material.

Under certain conditions specified in the law, libraries and archives are authorized to furnish a photocopy or other reproduction. One of these specified conditions is that the photocopy or reproduction is not to be "used for any purpose other than private study, scholarship, or research." If a, user makes a request for, or later uses, a photocopy or reproduction for purposes in excess of "fair use" that user may be liable for copyright infringement,

This institution reserves the right to refuse to accept a copying order if, in its judgment, fulfillment of the order would involve violation of copyright law.

Please Note: The author retains the copyright while the New Jersey Institute of Technology reserves the right to distribute this thesis or dissertation

Printing note: If you do not wish to print this page, then select "Pages from: first page # to: last page #" on the print dialog screen

SEPARATIONS OF MULTICOMPONENT MIXTURES VIA THERMAL PARAMETRIC PUMPING

BY

JOHN DANIEL STOKES

A DISSERTATION

PRESENTED IN PARTIAL FULFILLMENT OF

THE REQUIREMENTS FOR THE DEGREE

OF

DOCTOR OF ENGINEERING SCIENCE IN CHEMICAL ENGINEERING

AT

NEW JERSEY INSTITUTE OF TECHNOLOGY

Newark, New Jersey

1976

ABSTRACT

This dissertation covers the separation of solutes from multicomponent solutions via direct mode thermal parametric pumping.

Dilute solution separations were predicted from existing binary equations by assuming the existence of pseudo binary systems, each system consisting of one solute and the common solvent. Two systems, toluene-aniline-n-heptane and toluene-acetophenone-n-heptane with a silica gel adsorbent were used to experimentally demonstrate the separation. Experimental results were in good agreement with the mathematical predictions.

For concentrated multicomponent solutions, the separation was demonstrated by the system, toluene-acetophenone-n-heptane on silica gel. The effects of mass transfer and nonlinear adsorption isotherms became significant and a numerical solution of the basic mass balance, rate, and equilibrium expressions was used to predict the product concentration profiles. These predictions were in reasonable agreement with the experimental results. Separation efficiency was increased by decreasing the bottom product rate and increasing the cycle time. Separation efficiency fell off sharply and the system appeared to be saturated as the total solute concentration

reached 40 volume percent.

The dilute solution (pseudo binary) theory was used to develop design equations for pilot plant and commercial systems. The parametric pumping assembly has the configuration of a multi-tube heat exchanger due to the necessity of "instantaneous" temperature changes between the hot and cold half-cycles. In addition to the main assembly, the requirements for auxiliary tanks, pumps, and instrumentation are outlined along with a process description for the operation of the entire system.

Equations are also given for the required energies (steam, refrigeration, electrical) and the total energies compare favorably with conventional separation processes such as distillation. For the system studied, energy requirements were estimated at 600-900 BTU/lb. of bottom product for separation efficiencies of 50-100%. This was compared to distillation stripping and fractionating column separations where, for similar product purities, 310 and 1,250 BTU/lb. of bottom product are required.

APPROVAL OF DISSERTATION

SEPARATIONS OF MULTICOMPONENT MIXTURES

VIA THERMAL PARAMETRIC PUMPING

BY

JOHN DANIEL STOKES

FOR

DEPARTMENT OF CHEMICAL ENGINEERING

NEW JERSEY INSTITUTE OF TECHNOLOGY

BY

FACULTY COMMITTEE

APPROVED: _____ Chairman

_____

_____

_____

_____

NEWARK, NEW JERSEY

1976

PREFACE

Parametric pumping is a new separation technique that should rightfully take its place alongside unit operations such as distillation, adsorption, and extraction. It is hoped that this dissertation with emphasis on the separation of solutes in concentrated solutions and on design and scale-up will further this goal.

ACKNOWLEDGEMENTS

This dissertation is dedicated to Professor H. T. Chen, my advisor and friend whose enthusiasm, guidance, and encouragement made this work possible.

I also express my gratitude to Professor W. Snyder and the other members of my advisory committee for their help and encouragement.

To Dr. William J. Knebel and Mr. Sol Bravman I express my thanks for their valuable advice and suggestions regarding the analytical work.

And for their expert help and guidance in the drafting and textual aspects of the dissertation I wish to thank Mr. Cassius F. Brown and Ms. Anne Toto.

And in conclusion I thank my wife, Sabina, for her patience and encouragement, without which this work could not have been completed.

TABLE OF CONTENTS

LIST OF FIGURES

LIST OF TABLES

CHAPTER 1

INTRODUCTION

Thermal parametric pumping is a new unit operation that combines the effect of temperature change on solute adsorption with a reciprocating flow of the solute bearing stream. By alternately adsorbing and releasing the solute into the synchronously reversing stream, a wave front of concentrated solute is "pumped" up the packed adsorbent bed, thereby resulting in a purified solvent or solution leaving the bottom of the column and a concentrated stream leaving the top.

The most convenient basis for analyzing a thermal parametric pumping system is the equilibrium theory originated by Pigford et al (1969), generalized by Aris (1969), and extended to continuous and semicontinuous single solute operation by Chen et al (1972, 1973) and to continuous multicomponent operation by Chen et al (1974).

The equilibrium theory postulates that local interphase equilibrium exists with a linear distribution law having a temperature-dependent distribution coefficient and that there is negligible axial diffusion. This model generally applies to dilute solutions and has led to relatively simple analytical equations. These basic equations and their extension from binary systems to

multicomponent systems is covered in Chapter 3.

Many systems of commercial interest, however, are not only multicomponent systems but involve solutions which are not dilute but have solute concentrations of up to ten percent or more. With these systems, it is no longer reasonable to expect the existence of local interphase equilibrium or of independent linear binary isotherms and other basic assumptions of the equilibrium theory. It becomes necessary to allow for the effect of high concentrations of solute species which can create conditions in the system which include non-equilibrium and non-linear isotherms. These conditions and their effects on the mathematical model and the experimental system toluene-acetophenone-n-heptane on silica gel are covered in Chapter 4.

With this background on the performance of multicomponent systems, the next logical step was to provide the means for scale-up and design and this is covered in Chapter 5. The dilute solution theory is used because the basic analytical equations needed for predicting separation exist for this theory and can be incorporated into relatively simple design equations and graphs expressing the heating, cooling, and power requirements for the system components.

Before proceeding to the dilute solution theory, it is desirable to put the operation defined as "direct mode thermal parametric pumping" into its proper perspective as merely one subdivision of a very broad group of processes operating under the parametric pumping principle, to define that principle, and to describe some of the other processes operating under that general principle.

CHAPTER 2

BACKGROUND

Parametric pumping is the forcing of a desired concentration effect by synchronizing a cyclic change in a parametric variable with an oscillating field--actually pumping to a desired concentration level by utilizing energy from a cyclic parameter change.

In the field of physics, parametric pumping is the formation of a laser beam by "coupling electromagnetic waves (light) with quantum mechanical electronic fields of atoms" (Wilhelm, 1966). In the field of biology, parametric pumping is associated with Na^+ transport in membranes (Wilhelm, 1966). In the field of chemical technology, parametric pumping achieves a separation by forcing the migration of fluid species in desired directions by coupling an oscillating change in pH, temperature, pressure, or other state variable with the cyclic flow of a fluid phase past a stationary phase.

Conventional separation processes involve two phases in close proximity, the unidirectional movement of one phase relative to the other, an equilibrium function relating the compositions of the two phases, and steady state operation with state variables such as pressure or temperature held constant. Parametric pumping represents a whole new approach

to separation and differs from the conventional processes in that the relative motion of the two phases is reciprocal rather than unidirectional and the key state variable is not held constant but is caused to oscillate between fixed levels and is coupled to the reciprocating flow.

The first known application of the parametric pumping principle was heatless or pressure-swing adsorption (Skarstrom, 1959). A solute from a gas stream was adsorbed at high pressure and then purged from the adsorbent bed at low pressure using a fraction of the high pressure product stream. Two columns were used, one for the high pressure adsorption and the other for the low pressure desorption. After each half-cycle, the flows were switched and the operation repeated, restoring the beds to their original condition and completing the cycle. The process worked because, during the high pressure period, the solute concentration in the gas phase was high and the driving force was from the gas to the adsorbent bed. When the bed was exposed to the solute-depleted low pressure gas, the direction of the driving force was reversed and the solute desorbed from the bed. Heat was not required because the cycles were very short and the heat from the adsorption remained in the bed and was available for the desorption.

Skarstrom's invention was used commercially for drying air over a silica gel bed. Other uses of heatless

adsorption were the purification of hydrogen (Alexis, 1967), and the production of oxygen-rich gas from air (Lee and Stahl, 1972). In these operations the numbers of beds and the cycles were changed but the basic principles remained the same. An excellent review of these and other parametric pumping operations was given by Wankat (1974).

Despite the commercial success of heatless adsorption, the process was complicated and difficult to model. A mathematical model by Shendalman and Mitchell (1972) incorporated the assumptions of local equilibrium, linear adsorption isotherms, and no axial dispersion as did the equilibrium theory of Pigford et al (1969). This model showed the importance of a high purge to feed ratio and was in reasonable agreement with experimental results at high ratios. When mass transfer was taken into account, the prediction was conservative.

A semicontinuous modification of Skarstrom's basic process by Turnock and Kadlec (1971) and Kowler and Kadlec (1972) involved the admission of high pressure feed followed by feed shut-off and exhaustion of the column at the feed end. Product was withdrawn continuously from the other end. The basis of the separation was the same as before--adsorption of solute from the high pressure gas and purging the solute from the bed with a portion of the solute-depleted gas as exhaust, the remainder of the

solute-depleted gas leaving the other end of the column as a steady product stream. The mathematical model, based on the assumptions of local equilibrium, no axial dispersion, and a Freundlich isotherm was in good agreement with the experimental data. Reasons for the good agreement could be the assumption of a non-linear isotherm and the inclusion of the depressurization and repressurization steps in the mathematical model.

Another form of parametric pumping is pH parametric pumping based on a change in chemical potential. The work of Sabadell and Sweed (1970) was in the recuperative mode because the H^+ and OH^- ions could not be impressed on the packed bed through the walls of the column but travelled through the bed with the reciprocating fluid flow. The closed end of the bed was maintained at a low pH by titration with concentrated HCl. When the flow to the column is from the acidic closed end, H^+ ions are carried into the bed to release the Na^+ and K^+ ions attached to the resin. On the next half-cycle, the feed solution carries OH^-, Na^+, and K^+ ions into the bed. The OH^- ions neutralize the H^+ ions attached to the resin and the Na^+ and K^+ ions attach themselves to the sites on the resin made available due to the neutralization reaction. The excess Na^+ and K^+ ions move towards the closed end of the column and accumulate at this acidic end of the column.

The neutralization that occurs in the alkaline downflow half-cycle is the source of energy for the separation. This energy is supplied externally by the addition of HCl to maintain the low pH at the acidic end of the column.

No mathematical model was developed for pH parametric pumping but the model for recuperative thermal parametric pumping was suggested as a starting basis. The efficiency of the separation was poor but the principle of the separation was clearly demonstrated. pH parametric pumping may have applications in the separation of biological materials because it has been associated with Na^+ transport in membranes (Wilhelm, 1966) since the K^+, Na^+ equilibrium on proteins is known to be pH sensitive.

Miscellaneous applications of parametric pumping were liquid-liquid extraction parametric pumping (Wankat, 1973), thermal parametric pumping as a chemical reactor (Apostolopoulos, 1975), and the effects of parametric pumping on chemical reactions (Kim and Huburt, 1971). The range of possible applications of the parametric pumping principle is very large and more applications may be expected in the future.

The most widespread use of the parametric pumping principle has, thus far, been in the thermal field. Thermal parametric pumping has been effective because of the large

effect of thermal energy on forcing the migration of solute species in achieving a separation. Two methods of transferring heat to the packed bed have been used: the recuperative mode by Wilhelm et al (1966) in which the fluid entering the packed bed is heated and cooled by alternate half-cycles by external heat exchangers; and the direct mode developed independently by Wakao et al (1968) and by Wilhelm and Sweed (1968) in which the heat was transferred through the walls surrounding the packed bed. This direct process allowed isothermal operation during the hot and cold half-cycles and increased the efficiency of the separation, but tended to limit the diameter of the packed column due to heat transfer considerations.

The recuperative mode of thermal parametric pumping utilizes the moving fluid phase to transport the thermal energy as well as the solute species through the packed bed. The fluid is heated as it enters the top of the column and, as the thermal wave travels down the bed, the solutes are desorbed and move down the column with the flowing stream. The flow is then reversed and cold fluid enters the bottom of the column. The solutes are now adsorbed and held back as the solvent moves upwards. By repeating this pattern of hot and cold half-cyles, a concentration wave pattern is generated in the bed and, eventually, a cyclic steady state condition prevails; a dilute stream

leaves the top of the column and an enriched stream leaves the bottom.

Recuperative parametric pumping has been applied to both batch and open systems. The mathematical model (Wilhelm et al, 1968) (Rolke and Wilhelm, 1969) included mathematical expressions for equilibrium, rate, and continuity for both heat and mass transfer and were quite complicated. The equations were solved numerically and were in good agreement with the experimental results, but the separations were poor in comparison to those achieved by the direct mode. Sweed and Rigaudeau (1973) explained that good separations required that the thermal wave pass through the entire column. Since this would not normally happen (because the thermal wave travelled with the flowing fluid), it was proposed that in-bed heat exchangers be installed to advance the thermal wave beyond the concentration wave front. This was proposed as a means of successful scale-up of recuperative thermal parametric pumping (Sweed and Rigaudeau, 1973). The use of multiple bed units for scale-up via direct mode thermal pumping was described as undesirable due to column packing and operational difficulties.

The direct mode of thermal parametric pumping differs from the recuperative mode in that the transfer of heat is directly through the column walls. For this reason,

the operation is isothermal throughout each of the hot and cold half-cyles and the separation is increased to the maximum possible within a given temperature range. The separation factors, at least for certain systems, appeared to be limited only by the ability to analyze the product solutions for trace quantities of solute.

In the typical direct mode of operation, the column is heated and the solutes desorb and are carried upwards toward the top of the column with the flowing fluid. Then the flow is interrupted, the column is cooled, and the flow is reversed. The solutes are adsorbed and held in place while the cold solvent flows down the column. This pattern of hot upflow and cold downflow is repeated and a wave pattern is generated that leads to the migration of the strongly adsorbed solutes to the top of the column and the solvent and weakly adsorbed solutes to the bottom. Depending on the operating conditions, any desired separation split of the solutes between the top and bottom effluent streams is possible, including a solute-free bottom product.

The direct mode was first modeled by Wilhelm et al (1968) for the batch operation in which the fluid was pumped between two reservoirs located at the opposite ends of the column. The system was loaded with feed solution, operated for a required number of cycles, and

the top and bottom products were unloaded from the two reservoirs. The procedure was repeated until the desired amount of production was obtained.

The mathematical analysis of the batch pump was greatly simplified by the equilibrium theory originated by Pigford et al (1969) and generalized by Aris (1969). This equilibrium theory postulated that local interphase equilibrium exists with a linear distribution law having a temperature dependent coefficient and negligible axial diffusion. With these assumptions, it was possible for Pigford and his coworkers to solve the partial differential equations by the method of characteristics and to fit the analytical solution to the data of Wilhelm et al (1968). This equilibrium theory stimulated some additional work on batch systems which included a batch separation scheme for multicomponent mixtures (Butts, Gupta, and Sweed, 1972).

The equilibrium theory also led to the increased development of open systems. Gregory and Sweed (1970) presented mathematical models and analytical solutions for two open systems in which the feed and product flows occur during different portions of each cycle. The sequencing of the various flows is complex and can best be described as sequenced cyclic operations. In a later paper, Gregory and Sweed (1972) presented three additional open

systems and experimental verification for two systems.

Chen and Hill (1971) extended the equilibrium theory to batch, semicontinuous, and continuous systems with allowance for dead volume. The inclusion of dead volume increased the accuracy of separation prediction in the transient period prior to cyclic steady state operation. Details of the mathematical models, the analytical solutions, and the experimental verifications were presented by Chen et al (1972) for the continuous system and by Chen et al (1973) for the semicontinuous system. The semicontinuous operation differed from those of Gregory and Sweed in that the sequence of feed and product flows were basically simple--batch operation during the hot upflow half-cycle and continuous feed and product flows during the cold downflow half-cycle. For the continuous mode of operation, all flows were continuous and constant for all half-cycles. In a comparison between the sequenced cyclic operations of Gregory and Sweed (1970) and the semicontinuous operation of Chen and Hill (1971), it was pointed out (Chen et al,1973) that a sequenced cycle system with equal reservoir displacement for cold and hot cycles would correspond to a limiting case of no top product for the semicontinuous pump. It was further pointed out that both systems have the capability of infinite separation.

In their extended analysis of the equilibrium theory Chen and Hill (1971) showed that the basis of separation was the relationship of the penetration distances of the hot upflow and cold downflow wave fronts to each other and to the height of the packed column. To achieve maximum separation, it was necessary that the penetration distance of the cold downflow wave front never exceed either the penetration distance of the hot upflow wave front or the height of the column. Since these penetration distances were defined in terms of the column interstitial velocities and the adsorption isotherm parameters, it was simple to operate the column for maximum separation once these parameters were established.

Chen and his coworkers further extended their analysis to dilute multicomponent systems (Chen et al, 1973) which will be discussed in some detail in Chapter 3.

At this point, it would be pertinent to mention some of the chemical systems that have been investigated via direct thermal mode parametric pumping. The emphasis in the selection of most of the systems has naturally been oriented towards simple, easily analyzed, chemical systems that lend themselves to testing theories rather than systems whose separations have commercial significance.

Some of the binary liquid systems which have been used experimentally in direct mode thermal parametric pumping are toluene and n-heptane on silica gel (Wilhelm and Sweed, 1968) (Chen et al, 1972, 1973); benzene and n-hexane on silica gel (Wakao et al, 1968); sodium chloride and water on ion retardation resin (Sweed and Gregory, 1970); urea and water on activated carbon (Goldstein, 1969) (Bringhurst, 1970); sodium nitrate and water on ion retardation resin (Chen and Manganaro, 1974).

Binary gas system separations have also been reported despite some inherent problems with gas systems. Since most systems would be operated at constant volume, the high pressure corresponding to the high temperature during the hot upflow half-cycle would tend to counteract the normal desorption effect due to the temperature; and conversely, during the cold downflow half-cycle, the low pressure would tend to counteract the normal adsorption effect. A second major problem occurring with gas systems would be the lag between the jacket and bed temperatures due to the poor heat conduction of the gases. Despite these disadvantages, some binary gas separations have been reported and some may have commercial potential. Some of these were ethane and propane on activated carbon (Jenczewski and Myers, 1968); argon and propane on activated carbon (Jenczewski and Myers, 1970); ethane

and propane on activated carbon (Jenczewski and Myers, 1970); sulfur dioxide and air on silica gel (Patrick et al, 1972); and boron trifluoride isotopes on boron trifluoride-dimethylsulfoxide complex (Schroeder and Hamrin, Jr., 1975).

Multicomponent mixture separations are a logical extension of binary separations. Chen et al (1974) applied the analytical expressions for the continuous binary parametric pump (Chen et al, 1972) to pairs of pseudo binaries and thus developed a mathematical basis for dilute multicomponent systems. Examples of multicomponent systems studied thus far are glucose-fructose-water on Fullers earth (Chen et al, 1972); Na^+-H^+-K^+-H_2O on ion exchange resin (Butts et al, 1973); aniline-toluene-n-heptane on silica gel (Chen et al, 1974); and glucose-fructose-water on ion exchange resin (Chen and D'Emidio, 1975).

The multicomponent systems selected for study in this thesis are aniline-toluene-n-heptane on silica gel and a new system, acetophenone-toluene-n-heptane on silica gel. The latter system was selected because there were no solubility limitations that would interfere with an extension of the study to concentrated solutions. It is hoped that the dilute solution theory for multicomponent systems, the section on the effect of concentration, and

the equations for scale-up and design will stimulate interest that will result in the application of thermal parametric pumping on an industrial scale.

CHAPTER 3

MULTICOMPONENT SEPARATION OF DILUTE SOLUTIONS

This chapter comprises four sections: a review of the basic model, a review of the equilibrium theory, adaptation of this previous work to multicomponent separation of dilute solutions, and experimental verification of the dilute solution theory.

Basic Model

The basic model equations for parametric pumping were discussed in detail by Wilhelm et al. (1968). These equations are:

The material balance equation

$$\varepsilon \frac{\partial y_i}{\partial t} + \varepsilon v \frac{\partial y_i}{\partial z} + (1-\varepsilon)\rho_s \frac{\partial x_i}{\partial t} - \varepsilon \not{D} \frac{\partial^2 y_i}{\partial z^2} = 0 \qquad (1)$$

The interphase rate equation

$$\frac{\partial x_i}{\partial t} = \lambda (y_i - y_i^*) \qquad (2)$$

and the equilibrium expression

$$y_i^* = y_i^*(T, y_j^*, x_j^*) \text{ where } j = 1,2...., n \text{ including } i \qquad (3)$$

where y_i is the fluid concentration of component i in moles of i per unit volume of fluid, x_i is the moles of i adsorbed per unit weight of adsorbent, y_i^* is the equilibrium concentration of i in the fluid, v is the

interstitial velocity of the fluid, t is the time, z is the axial distance along the packed bed, ρ_s is the density of the solid adsorbent, ε is the void fraction of the adsorbent, T is the absolute temperature, λ is the mass transfer coefficient, and $\mathcal{D}$ is the axial diffusivity.

In this chapter, these equations are applied to continuous direct mode thermal parametric pumping for the separation of dilute multicomponent solutions. The particular method followed was originally proposed by Chen and Hill (1971) and developed for the toluene-aniline-n-heptane-silica gel system by Chen et al. (1974). In Chapter 5, this dilute solution theory is incorporated into the design equations for the scale-up of laboratory systems into pilot plant and larger size parametric pumping systems.

The continuous parametric pump, characterized by a steady flow of both feed and product streams during the hot upflow and cold downflow half cycles, is shown in Figure (1). Flow is upward during the hot half cycle and downward during the cold half cycle. Each half cycle is π/ω time units in duration and the reservoir displacement volume is $Q\pi/\omega$ where Q is the reservoir displacement rate. The pump has dead volumes V_T and V_B for the top and bottom reservoirs, respectively. The feed is directed to the top of the column at the flow rate $(\phi_T+\phi_B)Q$. The top product flow rate is $\phi_T Q$ and the bottom product flow rate

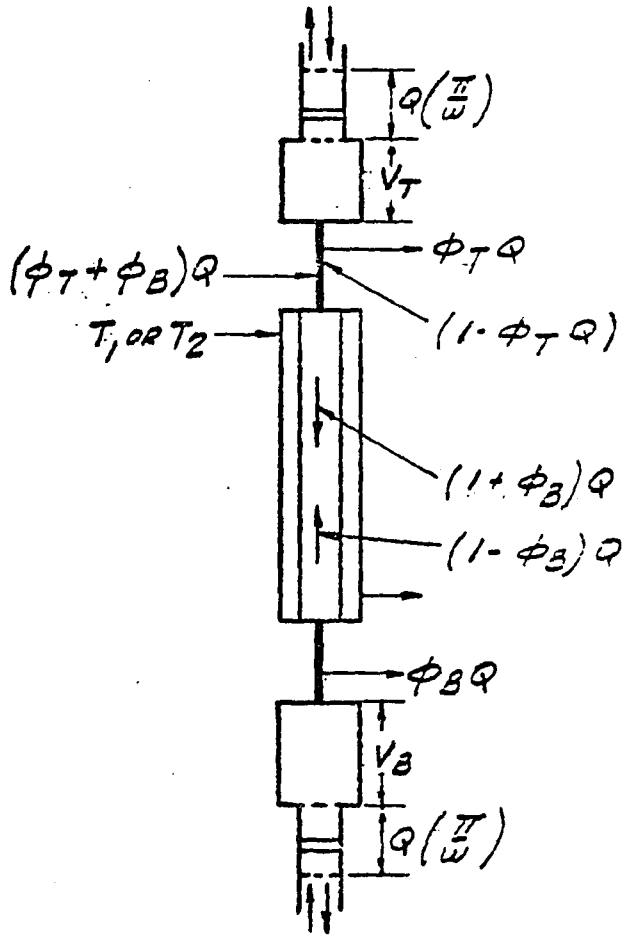

FIGURE (1)

Parametric Pump Schematic Diagram

is $\phi_B Q$ and ϕ_T and ϕ_B are the ratios of the top and bottom product rates to the reservoir displacement rate.

These parameters are involved in the mathematical development which requires: a mathematical description of the adsorption-desorption and flow processes occurring within the column (internal equations); material balances connecting the column to the reservoirs and all external streams; and a combination of these equations to produce the performance guidelines and concentration profiles which enable the researcher or designer to manipulate the parametric pumping separation to suit his particular needs.

Review of the Equilibrium Theory

First it is necessary to review the equilibrium theory originated by Pigford et al. (1969), generalized by Aris (1969), and extended to continuous direct mode parametric pumping by Chen and Hill (1971) and Chen et al. (1972).

Now in the case of the equilibrium theory, the following assumptions are made:

1. No axial dispersion ($\mathcal{D} = 0$).
2. Instantaneous equilibrium ($y_i = y_i^*$).
3. Linear equilibrium adsorption ($x_i = M_i(T) y_i$).
4. Instantaneous temperature changes.
5. Plug flow (steady unidirectional flow of all fluid elements).

6. Constant fluid density (Total moles of fluid per unit volume of fluid is a constant. In the equations, the term y_i incorporates the fluid density term shown by Pigford et al. (1969) as ρ_f.)

With these simplifying assumptions, the material balance is:

$$\frac{\partial y_i}{\partial t} + v\frac{\partial y_i}{\partial z} + \frac{(1-\varepsilon)\rho_s}{\varepsilon}\frac{\partial x_i}{\partial t} = 0 \tag{4}$$

Now if the linear isotherm is differentiated

$$\frac{\partial x_i}{\partial t} = M_i(T)\frac{\partial y_i}{\partial t} + y_i\frac{\partial M_i(T)}{\partial T}\frac{\partial T}{\partial t} \tag{5}$$

And if

$$m_i = \frac{(1-\varepsilon)\rho_s M_i(T)}{\varepsilon} \tag{6}$$

Then

$$\frac{\partial m_i}{\partial T} = \frac{(1-\varepsilon)\rho_s}{\varepsilon}\frac{\partial M_i(T)}{\partial T} \tag{7}$$

And by substitution Equation (4) becomes

$$(1+m_i)\frac{\partial y_i}{\partial t} + v\frac{\partial y_i}{\partial z} + \frac{\partial m_i}{\partial T}\frac{\partial T}{\partial t}y_i = 0 \tag{8}$$

Then by the method of characteristics we get

$$\frac{dt}{1+m_i} = \frac{dz}{v} = \frac{-dy_i}{\frac{dm_i}{dT}\frac{dT}{dt}\,y_i} \tag{9}$$

which become

$$\frac{dz}{dt} = \frac{v}{1+m_i} \tag{10}$$

and

$$\frac{dy_i}{y_i} = \frac{dm_i}{1+m_i} \tag{11}$$

Considering the definitions of Pigford et al. (1969),

$$v = v_o sq(\omega t) \tag{12}$$

$$m_i = m_{oi} - a_i sq(\omega t) \tag{13}$$

$$u_{oi} = v_o/(1+m_{oi}) \tag{14}$$

$$b_i = a_i/(1+m_{oi}) \tag{15}$$

as the interstitial velocity (v), the dimensionless equilibrium constant (m_i), the wave front velocity (u_{oi}), and the dimensionless equilibrium parameter (b_i). The subscript (o) denotes the value at the mean of the two operating temperatures, the constant a_i denotes the deviation of m_i from the mean, and the $sq(\omega t)$ term denotes whether the deviation from the mean is positive or negative in sign.

With these definitions, Equation (10) becomes

$$\frac{dz}{dt} = \frac{u_{oi}\,sq(\omega t)}{1-b_i\,sq(\omega t)} \tag{16}$$

showing that in the z-t plane, the characteristic curves are straight lines having slopes of $u_{oi}/(1-b_i)$ for hot upflow and $-u_{oi}/(1+b_{oi})$ for cold downflow.

Now if Equation (16) is integrated between the limits of t = 0 and π/ω, we get the wave front penetration distances for hot upflow and cold downflow, respectively, which were first defined by Chen and Hill (1971) as follows:

$$L_{1i} = \frac{u_{oi}(\pi/\omega)}{(1-b_i)} = \frac{v_o(\pi/\omega)}{(1-b_i)(1+m_{oi})} \tag{17}$$

$$L_{2i} = \frac{-u_{oi}(\pi/\omega)}{(1+b_i)} = \frac{-v_o(\pi/\omega)}{(1+b_i)(1+m_{oi})} \tag{18}$$

Now from Figure (1), the flow rates in the column during hot upflow and cold downflow are $Q(1-\phi_B)$ and $Q(1+\phi_B)$ and Equations (17) and (18) become

$$L_{1i} = \frac{v_o(1-\phi_B)(\pi/\omega)}{(1-b_i)[1+0.5(m_{1i}+m_{2i})]} \tag{19}$$

$$L_{2i} = \frac{v_o(1+\phi_B)(\pi/\omega)}{(1+b_i)[1+0.5(m_{1i}+m_{2i})]} \tag{20}$$

where m_{1i} and m_{2i} are the dimensionless equilibrium constants during hot upflow and cold downflow defined by Equation (6). The quantity b_i, defined by Equation (15), may be expressed as

$$b_i = \frac{0.5(m_{2i}-m_{1i})}{1+0.5(m_{1i}+m_{2i})} \tag{21}$$

Now

$$\frac{L_{1i}}{L_{2i}} = \frac{(1-\emptyset_B)}{(1+\emptyset_B)} \frac{(1+b_i)}{(1-b_i)} \tag{22}$$

Chen and Hill (1971) showed that the pump performance depends on the relative magnitudes of L_{1i}/L_{2i} and the height of the column, h. There are three possible regions of pump operations depending on L_{1i}/L_{2i} and h,

$$\text{Region 1, } \frac{L_{1i}}{L_{2i}} \geq 1 \text{ (or } \emptyset_B \leq b_i) \text{ and } L_{2i} \leq h \tag{23}$$

$$\text{Region 2, } \frac{L_{1i}}{L_{2i}} < 1 \text{ (or } \emptyset_B > b_i) \text{ and } L_{1i} \leq h \tag{24}$$

$$\text{Region 3, } L_{1i} \text{ and } L_{2i} > h \tag{25}$$

Equations (9) through (25) provide the operating guidelines for column performance. They were obtained by combining the column flow rates (external equations) with the internal equations (17, 18) that represent half of the analytical solution of Equations (1, 2, 3).

The other half of the analytical solution of Equation (9) leads to the concentration profiles. Equation (11) is combined with Equations (13, 15) and is integrated without definite limits (Pigford et al., 1969).

$$y_i(z,t)\left[1-b_i sq(\omega t)\right] = \text{integration constant} \qquad (26)$$

This means that $y_i(z,t)$ undergoes a change in value proportional to the ratio $(1+b_i)/(1-b_i)$ when the characteristic line passes from a cold region into a hot one. The reverse is true when passing from a hot to a cold region. Now if the change in $y_i(z,t)$ is followed for n cycles, the value of y_i <u>for the bottom of the column</u> is

$$\langle y_{B2i}\rangle_n = \langle y_{B1i}\rangle_n \frac{(1-b_i)}{(1+b_i)} = y_{oi}\left[\frac{1-b_i}{1+b_i}\right]^n \qquad (27)$$

where $\langle y_{B2i}\rangle_n$ is the concentration of the i component at the bottom of the column during the cold downflow half cycle, $\langle y_{B1i}\rangle_n$ is the concentration of the i component at the bottom of the column during the preceding hot upflow cycle, and y_{oi} is the concentration of the i component in the original or feed solution.

Chen and Hill (1971) modified Equation (27) to include the effect of dead volume in the reservoirs, which is always present in actual systems. With this correction for dead volume, Equation (27) becomes

$$\frac{\langle y_{BP2i}\rangle_n}{y_{oi}} = \frac{(1-b_i)}{(1+b_i)}\left[\frac{(1-b_i)/(1+b_i)+C_2}{1+C_2}\right]^{n-1} \qquad (28)$$

This correction for dead volume was made by solving the first part of Equation (27) simultaneously with an external material balance equation (Chen and Hill, 1971).

Chen and Hill also gave the bottom product-to-feed ratio for cyclic steady state, which for multicomponent systems is

$$\frac{\langle y_{BP2i} \rangle_{\infty}}{y_{oi}} = 0 \qquad (29)$$

The equations for the top product stream were developed in the same manner as those for the bottom product stream, cycle by cycle to the n^{th} cycle. But the top product stream is somewhat more complicated. The equations by Pigford et al. (1969) were generalized by Aris (1969) to apply to all batch pumps with no dead volume. Chen and Hill (1971) extended these equations to include batch, continuous, and semicontinuous pumps with dead volume and the transient equations were given for the continuous and semicontinuous pumps by Chen et al. (1972, 1973). The development of the equations for the continuous pump proceeds as follows:

As the progress of the concentration wave fronts is traced to the top of the column, it is found that after a certain number of cycles, a pattern develops--characteristic regions of constant concentrations from the bottom to the

top of the column. This pattern is established (for operation in Region 1) p_1+1 cycles after time zero, where

$$p_{1i} + q_{1i} = \frac{(h-L_{2i})}{(L_{1i}-L_{2i})} = \frac{(h-L_{2i})}{\Delta L_i} \tag{30}$$

The internal equation for the average concentration of the effluent stream leaving the top of the column after $P_{1i}+1$ cycles, as given by Chen and Hill (1971) and adapted to multicomponent systems is

$$\langle y_{T1i} \rangle_n = \frac{L_{2i}}{L_{1i}} \frac{(1+b_i)}{(1-b_i)} \langle y_{T2i} \rangle_{n-1} +$$

$$\left[1 - \frac{L_{2i}}{L_{1i}}\right] \left[q_{1i} \langle y_{Bli} \rangle_{n-p_{1i}-1} + (1-q_{1i}) \langle y_{Bli} \rangle_{n-p_{1i}}\right] \tag{31}$$

and shows that the average concentration of component i in the top effluent stream after n cycles comprises contributions from three sources: the column bottom compositions from time zero and the first cycle, and the top composition from the previous downflow cycle.

This internal equation (31) must be solved simultaneously with the corresponding external equations around the top of the column. This was done by Chen and Hill (1971) for the binary system and the resulting transient equations were given by Chen et al. (1972) for the continuous column.

A total of ten equations for the concentration transients was given, including the binary system version of Equation (28). The equations present the concentration transients for the top and bottom product streams for operation in Regions 1, 2, and 3, and for ranges of time cycles from time zero ($n \geq 1$) to constant wave pattern development ($n \leq p_1+1$ for Region 1 and $n \leq p_2+1$ for Region 2) and beyond ($n \geq p_1+2$ for Region 1 and $n \geq p_2+2$ for Region 2). The equations for cyclic steady state ($n = \infty$) were previously given by Chen and Hill (1971). In the case of Region 3, there are no specific ranges of n to achieve constant wave front patterns because this mode of operation is characterized by wavefront breakthrough (L_{1i} and $L_{2i} > h$) on both hot upflow and cold downflow half cycles.

Most components found in normal multicomponent mixtures have exothermic heats of adsorption and the slopes of the isotherms, $M_i(T)$ and $m_i(T)$, are positive. Some of these components will be in Region 1 and some in Region 2, depending on their values of b_i and on the manner in which the column is operated (values of $\emptyset_B$ and $\emptyset_T$ selected by the operator). However, it is possible for some components in this same mixture to be in the Region 3 mode of operation, especially those with endothermic heats of adsorption and negative isotherm slopes.

Therefore, all three Regions of operation are possible and all the concentration transient equations are necessary in any given multicomponent system. The binary forms of the equations given by Chen et al. (1972) are simply applied to each pseudo binary pair in the multicomponent system.

Two of the equations applicable to the top product concentration profiles for operation in Region 1 are:

$$\frac{\langle Y_{TP2i} \rangle_n}{Y_{oi}} = -\frac{\phi_B+\phi_T}{1-\phi_T} + \frac{1+\phi_B}{1-\phi_T}\left[\frac{C_1+(1-\phi_T)/(1+\phi_T)}{1+C_1}\right]^{n-1}$$

$$+ \frac{1+\phi_B}{1-\phi_T}\frac{1+\phi_T}{2\phi_T}\left[1 - \frac{1-\phi_T}{1+\phi_T}\frac{1-b_i}{1+b_i}\right] \qquad (32)$$

$$\left[1 - \left(\frac{C_1+(1-\phi_T)/(1+\phi_T)}{1+C_1}\right)^{n-1}\right] \qquad \text{for } n \leq p_1+1$$

and

$$\frac{\langle Y_{TP2i} \rangle_\infty}{Y_{oi}} = 1 + \frac{\phi_B}{\phi_T} \qquad \text{for } n = \infty \qquad (33)$$

Multicomponent Separation of Dilute Solutions

The adaptation of the binary equations to multicomponent separations has been published (Chen, Lin, Stokes, and Fabisiak, 1974). The binary system equations are applicable to a multicomponent mixture if the multicomponent mixture is

treated as a series of independent pseudo-binary systems, each binary behaving as though the other systems were not present. Chen and Hill (1971) first suggested that multi-component separations could be predicted by existing mathematical expressions for binary systems (Chen et al., 1972, 1973), and Chen et al. (1974) used this procedure on the toluene-aniline-n-heptane silica gel system. Their derivations will not be repeated here, but note that they found that at steady state ($n \to \infty$) solute removal from the bottom product stream, $\phi_B Q$, was complete in Region 1 and only partially complete in Regions 2 and 3.

Now, consider a mixture containing s solutes, each with its own b_i and

$$b_i > b_2 >--- \; b_k = \phi_B > b_{k+1} >---> b_s \tag{34}$$

where subscripts 1, 2, etc., refer to solutes 1, 2, etc. Furthermore,

$$L_{2i} \leq h \text{ when } i = 1, 2, \text{--- } k \tag{35}$$

$$L_{1i} \leq h \text{ when } i = k+1, \text{--- } s \tag{36}$$

At steady state, the components, i = 1, 2, --- k, for which the operations are indicated in Region 1, would appear only in the top product stream, and the remaining components (k+1, --- s) would appear in both the top and bottom product

streams. In the extreme case where k = s, the bottom product stream would consist only of pure solvent. By proper adjustment of $\emptyset_B$ in Equation (26), a solute split could be made which is analogous to that obtained by a multicomponent distillation column.

Experimental Verification of the Dilute Solution Theory

The experimental verification of the theory has been published (Chen, Lin, Stokes, and Fabisiak, 1974) and the experimental details presented by Lin (1974). The experimental apparatus and procedure was the same as that used previously (Chen et al., 1972) and included two dual infusion-withdrawal syringe pumps manufactured by the Harvard Apparatus Co., one for the feed and one for the reservoirs. The jacketed column was packed with 30 to 60 mesh chromatographic-grade silica gel. Prior to each run, the column and the bottom reservoir were filled with the feed mixture of concentrations, y_{oi}. Hot and cold water baths were connected to the column jacket and solenoid valves were wired to a dual timer to insure that hot water was directed to the column during upflow and cold water during downflow. Feed was pumped continuously to the top of the column and the continuous top and bottom product streams were throttled by micrometer capillary valves to regulate flow and to impose a small back pressure on the system. Samples were taken at the end of each cycle and analyzed by ultraviolet spectrophotometry.

Four runs were made. The experimental and model parameters are presented in Table (1) and the results in Figures (2) and (3).

Figure (2) illustrates the concentration profile of $\langle y_{BP2i} \rangle_n / y_{oi}$ versus n for both toluene and aniline in both binary and ternary systems. It can be seen that this ratio of bottom product to feed decreases as the number of cycles increases and, as indicated by Equation (29), approaches zero as n becomes large. The slope of log $(\langle y_{BP2i} \rangle_n / y_{oi})$ versus n of the solute in the binary mixture coincides with that in the ternary system. This means that for a given set of operating temperatures and dimensionless top reservoir dead volume, the value of b_i was essentially the same for the binary and ternary systems. Since b_i is a measure of the extent of adsorption and desorption of a solute between the two operating temperatures (Equation 21), the separation is increased by a large b_i and solute concentration in the bottom stream becomes smaller (see Equation 28). The b_i values in the present case were 0.15 for toluene and 0.31 for aniline.

Figure (3) shows the effects of the hot upflow and cold downflow wavefront penetration distances (L_{1i}, L_{2i}) and the height of the column (h) on product concentrations. As long as the wavefront penetration on cold downflow is less than or equal to that on hot upflow or the height of

TABLE 1

EXPERIMENTAL AND MODEL PARAMETERS

$\frac{\P}{\omega}$ = 1,200 sec., T_1 = 333°K, T_2 = 298°K, h = 0.9 m, $\phi_T + \phi_B = 0.4$

	Y_{oi}								
	Toluene	Aniline	ϕ_B	C_1	C_2	b_i	L_{1i}(m)	L_{2i}(m)	Region
1. Toluene-n-heptane	0.025	0	0.07	0.12	0.13	0.15	0.51	0.43	1
2. Aniline-n-heptane	0	0.025	0.10	0.11	0.13	0.31	0.70	0.45	1
3. *Aniline-toluene-n-heptane	0.025	0.025	0.09	0.12	0.13				
a. Toluene-n-heptane						0.15	0.49	0.44	1
b. Aniline-n-heptane						0.31	0.71	0.45	1
4. *Aniline-toluene-n-heptane	0.025	0.025	0.22	0.12	0.13				
a. Toluene-n-heptane						0.15	0.42	0.49	2
b. Aniline-n-heptane						0.31	0.62	0.51	1

* Assume that a ternary system contains two pseudo-binaries.

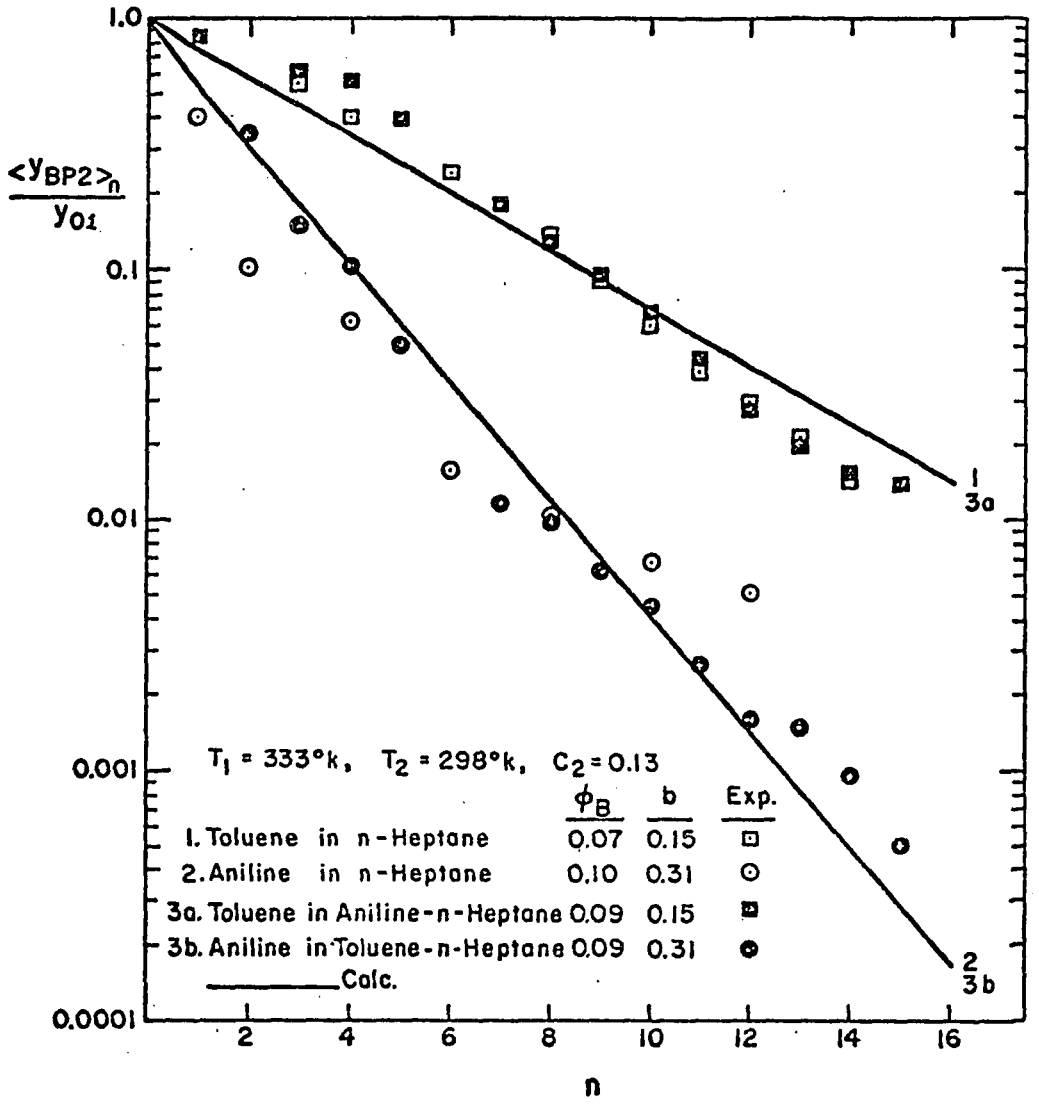

FIGURE (2)

Effect of b_i on Multicomponent Separation

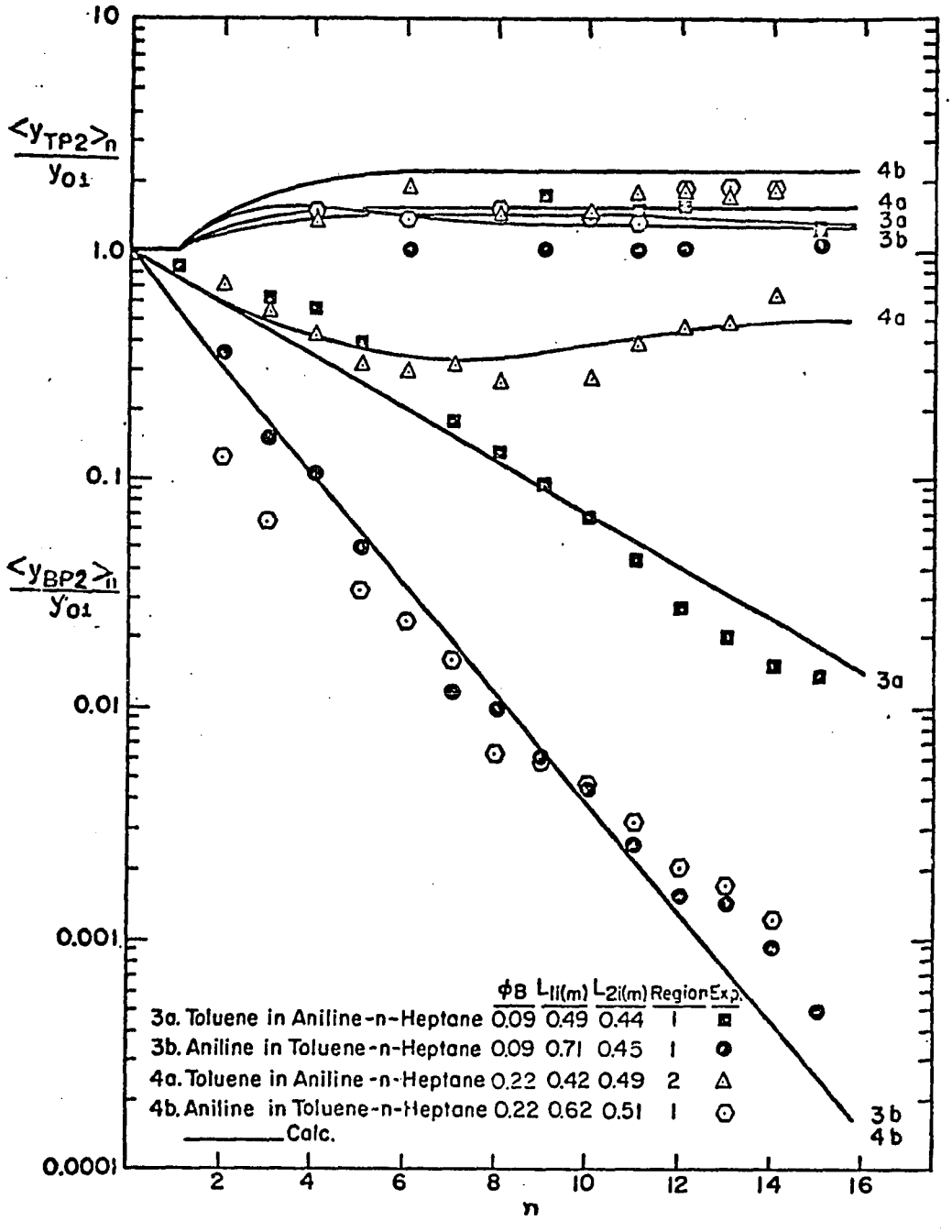

FIGURE (3)

Effect of ϕ_B on Multicomponent Separation

the column, the solute concentration in the bottom stream approaches zero as n becomes large. But this steady state behavior can abruptly change if pump operation moves out of Region 1. If L_{2i} is increased until it exceeds h, or if L_{1i} becomes less than L_{2i}, switching points are encountered which causes pump behavior to abruptly switch from a mode in which solute is completely removed from the bottom product stream to one in which solute removal is incomplete. One may visualize crossing the boundary $L_{2i}=h$ as a result of increasing L_{2i} by increasing reservoir displacement volume, $Q\pi/\omega$. Crossing of the boundary $L_{1i}=L_{2i}$ may be viewed as resulting from an increase of ϕ_B so that $\phi_B > b_i$, or $L_{2i} > L_{1i}$. At $T_1 = 333^oK$ and $T_2 = 298^oK$, the switching point for toluene corresponds to the condition $\phi_B = b_{toluene} = 0.15$. In the case of aniline, the condition is $\phi_B = b_{aniline} = 0.31$. Thus, when $\phi_B \leq 0.15$ (curves 3a and 3b), the operation is in Region 1 for both toluene and aniline, and solute removal from the bottom stream may be complete as n approaches infinity. If ϕ_B is increased to the interval range, $0.15 < \phi_B \leq 0.31$ (curves 4a and 4b), the operation switches to Region 2 for toluene, remains in Region 1 for aniline, and the bottom product could eventually contain only toluene. If ϕ_B is further increased, $\phi_B > 0.31 = b_{aniline}$, the operation is now in Region 2 for both toluene and aniline, and both toluene and aniline would appear in the bottom product stream as n approaches infinity. Note

that over the interval $\phi_B \leq b_i$ = switching point of solute i, the top concentration of i as n approaches infinity would be $\langle y_{TP2i} \rangle_\infty / y_{oi} = 1+\phi_B/\phi_T$. Beyond the switching point, $\langle y_{TP2i} \rangle_\infty / y_{oi}$ can be expressed according to the equations by Chen and Hill (1971).

Figures (4) and (5) show the net direction of concentration fronts moving through the adsorption column as n increases. In Figure (4), the operation for both toluene and aniline is in Region 1, and in Figure (5) the operations are in Regions 1 and 2, respectively, for aniline and toluene. If the net direction of solute i is upward, $L_{1i}/L_{2i} \geq 1$, and complete removal of solute i from the bottom product may be obtained. If the net direction is downward, $L_{1i}/L_{2i} < 1$, and solute i removal from the bottom product will be incomplete. This net downward direction will occur if the bottom product flow becomes too large. However, it must be noted that even though the net direction is upward, a modest separation will occur if the reservoir displacement volume is excessive, if $L_{2i} > h$ (Region 3).

The method presented here is a means of predicting multicomponent separations by assuming that solutes do not interact with one another. In Chapter 4, the effect of higher concentrations and the competition for adsorption sites will be examined.

Toluene- Aniline- n-Heptane

with ϕ_B= 0.09, h= 0.9meter

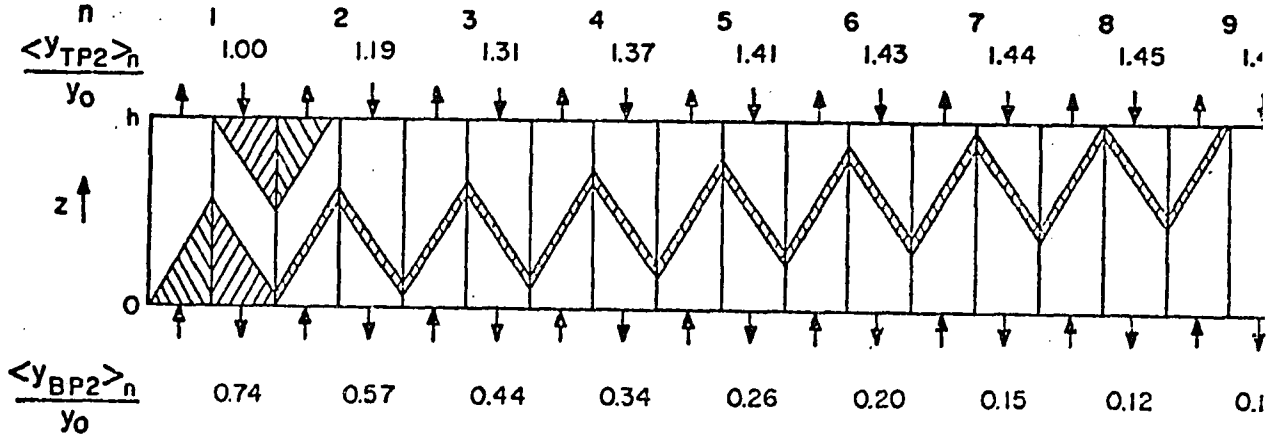

Toluene: b= 0.15, L_1= 0.49 meter

L_2= 0.44 meter

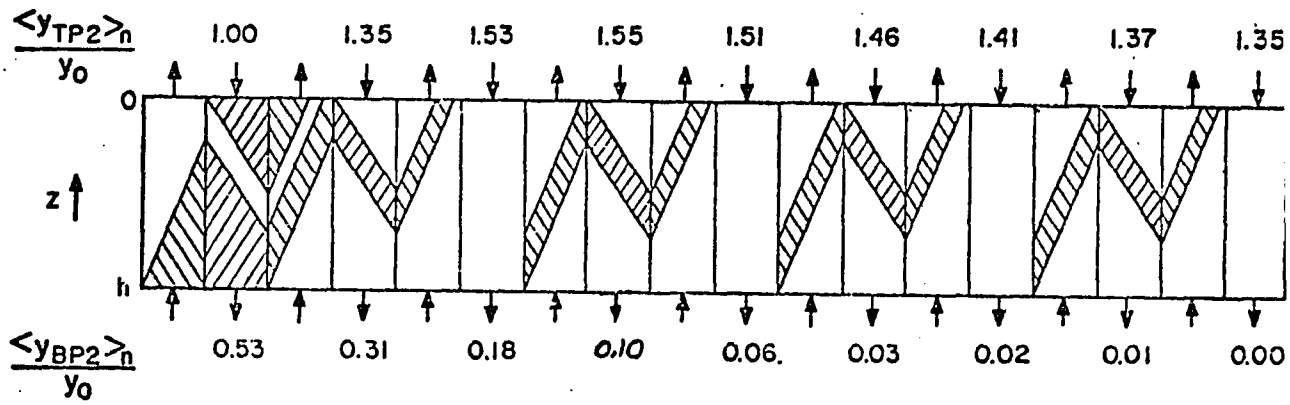

Aniline: b= 0.31, L_1= 0.71 meter

L_2= 0.45 meter

FIGURE (4)

Multicomponent Wave Fronts in Region 1 Operation

Toluene- Aniline- n-Heptane

with ϕ_B= 0.22, h= 0.9 meter

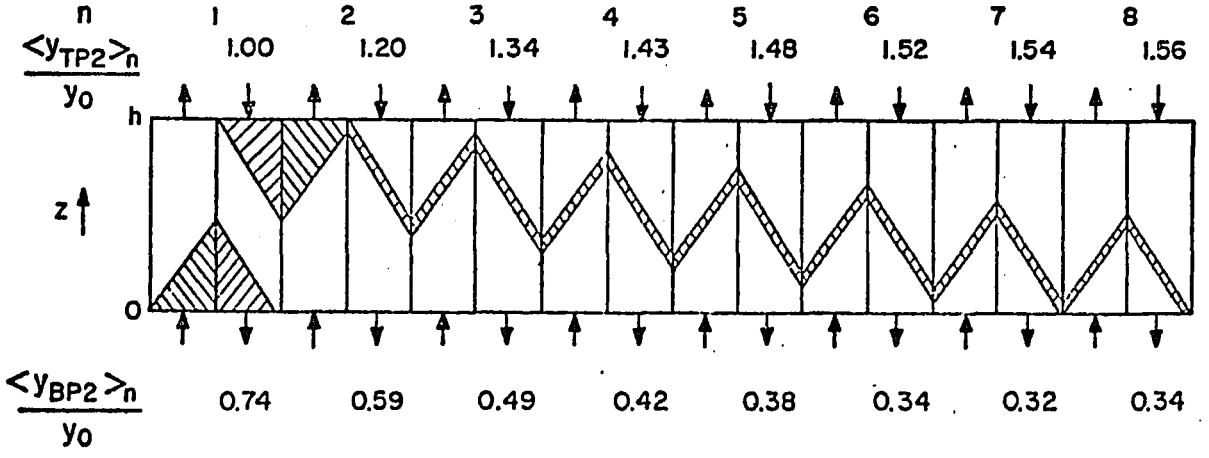

Toluene: b= 0.15, L_1= 0.42 meter

L_2= 0.49 meter

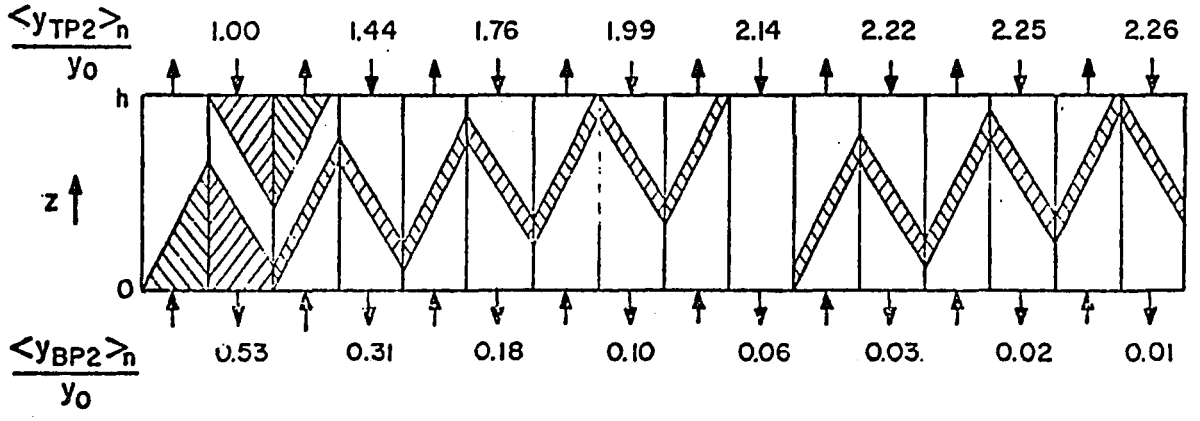

Aniline: b= 0.31, L_1= 0.62 meter

L_2= 0.51 meter

FIGURE (5)

Multicomponent Wave Fronts For Operation in Regions 1 and 2

CHAPTER 4

EFFECT OF CONCENTRATION ON MULTICOMPONENT SEPARATION

Chapter 3 covered multicomponent separations for dilute solutions. The mathematical model for the dilute solution theory was made up of analytical solutions to the basic mass balance, equilibrium, and rate equations. In the case of more concentrated solutions, analytical solutions have not been possible because the necessary simplifying assumptions (Chapter 3) are not valid and it is necessary to resort to techniques such as the method of characteristics to reduce the partial differential equations to solvable ordinary differential equations. But this method is far too tedious for hand calculations and a computer program is necessary. A suitable computer program developed recently (Kim, 1976) is used in this chapter to provide the required mathematical comparison for the experimental work described in this chapter.

This chapter is divided into three sections: the mathematical model, the experimental work, and the results and discussion section. In this way, the chapter covers the basic mathematical logic behind the behavior of concentrated multicomponent systems when exposed to parametric pumping separation. Also

covered in detail are the experimental and analytical procedures needed for verification. Finally, these are combined in the results where the experimental top and bottom product concentrations vs. time are compared with the mathematical predictions.

The results show that the transient and steady state product concentrations vary with feed concentration, bottom product product rate, and cycle time. The concentration of solute(s) in the bottom product stream is significantly reduced by decreasing the bottom product rate and increasing the cycle time. The computer program predicted the results with reasonable accuracy and could do so with systems other than the toluene-acetophenone-n-heptane system described. The results also show that the separation capability decreases sharply as total solute concentrations approach 40 vol. percent and the column tends to become saturated first with the least strongly adsorbed solute and then with the more strongly adsorbed solutes.

Mathematical Development

The basis for the mathematical development here is the same as for the dilute solution theory of Chapter 3: the material balance equation, the interphase rate equation, and the equilibrium expression.

$$\varepsilon\frac{\partial y_i}{\partial t} + \varepsilon v\frac{\partial y_i}{\partial z} + (1-\varepsilon)\rho_s\frac{\partial x_i}{\partial t} - \varepsilon\mathcal{D}\frac{\partial^2 y_i}{\partial z^2} = 0 \qquad (1)$$

$$\frac{\partial x_i}{\partial t} = \lambda_i(y_i - y_i^*) \qquad (2)$$

$$y_i^* = y_i^*(T, y_j^*, x_j^*) \text{ where } j = 1,2,\ldots, n \text{ including } i \qquad (3)$$

If there is no axial dispersion, $\mathcal{D} = 0$; and if z/v is set equal to $\hat{z}$, then Equation (1) becomes

$$\frac{\partial y_i}{\partial t} + \frac{\partial y_i}{\partial \hat{z}} = -\frac{(1-\varepsilon)\rho_s}{\varepsilon}\frac{\partial x_i}{\partial t} \qquad (37)$$

In Equation (37), y_i is a function of $\hat{z}$ and t, and the total differential of y_i is therefore

$$\frac{dy_i}{d\hat{z}} = \frac{\partial y_i}{\partial \hat{z}} + \frac{\partial y_i}{\partial t}\frac{dt}{d\hat{z}} \qquad (38)$$

According to the method of characteristics (Acrivos, 1956), the choice of paths in the $\hat{z}$ - t plane is optional. The two paths in the present case are along the diagonal

$$\frac{dt}{d\hat{z}} = 1 \tag{39}$$

and along the horizontal $\hat{z}$ = constant or

$$\frac{d\hat{z}}{dt} = 0 \tag{40}$$

If Equation (39) is substituted into Equation (38), the left hand sides of Equations (37) and (38) are equal. Furthermore, if Equation (2) is substituted into the right hand side of Equation (37), then Equation (37) becomes the ordinary differential equation (ODE) along the characteristic path defined by Equation (39) or

$$\frac{dy_i}{d\hat{z}} = - \frac{(1-\varepsilon)\rho_s}{\varepsilon} \lambda_i (y_i - y_i^*) \tag{41}$$

A second ODE along the other characteristic path defined by Equation (40) is derived in the following manner. In Equation (37), if y_i is a function of $\hat{z}$ and t, then x_i is also a function of these variables and the total differential of x_i with respect to t is

$$\frac{dx_i}{dt} = \frac{\partial x_i}{\partial \hat{z}} \frac{d\hat{z}}{dt} + \frac{\partial x_i}{\partial t} \tag{42}$$

Since the path to be followed is defined by Equation (40), $\partial x_i/\partial t$ becomes equal to dx_i/dt and Equation (2) becomes

$$\frac{dx_i}{dt} = \lambda_i (y_i - y_i^*) \tag{43}$$

which is the other ODE required, this time along the path in the $\hat{z}$ - t plane defined by Equation (40).

According to the method of characteristics, Equations (41) and (43) will be used to calculate fluid and adsorbent phase concentrations in the $\hat{z}$ - t plane along the characteristic paths defined by Equations (39) and (40) respectively. The starting points for these calculations are the initial conditions and the boundary conditions at the top and bottom of the adsorption column.

The initial conditions are, at t = 0 and $\hat{z} \geq 0$,

$$y_i = y_{oi}(\hat{z}) \tag{44}$$

and

$$x_i = x_i(\hat{z}) \tag{45}$$

The boundary conditions at the bottom of the column for hot upflow are, at $\hat{z} = 0$ and $t \geq 0$,

$$y_i = \langle y_{Bli} \rangle \tag{46}$$

for the fluid phase concentration and

$$\left.\frac{dx_i}{dt}\right|_{\hat{z} = o} = \lambda_i (\langle y_{Bli} \rangle - y_i^*) \tag{47}$$

for the solid phase concentration.

For cold downflow at the top of the column, the boundary conditions are, at $\hat{z} = h/v_2$ and $t = 0$,

$$y_i = \langle y_{T2i} \rangle \tag{48}$$

for the fluid phase concentration and

$$\left.\frac{dx_i}{dt}\right|_{\hat{z} = h/v_2} = \lambda_i (\langle y_{T2i} \rangle - y_i^*) \tag{49}$$

for the solid phase concentration

The next step is to calculate the concentration profiles in the $\hat{z}$ - t plane (along the packed column with time) along the characteristic paths (Equations 39 and 40). For this purpose, the plane will be divided into equal increments, Δt and Δz, along the horizontal and vertical axes respectively as shown in Figure (37). Let

$$\Delta z/v = \Delta \hat{z} = \Delta t = \delta \tag{50}$$

Now the concentrations will be calculated from

point to point along the characteristic lines and the finite difference equations needed for this are obtained by integrating Equations (41) and (43) between the limits of $\hat{z}$ and $\hat{z}_o$ and t and t_o to give

$$y_i\langle\hat{z}\rangle = y_i\langle\hat{z}_o\rangle - \frac{(1-\varepsilon)\rho_s}{\varepsilon} \lambda_i \int_{\hat{z}_o}^{\hat{z}} (y_i - y_i^*)\, d\hat{z} \qquad (51)$$

and

$$x_i\langle t\rangle = x_i\langle t_o\rangle + \lambda_i \int_{t_o}^{t} (y_i - y_i^*)\, dt \qquad (52)$$

Now, as previously mentioned and as shown in Figure (6), the calculations for y_i will be made step by step along the diagonals $\hat{z} = t$ (Equation 39) and the calculations for x_i will be made along the horizontal lines, $\hat{z}$ = constant (Equation 40). The position at the junction of the characteristic lines is designated by (i,j). Thus calculations for y_i at (i + 1, j + 1) will be made by adding the increment of y_i [from (i,j) to (i + 1, j + 1)] to the value of y_i at (i,j). Values for x_i at (i + 1, j + 1) will be calculated by adding the increment (from (i + 1, j) to (i + 1, j + 1) to the value of x_i at (i + 1, j). In this fashion the concentration profiles are calculated along the axis of the column and time.

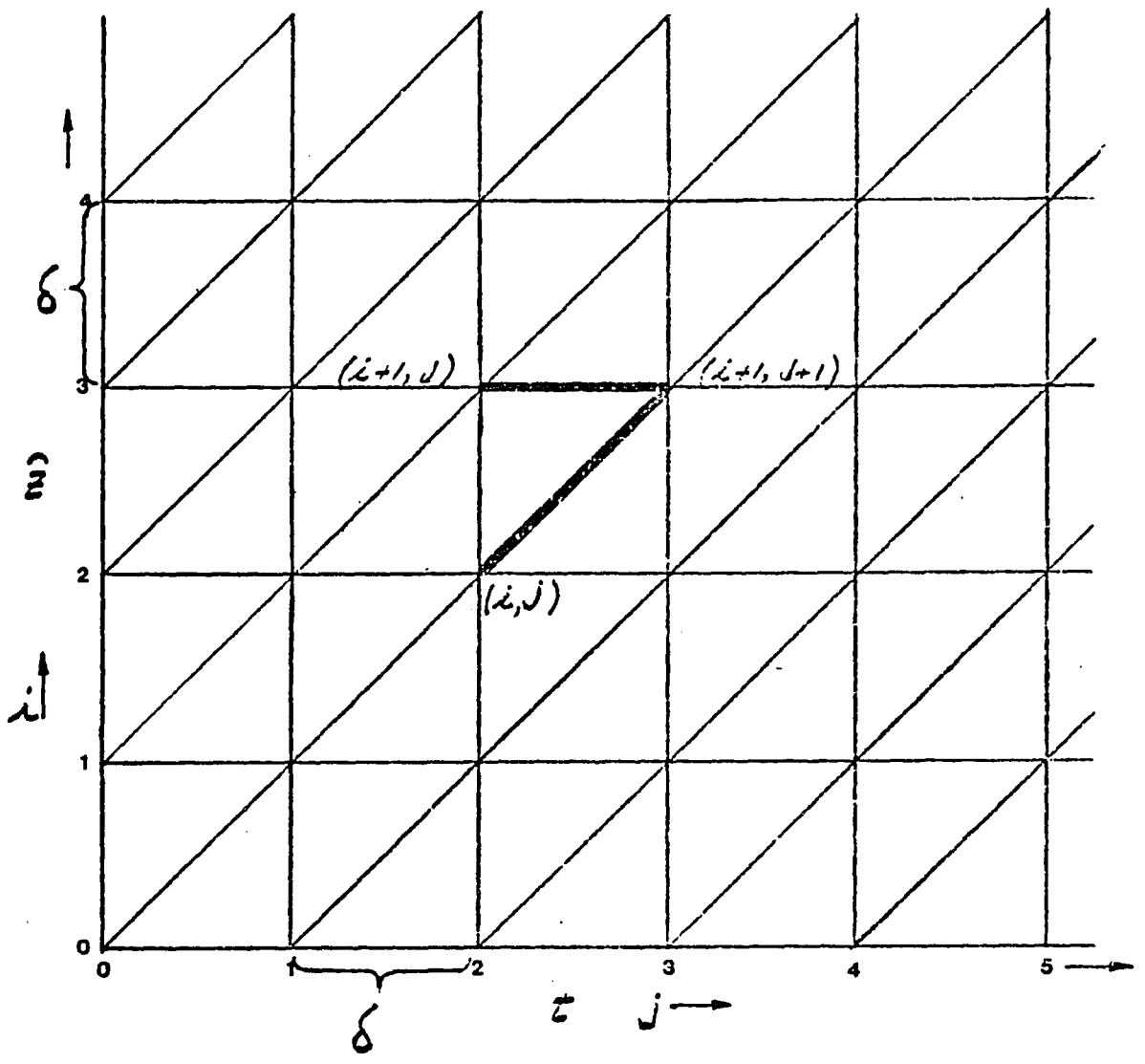

FIGURE (6)

Characteristic Calculation Paths in the $\hat{z}$-t Plane

If the intervals ($\delta = \Delta\hat{z} = \Delta t$) in Equation (50) and Figure (6) are small enough, then Equations (51) and (52) become

$$y_i(i+1,j+1) = y_i(i,j) - \frac{(1-\varepsilon)\rho_s}{\varepsilon}\frac{\lambda_i\delta}{2}\left[y_i(i+1,\ j+1)\right.$$
$$\left.-y_i^*(i+1,j+1) + y_i(i,j) - y_i^*(i,j)\right] \quad (53)$$

$$x_i(i+1,j+1) = x_i(i+1,j) + \frac{\lambda_i\delta}{2}\left[y_i(i+1,j+1)\right.$$
$$\left.-y_i^*(i+1,j+1) + y_i(i+1,j) - y_i^*(i+1,j)\right] \quad (54)$$

At the beginning of the first hot upflow half cycle, the entire column is filled with feed solution and $y_i = y_{oi}$ at $t = 0$ and $\hat{z} = 0$ to h/v. All corresponding values of x_i are equal to zero. Values of y_i and x_i at the end of the half cycle are calculated for various points along the column from Equations (53 and 54). The values of y_i and x_i at the end of the column ($\hat{z}$ = h/v) are then combined with external material balance equations (Chen and Hill, 1971) to account for the effect of the feed, product, and reservoir streams at the top of the column.

These external equations (Chen and Hill, 1971) are rearranged and modified for multicomponent systems. For the top of the column

$$\langle y_{TP1i}\rangle_n = \frac{(\phi_T+\phi_B)y_{oi} + (1-\phi_B)\langle y_{T1i}\rangle_n}{1+\phi_T} \qquad (55)$$

$$\langle y_{TP2i}\rangle_n = \frac{Q\pi/\omega\langle y_{TP1i}\rangle_n + V_T\langle y_{TP1i}\rangle_{n-1}}{V_T + Q\pi/\omega} \qquad (56)$$

$$\langle y_{T2i}\rangle_n = \frac{(\phi_T+\phi_B)y_{oi} + (1-\phi_T)\langle y_{TP2i}\rangle_n}{1+\phi_B} \qquad (57)$$

The value of $\langle y_{T1i}\rangle$ from Equation (53) is substituted in Equation (55) to get the value of $\langle y_{TP1i}\rangle$. This hot cycle top product concentration is then used in Equation (56) to obtain the cold cycle top product concentration $\langle y_{TP2i}\rangle$ which is used for plotting the top product vs. time graph shown in later in the chapter. It is also used in Equation (57) to obtain the value $\langle y_{T2i}\rangle$ which is used in the boundary condition equations for the top of the column (Equations 48 and 49). These equations give the values of y_i and x_i at the top of the column for the cold downflow half cycle. Then, Equations (53 and 54) are again used, this time to calculate the concentration profiles in the column during the cold downflow half cycle. The value of y_i at the bottom of

the column ($\hat{z} = 0$) is $\langle y_{B2i} \rangle$ and is used along with other known values in an external equation around the bottom of the column (Chen and Hill, 1971) rearranged for multicomponent systems.

$$\langle y_{B1i} \rangle_n = \frac{Q\pi/\omega \langle y_{B2i} \rangle_{n-1} + V_B \langle y_{B1i} \rangle_{n-1}}{Q\pi/\omega + V_B} \qquad (58)$$

Now $\langle y_{B2i} \rangle$ is equal to $\langle y_{BP2i} \rangle$ since both streams come from the same source. For the same reason, $\langle y_{BP1i} \rangle$ equals $\langle y_{B1i} \rangle$.

This value is used with the boundary equations at the bottom of the column (Equations 46 and 47) to give the values of y_i and x_i at the beginning of the next hot upflow half cycle. And Equations (53 and 54) are again used to calculate the concentration profile in the column for the second hot upflow half cycle.

This procedure is repeated for every cycle and the resulting top and bottom product concentrations calculated by the computer program are plotted along with the experimental data in the graphs presented in this chapter. The details of the computer program (including the incorporation of the external equations into the program) are given by Kim (1976).

Calculation of λ_i. Values of λ_i, the mass transfer coefficient, vary with temperature and solute concentration and must be calculated at every point in the column. The equations presented here were developed (Kim, 1976) for the particular system (toluene-acetophenone-n-heptane on silica gel) used for the experimental section of this thesis. The equations were generalized for multicomponent systems and may be used to extend the ternary system to additional solute contents.

$$\lambda_i = (A_p)(J_D)(v)(\varepsilon)(Sc)^{-2/3} \tag{59}$$

where

$$J_D = \alpha(Re)^{-0.78} \text{ for laminar flow} \tag{60}$$

$$Re = \frac{D_p v \rho_f \varepsilon}{\mu_f (1-\varepsilon)} = \text{Reynolds No. for flow in packed beds} \tag{61}$$

$$Sc = \frac{\mu_f}{\rho_f D_f} = \text{Schmidt No.} \tag{62}$$

$$A_p = a_p/\rho_s = \text{interfacial area/unit weight of adsorbent}$$

$$v\varepsilon = \text{superficial column velocity}$$

$$= v_1\varepsilon = (1-\phi_B)Qa_t \text{ for hot upflow}$$

$$= v_2\varepsilon = (1+\phi_B)Qa_t \text{ for cold downflow} \tag{63}$$

$$\rho_f = \Sigma_{n=1}^{n} \; y_i M_i \tag{64}$$

$$\mu_f = \Sigma_{n=1}^{n} \; y_i \mu_i / \Sigma_{n=1}^{n} \; y_i \tag{65}$$

where y_i (moles i/unit vol. solution) varies at each point in the column and μ_i varies with temperature (T_1, T_2).

α varies with the solute and the solute concentration (Kim, 1976), but usually becomes a single constant for all solutes at low concentrations.

D_f is the solute-solvent diffusivity which varies with the solute and with the temperature (Kim, 1976).

$$D_{fi} = \frac{7.4 \times 10^{-8} (60) (\psi_s M_s)^{0.5} T}{\mu_f V_{Mi}^{0.6}} \tag{66}$$

where

$T = T_1$ for hot upflow

$T = T_2$ for cold upflow

$\psi_s = 1.0$ for n-heptane

$M_s = 100.2$ for n-heptane

$V_{Mi} = 119$ for toluene (molecular volume)

$= 161$ for acetophenone

Calculation of y^*. y_i^* is the fluid concentration of solute in equilibrium with the adsorbent. In the present type of system, the equilibrium should be determined from a Langmuir type of isotherm (Wilhelm et al, 1968). The particular form of the Langmuir isotherm was originally proposed by Sweed (1969). In the present nomenclature, this isotherm is:

$$x_i^* = \frac{A_i y_i}{1+B_i y_i/\rho_i} + Dy_i \qquad (67)$$

or (Kim, 1976),

$$y_i^* = \frac{-(A_i+D-B_i x_i/\rho_i)+[(A_i+D-B_i x_i/\rho_i)^2+ 4B_i D x_i/\rho_i]^{1/2}}{2B_i D} \qquad (68)$$

where A_i and B_i are constants

	toluene		acetophenone	
	343°K	298°K	343°K	298°K
A_i	1.46	8.65	0.10	40.0
B_i	18.47	66.97	50.00	10.0

and

$D = 0.29$ cm^3 pores/gm dry silica gel

Experimental

The experimental apparatus is shown in Figure (7). The equipment consists of a jacketed glass column 1.0 cm in diameter and 90 cm long packed with 30-60 mesh chromatographic grade silica gel. The reservoirs for the top and bottom of the column were two 50 cc glass syringes operated by a dual infusion-withdrawal pump manufactured by the Harvard Apparatus Co. A micro-switch was wired into the pump circuit to automatically reverse the syringes at the end of each cycle.

The jacket was heated and cooled on alternate half cycles by water pumped from constant temperature hot and refrigerated baths kept at 343 and 298°K respectively. The baths were connected to the column and to recycle by solenoid valves wired to a timer so that hot water was always supplied to the jacket during the upflow half cycle and cold water during the downflow half cycle.

Feed solution was fed to the top of the column from a 50 cc syringe mounted in a second Harvard Apparatus Co. pump. Pump operation was interrupted to refill the syringe approximately every third cycle. The top and bottom product streams were regulated with micrometer capillary valves which also served to impose a slight back pressure on the column to exclude air

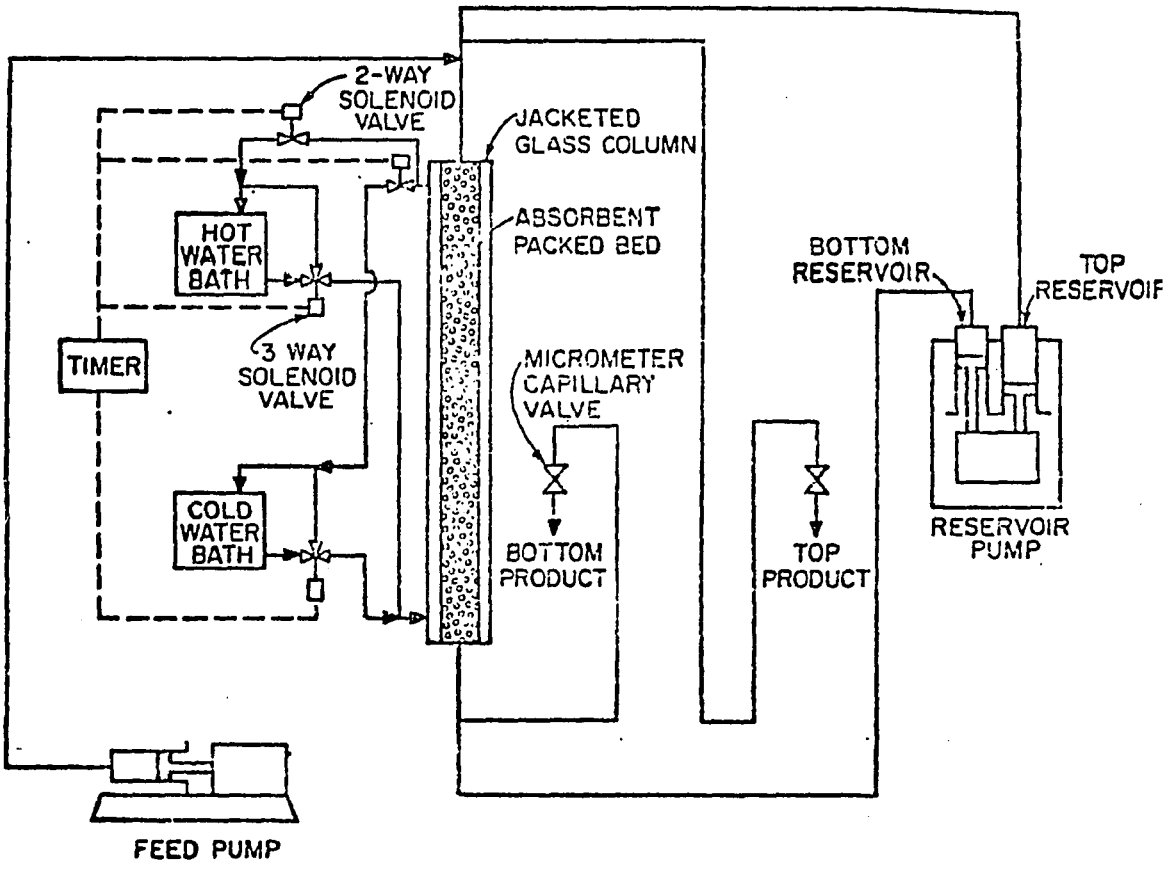

FIGURE (7)

Laboratory Parametric Pump

which could enter the system due to a small amount of thermal expansion and contraction of the process fluid.

In preparation for each run, the column was carefully packed with silica gel and feed solution so as to eliminate all air from the column. The reservoir and feed pumps and all connecting lines were filled with feed solution at ambient temperature. The reservoir syringes were set for the specified delivery with a dead volume of approximately 3 cc.

The run was started by switching on the syringe pumps and activating the timer. The bottom reservoir pumped fluid into the bottom of the column and, at the same time, the hot water bath pump supplied hot water to the column jacket. At the end of the hot half cycle, the microswitch reversed the action of the reservoir pump and the solenoid valves put the hot water bath system on recycle and supplied cold water to the jacket of the column. The top and bottom flow rates were adjusted to allow for thermal expansion so that the average rates for the complete cycle were correct.

The top and bottom products were collected for both hot and cold half cycles. The cold downflow product samples were analyzed by vapor phase chromatography.

A Hewlett Packard Model 5710A Chromatograph coupled with an electronic area integrator was used. For very low peaks, beyond the lower detection limit of the integrator, the areas were measured manually at one half the peak height. The helium rate was set at 86 cc/ minute with a soap bubble flow meter. The temperatures of the injection port, the conductivity detector, and the oven were maintained automatically at constant values of 250, 250, and 205 degrees C respectively. The detector current was set at a constant 160 milliamps and the chart speed at 0.2 inches per minute. Dual columns were used made of 0.25 inch o.d. copper tubing 6 feet long and packed with "Pennwalt 223 on 4% KOH" from Applied Science Laboratories, Inc. Under these conditions, the approximate peak times for n-heptane, toluene, and acetophenone were 1.1, 2.2, and 10.1 minutes respectively. A few peaks from most of the runs were checked with an F & M Model 810-29 Chromatograph with the same columns and approximately the same running conditions. Sample injections were all 5 microliters from a 10 microliter Hamilton syringe.

In the chromatograph calibration runs for this system, the area percent of the component peaks was only approximately equal to the weight percent of the corresponding component in solution. A better correlation is shown in Figure (8) which gives the area of the component peaks versus the actual volume (microliters) of the component injected into the chromatograph, either as a solution or as the pure material. This linear relationship of chart peak area to injection volume is fundamental to vapor phase chromatography and Figure (8) demonstrates its applicability to the present system.

With this calibration, the ratios of the areas of the component peaks in any given product sample to the areas of the corresponding peaks in the feed sample give the desired product/feed concentration ratios directly.

$$\langle y_{BPi} \rangle_n / y_{oi} = \frac{\text{area of the component peak in the product}}{\text{area of the component peak in the feed}}$$

Of course the same relationship applies to top product sample components. These concentration ratios apply equally well to volume, weight, or mole ratios because any conversion factors from volume to other units automatically cancel themselves out. To eliminate errors from variations due to the equipment or analytical techniques, feed and product samples are run the same day.

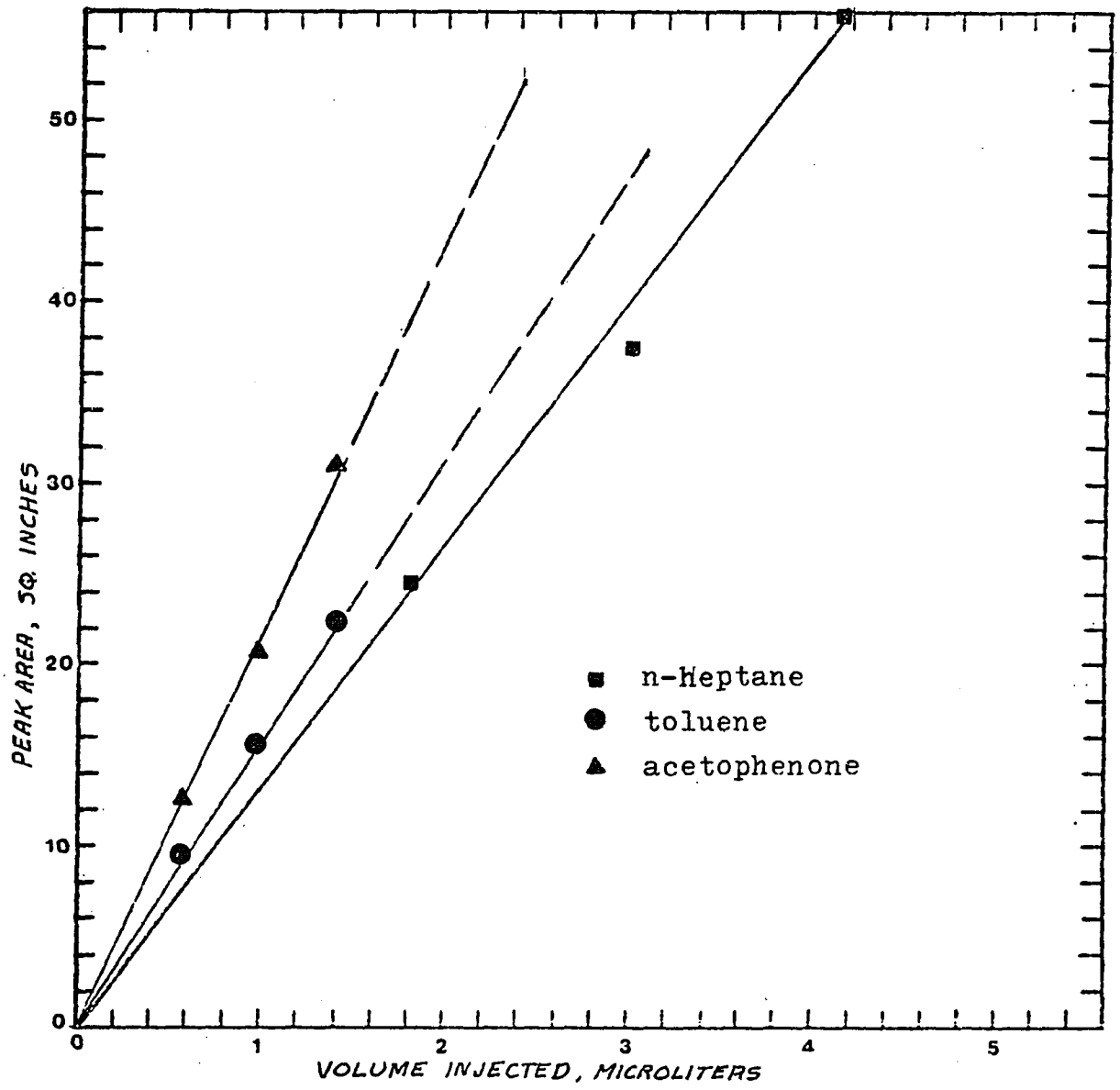

FIGURE (8)

Calibration: Solute Volume vs Peak Area

The chromatographic peak analysis, as previously mentioned, was by area integration. The large peaks as shown in Figure (9) were automatically integrated by the attached electronic integrator. For very small peaks (very low solute concentrations), it was necessary to calculate the area by hand as indicated in Figure (10). The results are presented as area or concentration ratios in the experimental data tables in Appendix I.

FIGURE (9)

CHROMATOGRAPHIC PEAK ANALYSIS (EXAMPLE)

Hewlett Packard Model 5710A, "Pennwalt 223+ 4% KOH" Packing, He = 86 cc/min, T.C. Detector, 160 ma current, Oven 205 C. I.P. 250 C., Detector 250 C., Col- ¼"o.d.x 6' copper.

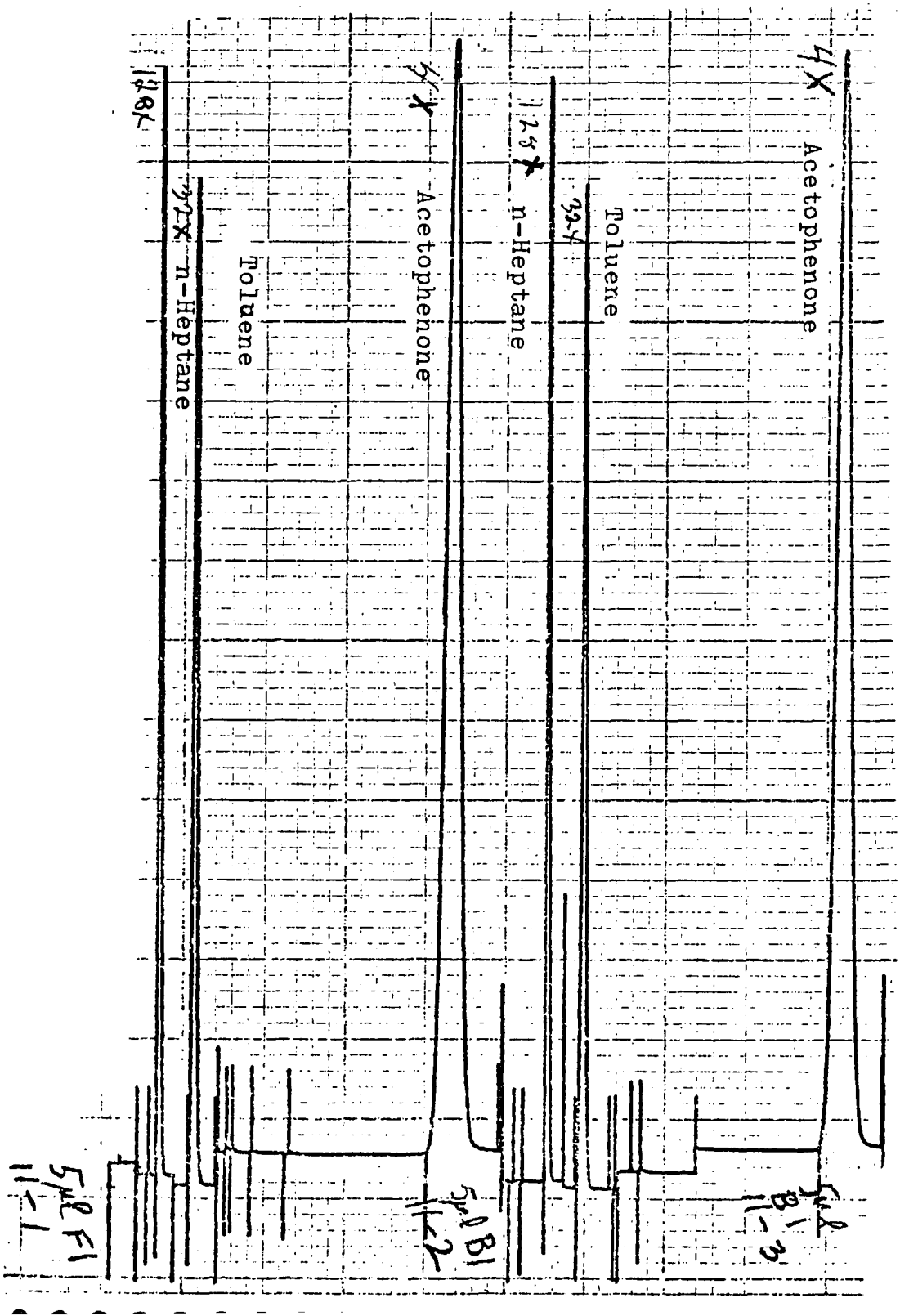

FIGURE (10)

CHROMATOGRAPHIC PEAK ANALYSIS (EXAMPLE)

(Small Solute Peaks)

Hewlett Packard Model 5710A
"Pennwalt 223+4% KOH" Packing
He = 86 cc/min
T.C. Detector
Current= 160 ma
Oven = 205 C.
Injection Port= 250 C.
Detector = 250 C.
Col.- ¼"o.d.x 6' copper

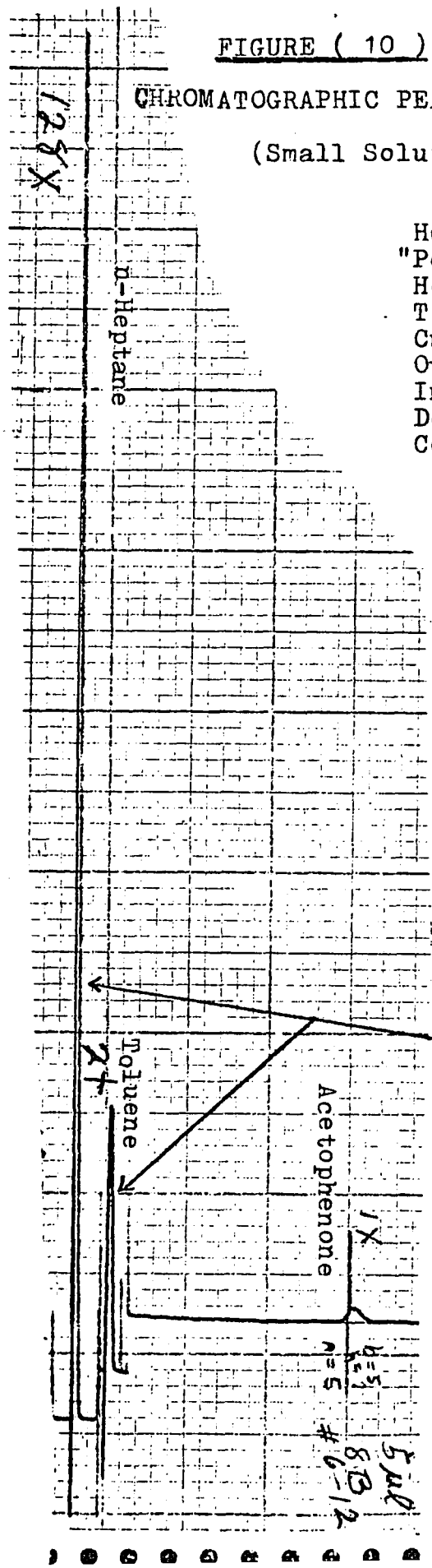

peak areas by electronic integrator

manual peak area calculation

Results and Discussion

Ten runs corresponding to various solute concentrations, cycle times, and bottom product rates were carried out. The experimental parameters are shown in Table (2). The complete experimental data are shown in tabular form in Appendix I. The data are plotted as product/feed solute concentration ratios vs. time (cycle number) in Figures (11) to (20) inclusive. In all cases, the hot upflow temperature was 343°K (70°C), the cold downflow temperature was 298°K (25°C), the ratio of the feed to reservoir volume was 0.4, and the top and bottom reservoir dead volumes were 5 $cm.^3$ Also, the column height and diameter were 90 cm. and 1.0 cm. for all runs.

Dilute solution runs. The runs with 2.5 volume percent toluene and acetophenone in n-heptane are shown in Figures (11,12,13). As pointed out in Chapter 3, the dilute solution theory applies to these low solute concentrations, and the dimensionless equilibrium parameter has special significance in predicting column performance. This parameter, b, depends only on the particular binary system and the two operating temperatures, T_1 and T_2. The value for toluene-n-heptane was 0.22 for 277° and 343°K (Chen et al, 1972, 1973) and 0.15 for 298° and 333°K (Chen et al, 1974). For the present temperatures, 298° and 343°K, the value of b

TABLE 2

EXPERIMENTAL PARAMETERS - CONCENTRATION EFFECT

Hot upflow half cycle temperature, °K	343
Cold downflow half cycle temperature, °K	298
Feed volume/reservoir ratio, $\phi_T+\phi_B$, dimensionless	0.400
Column height, h, cm.	90
Column diameter, d_1, cm.	1.0
Top reservoir dead volume, V_T, $cm.^3$	5.0
Bottom reservoir dead volume, V_B, $cm.^3$	5.0

Specific Run Data

Run No.	Fig. No.	Feed Composition, vol. %		$Q\pi/\omega$ $cm.^3$	ϕ_B		Cycle time π/ω, min.	
		Toluene	Aceto-phenone		Exp.	Calc.	Exp.	Calc.
1	-	2.5	0	20	0.15	0.15	20	20
2	-	0	2.5	35	0.10	0.10	20	20
3	11	2.5	0	35	0.035	0.035	20	20
4	12	0	2.5	35	0.035	0.035	20	20
5	15	10.0	10.0	25	0.25	0.25	20	20
6	13	2.5	2.5	25	0.25	0.30	20	20
7	16	10.0	10.0	25	0.035	0.085	20	20
8	17	10.0	10.0	25	0.035	0.035	10	15
9	18	10.0	10.0	25	0.035	0.035	5	10
10	20	20.0	20.0	25	0.035	0.035	10	10
11	19	20.0	10.0	25	0.035	0.035	10	10
12	14	0	10.0	35	0.035	0.035	20	20

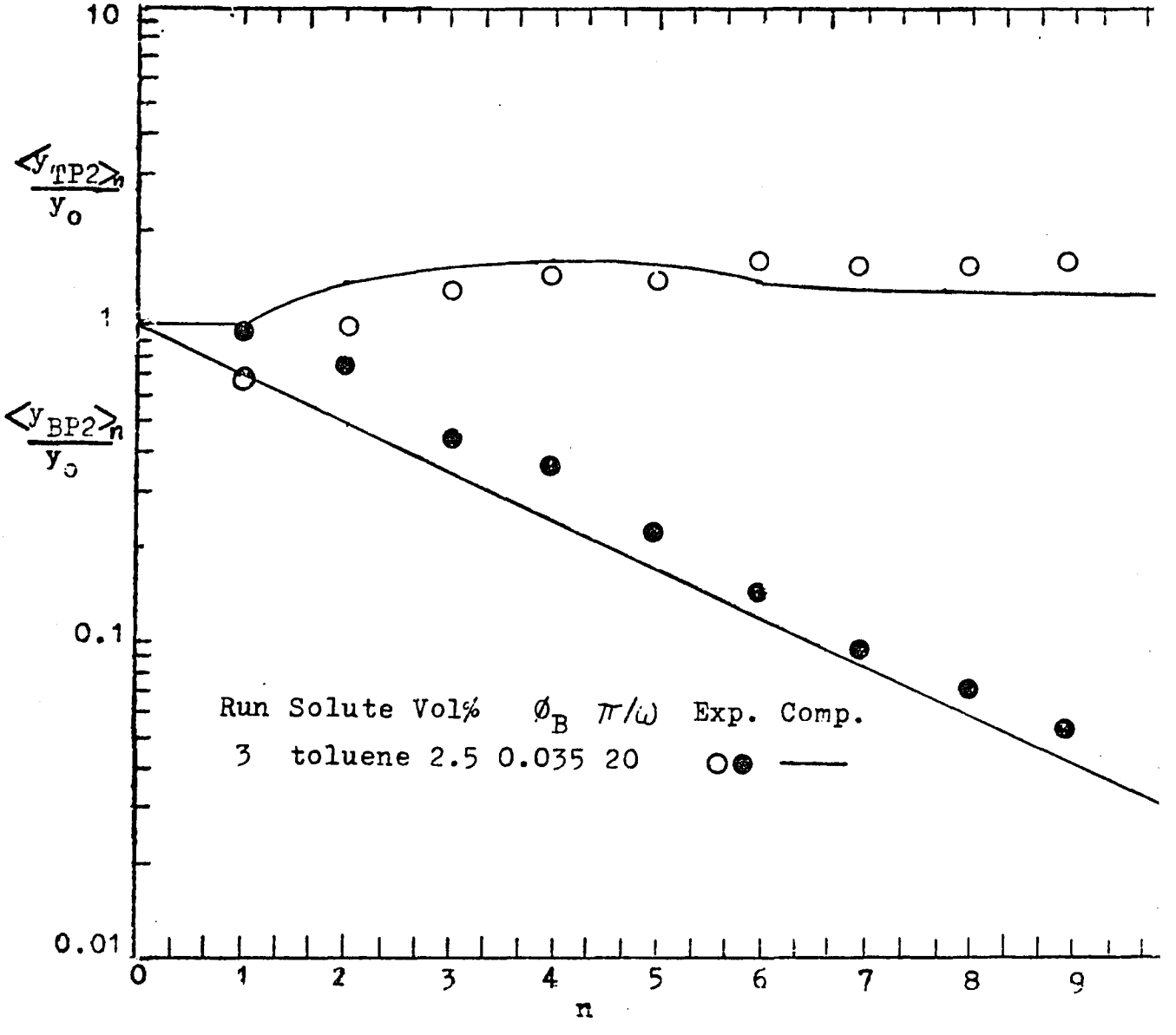

FIGURE (11)

Dilute Binary System: 2.5% Toluene in n-Heptane

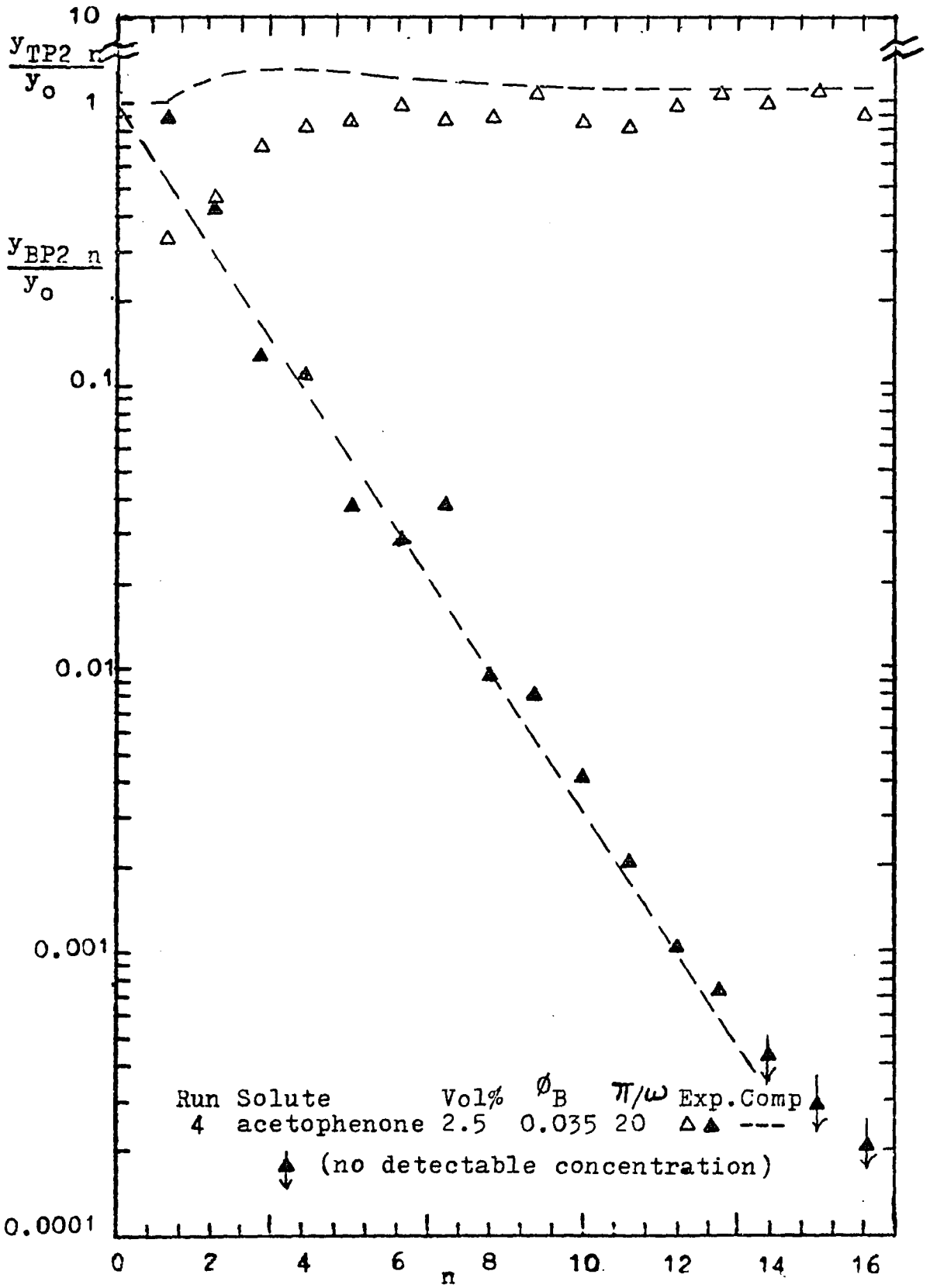

FIGURE (12)

Dilute Binary System: 2.5% Acetophenone in n-Heptane

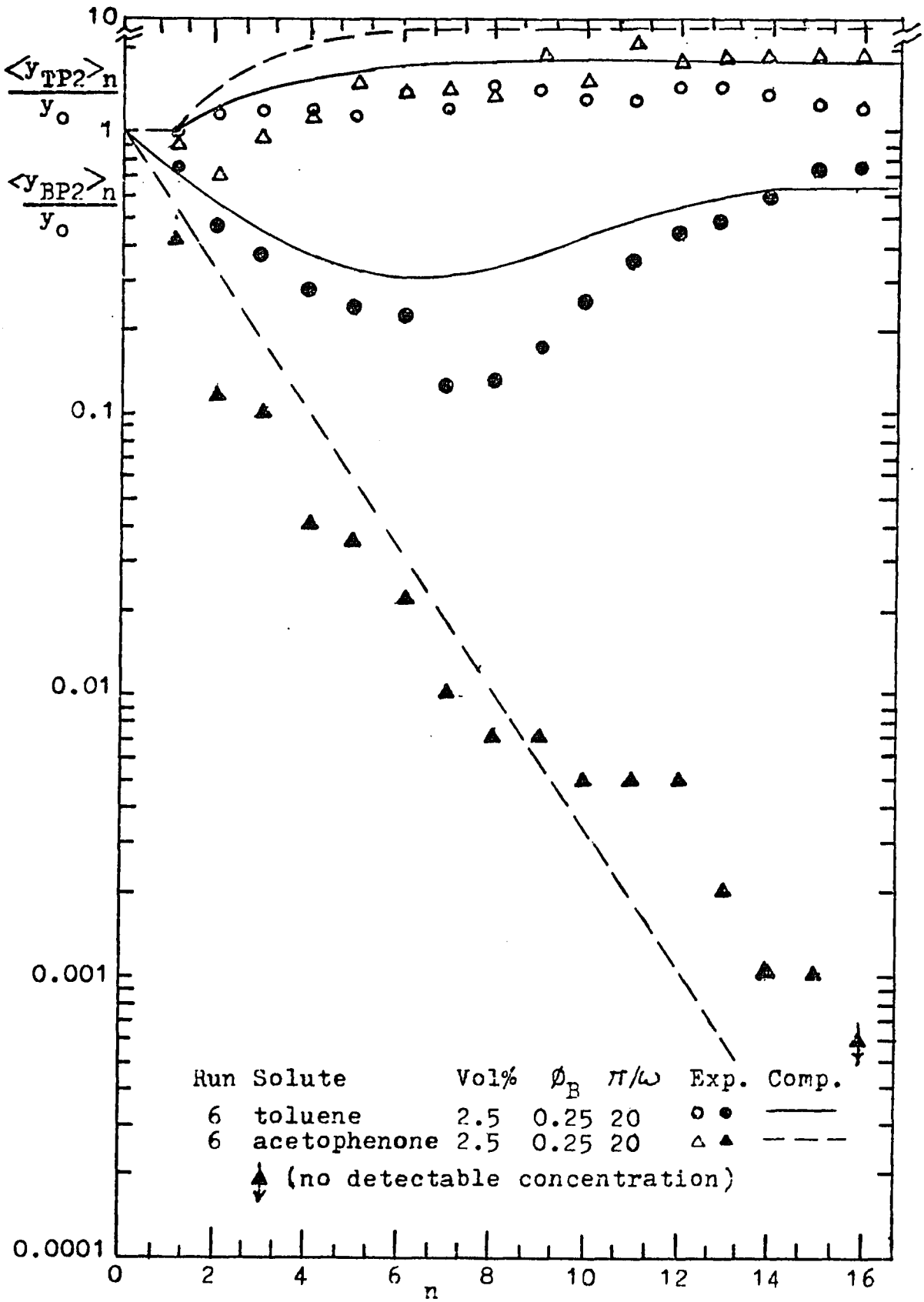

FIGURE (13)

Dilute Ternary System: 2.5% Toluene and Acetophenone in n-Heptane

for toluene-n-heptane was estimated at 0.20 from the bottom product curve in Figure (11) by the method of Chen et al (1972). The value of b for acetophenone was estimated at 0.33 by the same method from the bottom product curves for both the binary system (Figure 12) and the acetophenone toluene-n-heptane ternary (Figure 13). This is further proof (over that given in Chapter 3 for the toluene-aniline-n-heptane system) that the value of the parameter b is independent of the system for dilute multicomponent solutions. With these values of b (0.20 for toluene and 0.33 for acetophenone), the bottom product/reservoir ratio ($\emptyset_B$) was set at 0.25 for run no. 6, and acetophenone was separated from toluene in the bottom product stream (Figure 13). This result is easily predictable from the dilute solution theory of Chapter 3.

Figure (14) shows the product concentration profile for 10% acetophenone in n-heptane. This is comparable to the 10% toluene in n-heptane binary (Chen et al, 1972) in that it may be considered dilute since the 10% refers to total concentration. Actually, the bottom product profile was fitted better by the mathematical model for concentrated solutions and this model was used to compute the profile shown in Figure (14).

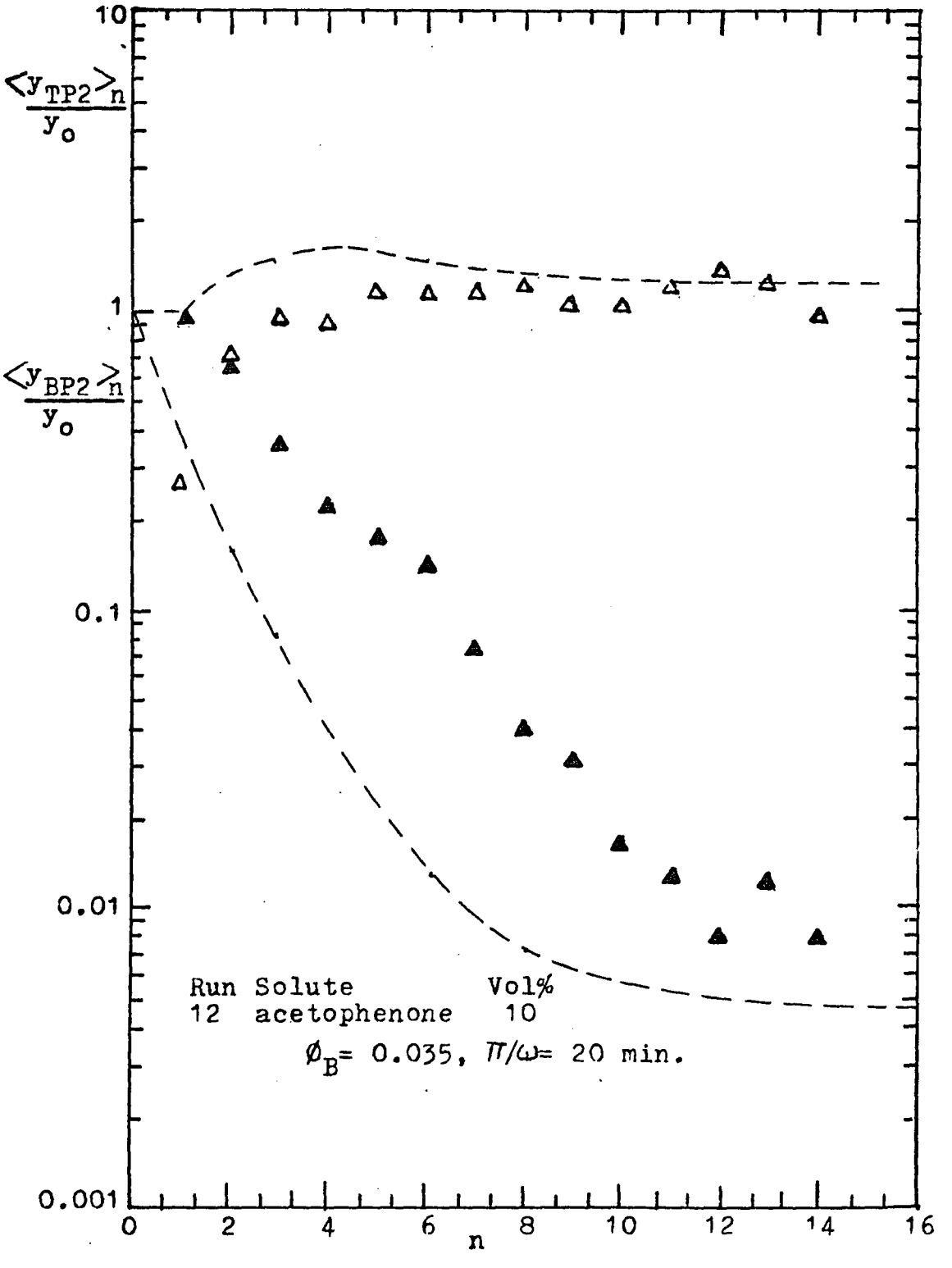

FIGURE (14)

10% Binary System: Acetophenone in n-Heptane

Concentrated solution runs. When the feed concentration was increased to 10 vol. percent for acetophenone and toluene, and the value of $\emptyset_B$ was held at 0.25, there was only a modest separation of acetophenone from toluene in the bottom product stream as shown in Run No. 5 (Figure 15). The initial downward slope of the acetophenone bottom product stream extends to the eighth cycle and is followed by a sharp turn upwards to the twelfth cycle and a levelling off after cycle no. 12. This dip in the bottom product curve is quite sensitive to the value of $\emptyset_B$ input to the computer program, the bulge tending to disappear at values of $\emptyset_B$ less than 0.20. Experimentally, this is shown in Run no. 7 (Figure 16) in which the dip disappears completely at a $\emptyset_B$ of 0.035. One physical interpretation of this phenomenon is that the acetophenone is rapidly adsorbed from the solution initially saturating the entire column and the dilute n-heptane solution is displaced down the column by the main stream until the normal acetophenone concentration wave front breaks through the bottom of the column at cycle 8. The bottom column effluent is then rapidly saturated with acetophenone until the acetophenone wavefront is no longer diluted by the residual n-heptane and assumes its steady state value as shown in Figure (15). Of course, the larger the value of $\emptyset_B$, the

sharper the bulge of the bottom product concentration curve. The same phenomenon is shown with toluene in the same run (No. 5), but the bulge is smaller because toluene is less strongly adsorbed.

The transient effect described above is interesting but less important than the steady state separation effect which is small (y_{BP2}/y_o = 0.8) for the concentrated solution run and large (y_{BP2}/y_o = 0) for the dilute solution run.

The computed curves tend to level out above the experimental points, indicating that the experimental separation is better than that predicted by the computer program. This usually occurs when the bottom product concentration is low (y_{BP2}/y_o) is 0.01 or less. The analytical results at this point tend to be inaccurate because the acetophenone peaks on the chromatographic charts are very small, cannot be detected by the electronic integrator and, if they show up at all, must be integrated by hand. The analytical results at this level are generally very uncertain and the data tend to scatter. Therefore, the levelling out trend indicated by the computer is not necessarily contradicted by the experimental data.

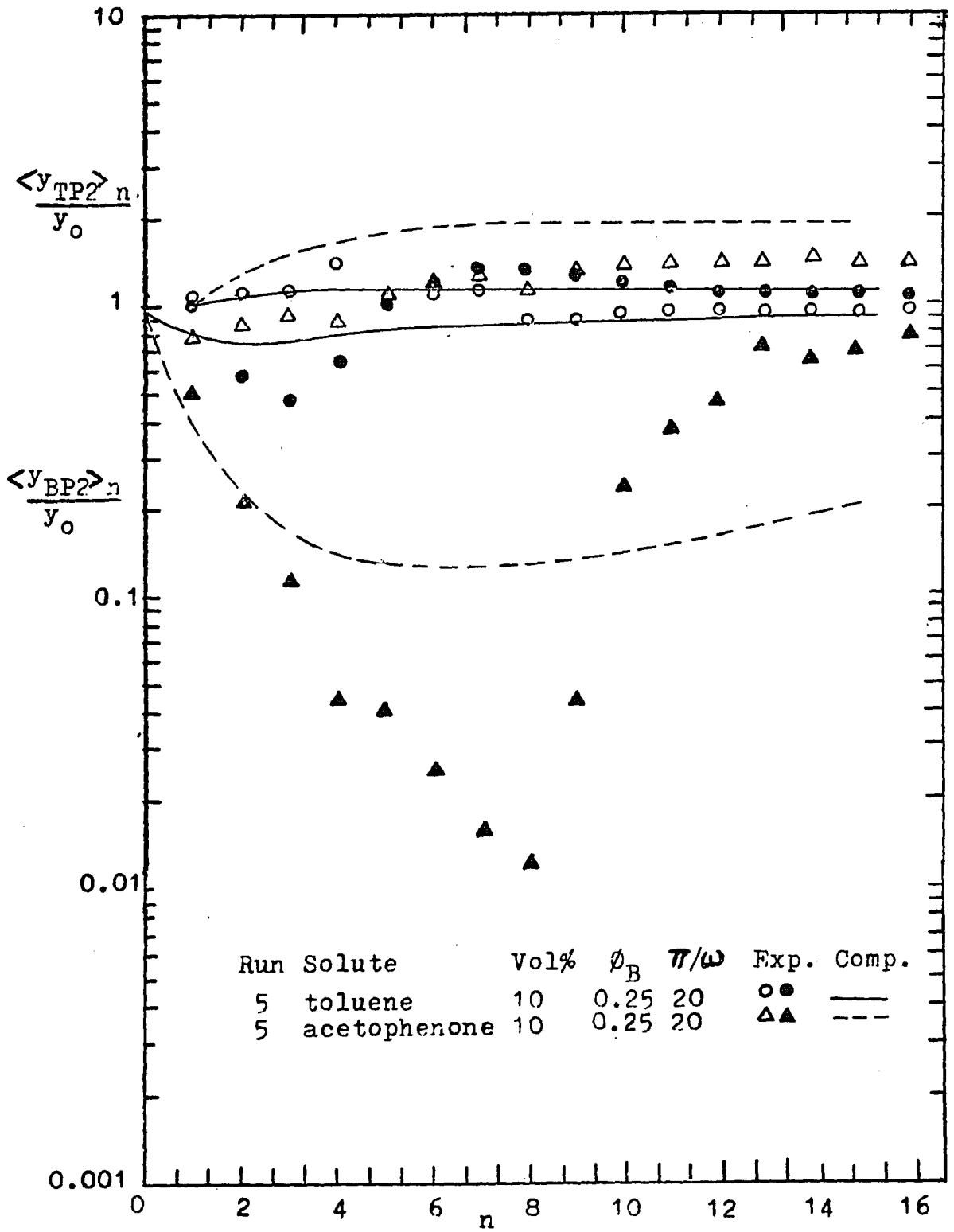

FIGURE (15)

Concentrated Ternary System: 10% Toluene and Acetophenone in n-Heptane

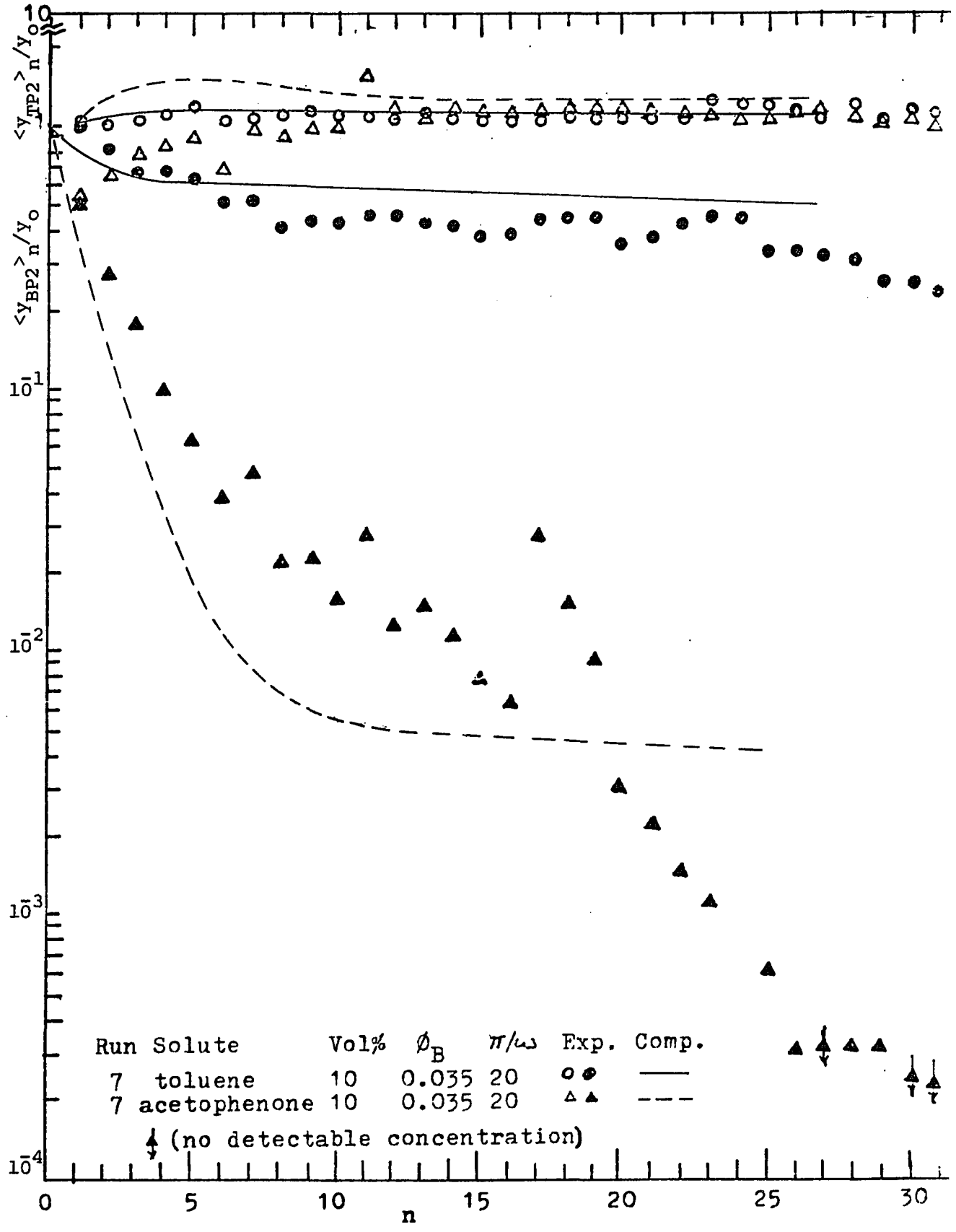

FIGURE (16)

10% Ternary System: Effect of Reducing ϕ_B

Effect of cycle time. The length of the cycle affects the separation by changing the approach to equilibrium. In the mathematical logic and in the computer program, the cycle time shows up in the column velocity and in the mass transfer coefficients which are automatically computed for every point in the column and incorporated into the calculated concentration profiles. The net result is shown in Runs 7, 8, and 9 (Figures 16, 17,18) for half cycle times (π/ω) of 20, 10, and 5 minutes.

Experimentally, the net effect of reducing the cycle time and decreasing the approach to equilibrium appears to be a tendency of the bottom product concentration to level out at increasingly higher solute concentrations. For 10 vol. percent feed solutions with dimensionless bottom product rates (ϕ_B) of 0.035, the bottom product concentration ratios (y_{BP2}/y_o) appear to level out at values of 0.0003, 0.001, and 0.008 for the respective half-cycle times of 20, 10, and 5 minutes. As previously mentioned, the analytical accuracy in this concentration range is uncertain and the computed results should show the actual trends.

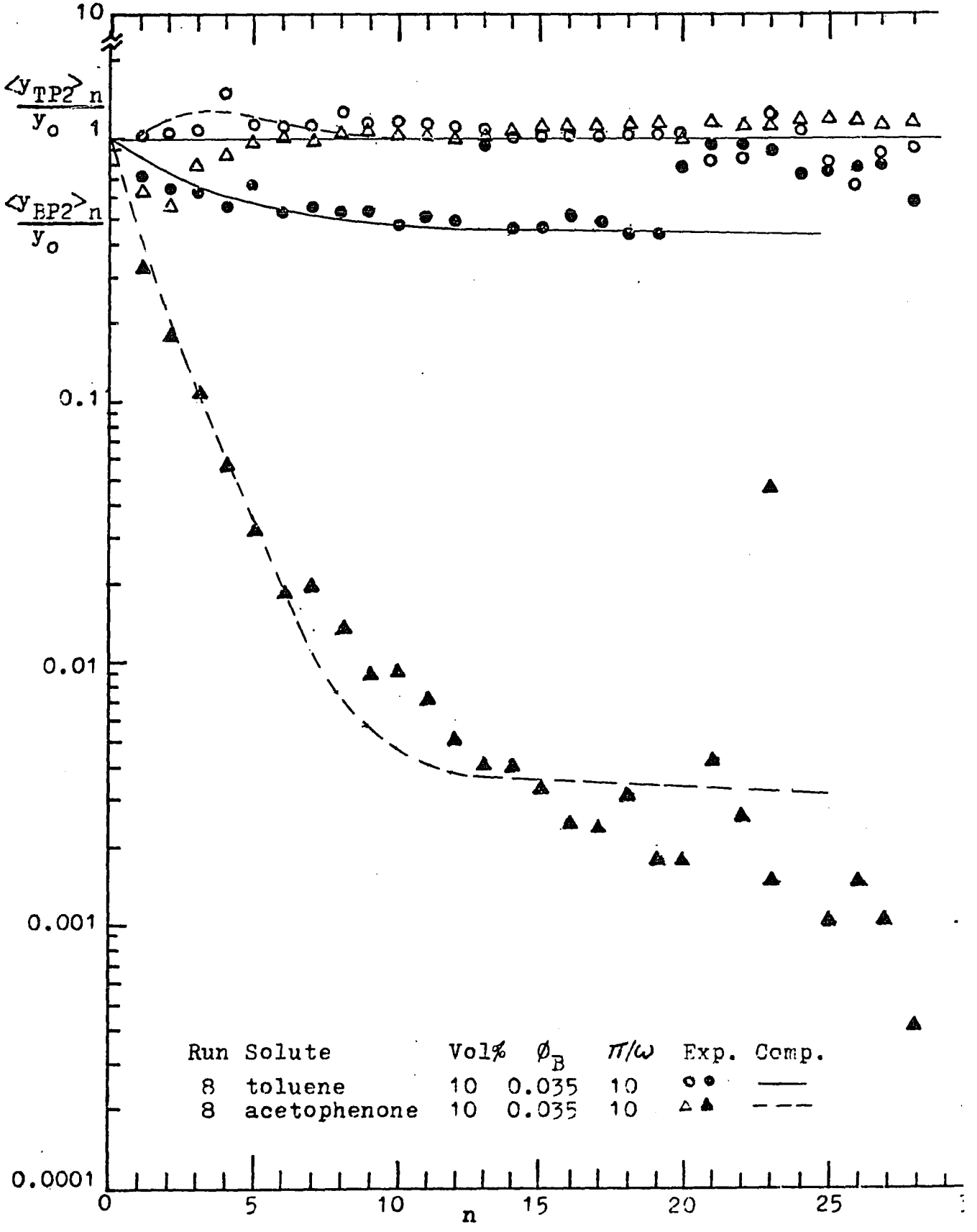

FIGURE (17)

10% Ternary System: Effect of Increasing Separation Rate by 100%

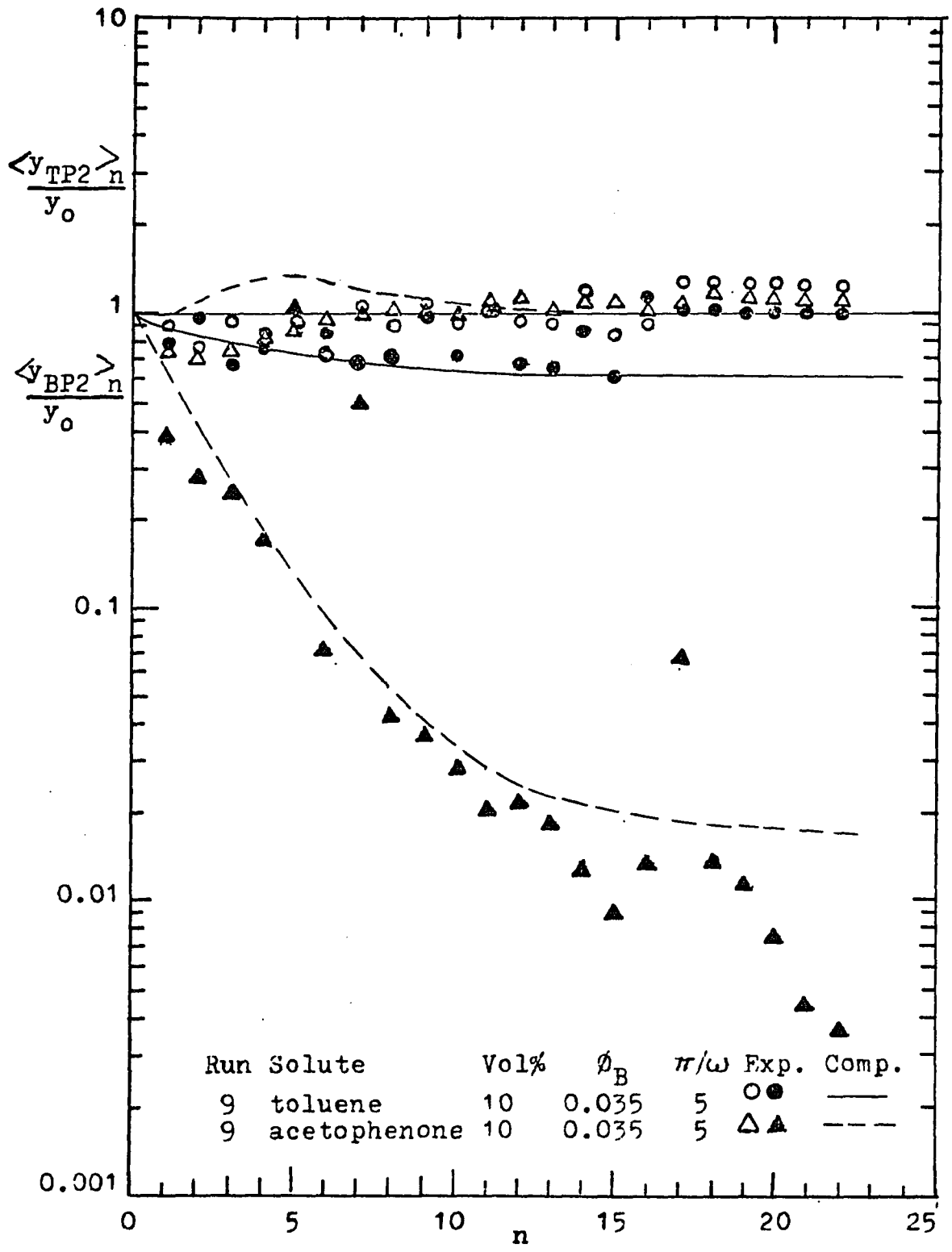

FIGURE (18)

10% Ternary System: Effect of Increasing Separation Rate by 400%

Effect of high solute concentrations. The effect of going from dilute (2.5 vol. %) solute concentrations to higher concentrations (10 vol. %) has been described as a changeover from the dilute solution theory of Chapter 3 to the concentrated solution mathematical model of this chapter. The effect of increasing solute concentrations to 20 vol. percent can now be considered. If two solutes are involved, the total concentration is 40% and proceeding beyond this point is not warranted unless the solvent is redefined.

Runs 8, 10, and 11 (Figure 17,19,20) show the effect of varying solute concentration in the concentrated solution range (above that of the dilute solution theory). All of these runs used the same value of $\emptyset_B$ (0.035) and a half cycle time (π/ω) of 10 minutes. In Run 8, the concentrations of toluene and acetophenone were 10 volume % each. The toluene concentration was increased to 20% in Run 11 and both solute concentrations were increased to 20% in Run 10.

In all three runs, the concentrations of toluene and acetophenone in the top product stream were almost identical and the same as the feed concentration. In Run 8, there was some separation of toluene in the bottom product stream ($y_{BP2}/y_o = 0.5$) and acetophenone

was separated to a greater extent ($y_{BP2}/y_o = 0.002$). When the toluene concentration of the feed was increased to 20 vol. %, the toluene concentration in the bottom product relative to the feed rose to 0.9 and the acetophenone bottom product concentration rose to 0.009. When the feed concentration of acetophenone was also increased to 20 vol. % (Run no. 10), the toluene concentration in the bottom product was actually greater than that of either the feed or the top product. The concentration of acetophenone in the bottom product rose to a steady state value of approximately 0.1 relative to that of the feed.

Thus the overall effect of increasing the solute concentration in the feed is to decrease the separation of the solutes in the bottom product. In the case where both toluene and acetophenone feed concentrations were 20%, the column behaved as though it were completely saturated with toluene and no separation was possible. Acetophenone was still separable, but the separation was relatively poor and it is doubtful that the column could handle a more concentrated feed unless the feed rate was reduced.

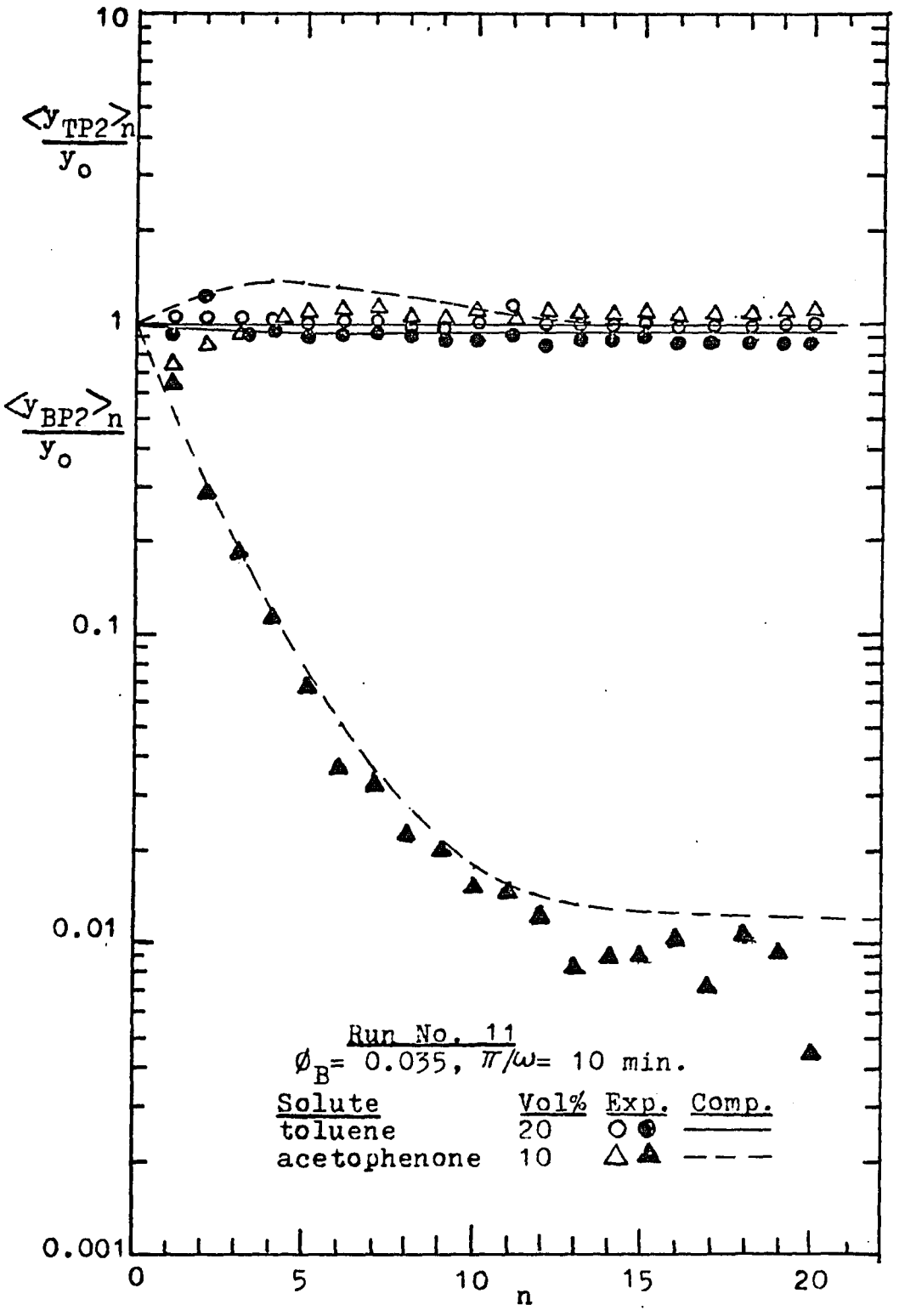

FIGURE (19)

Concentrated Ternary System: Effect of Increasing Concentration of One Solute (Toluene) to 20%

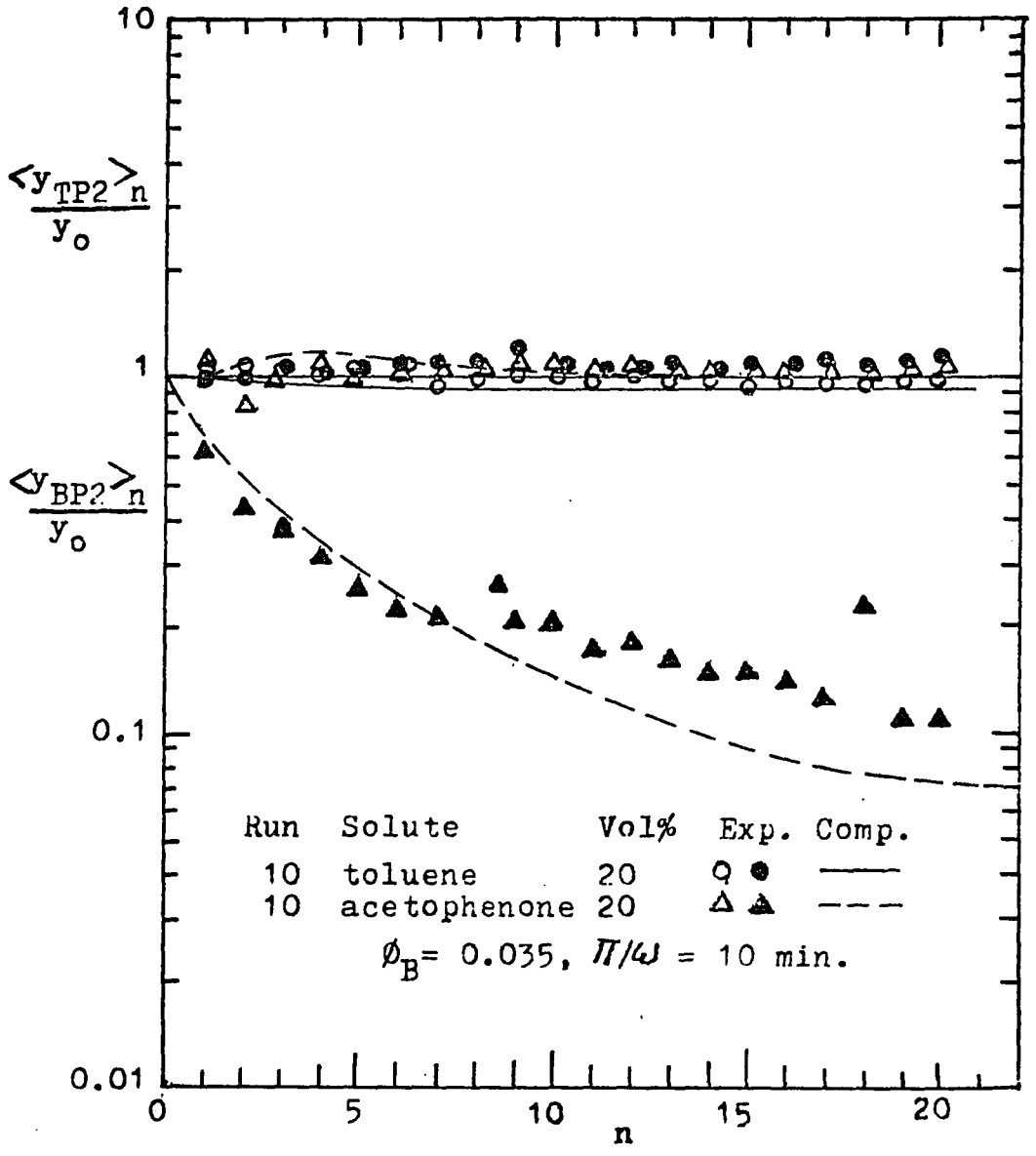

FIGURE (20)

Effect of Increasing Concentration of Both Solutes to 20%

CHAPTER 5

APPLICATION OF THE DILUTE SOLUTION THEORY TO SCALE-UP, DESIGN, AND ENERGIES

In this chapter the dilute solution theory of Chapter 3 is applied to the scale-up, design, and energies of parametric pumping systems. The four main sections of the chapter are: the basic design concepts and equations; a process design example to illustrate the use of these concepts in the design of a separation system for toluene-n-heptane-silica gel; a further expansion of the equations and concepts to correlate process energy and product purity requirements with equipment size and key operating parameters; and a description of a full scale parametric pumping system with the associated equipment and instrumentation.

It is hoped that this information will encourage the development of the parametric pumping separation technology into industrial processes. Gregory (1974) contributed towards this goal in his comparison of parametric pumping with conventional adsorption. Gregory's comparison dealt with the recuperative rather than the direct mode, but is generally valid for both approaches. The broad conclusion was that the parametric pumping process can handle larger volume feed streams than conventional adsorption processes

for equivalent separations. But, because of the frequent temperature changes, the energy requirements will, in general, be higher than those of conventional adsorption.

The energy requirements are highly significant in process separations, especially in an era of rising fuel costs. Nevertheless, the overall process must be considered and it is quite possible that the higher volumes processed by the parametric pumping system will outweigh any higher energy costs on a unit volume basis. In the section describing the full scale plant operation, methods are proposed to minimize energy requirements. And the section on energies predicts what those requirements would be for different size plants.

A series of four graphs relate equipment size and product draw-off rate to separation efficiency and to the energies required on both a BTU per operating cycle basis and a BTU per pound of product basis. As an example, a system with a 10 $ft.^3$ reservoir and a 9 $ft.^3/hr.$ draw-off rate could have a total minimum energy consumption of 171,000 BTU per cycle (heating, refrigeration, and pumping) for a product solute concentration reduced to 55% of the feed. For complete separation, the energy costs would rise to 237,000 BTU per cycle. The practical operating range of solute separations of 0-100%, required 540-900 BTU/lb. of product.

Design Concept and Equations

The dilute solution theory presented in Chapter 3 is well established for both the multicomponent systems and the binary systems, and therefore forms a reliable design basis for the present work. The design equations derived in Appendix III and summarized in this section are based on the dilute solution theory. Modifying these equations to account for the effect of solute concentration covered in Chapter 4 is beyond the scope of the present work.

In developing the design equations, as explained in Appendix III, the mathematic expressions for the binary or the multicomponent systems are identical and equally valid because the design is focussed on the separation of one particular solute. Whether that solute is the only one, as in a binary system, or only one of many, the design is the same because the equipment can produce only two product streams (as in a distillation column). Further separation of one or both streams requires another parapump for each separation and repetition of the design procedures described below.

Packed column diameter and switchover time. The basic configuration of a pilot plant or commercial parapump unit depends on a minimal switchover time

between hot and cold half-cycles. And the relationship between this switchover time and the column diameter or radius is (III-1)

$$t_{90} = 0.5\ r^2/k \qquad (70)$$

in which t_{90} is the time required for the temperature at the axis of the column to reach 90% of the external fluid temperature, r is the column radius, and k is the thermal diffusivity. This equation, as explained in Appendix III, was first applied by Sweed (1969) to a single laboratory column to explain that the switchover time for laboratory size columns was sufficiently small to consider the switchover "instantaneous" as required by the equilibrium theory.

In Appendix III, this equation was extended to (III-2,3)

$$t_1/t_2 = d_1^2/d_2^{\ 2} = N \qquad (71)$$

where d_1 is the diameter of one large column equal in cross section area (or capacity) to N small tubes of diameter d_2.

Therefore, if the equilibrium theory is to be applied and the temperature change is to be instantaneous by means of externally applied heating or cooling, the design must be based on multiple tubes in a heat exchanger configuration and the first scale up criteria is to use multiple tubes rather than a single large tube in which an internal

heat transfer device could interfere with the adsorption wave pattern and plug flow, also basic to the equilibrium theory.

Packed column length and capacity. The second scale-up concept relating to capacity is the length of the columns. As shown in the derivation in Appendix III, optimum separation is achieved when the ratio of the bottom product take-off rate to the reservoir flow rate is equal to or less than the value of the equilibrium separation parameter b. Theoretically, the capacity is at a maximum when this ratio is equal to b. Under these conditions, the penetration distance of the adsorption wavefront during the cold downflow is at a maximum and this penetration distance must be equal to or less than the length of the column. In terms of column length, h, and the superficial column velocity v, this relation was shown to be (III-9, 10)

$$h \geq K'v \tag{72}$$

where

$$K' = \frac{(1+\phi_B)(\pi/\omega)}{(1+b_i)(1+m_{oi})(\varepsilon)} \tag{73}$$

and ϕ_B is the ratio of the bottom product rate to the reservoir rate, b_i is a dimensionless equilibrium parameter, π/ω is the half cycle time, m_{oi} is a dimensionless

equilibrium parameter, and ε is the dimensionless void fraction of the adsorbent packing.

In terms of the column volumetric flow rate, the length of the column is (III-12, 13)

$$h \geq K''Q/N \tag{74}$$

where

$$K'' = \frac{(1+\phi_B)(\pi/\omega)}{(1+b_i)(1+m_o)(\varepsilon)(a_t)} \tag{75}$$

and a_t is the cross section area of one tube, N is the number of tubes, and Q is the volumetric reservoir rate.

Now K' and K" are, in fact, constants for a given system operating under a fixed set of conditions because b_i and m_{oi} are constants for any given system operating at specific temperatures for hot upflow and cold downflow, ϕ_B is a fixed ratio of the bottom product rate to the reservoir rate, π/ω is usually the minimum half cycle time required to give a separation, ε is the void fraction characteristic of the packing, and a_t is usually fixed.

Heat requirements during the hot upflow half cycle. The heat requirements may be divided into two sections as shown in the following equation derived in Appendix III (III-17).

$$q_1 = (w_t c_t + w_s c_s + w_f c_f) Nh (T_1 - T_2) n$$

$$+ Q(1-\phi_B)(\rho_f c_f)(\pi/\omega)(T_1 - T_2) n \quad (76)$$

The first half of the equation represents the heat required to raise the temperature of the tubes and tube contents from T_2 to T_1. The second half represents the heat required to raise the temperature of the fluid pumped through the column from T_2 to T_1. In this equation w_t, w_s, and w_f represent the mass per unit length of the tube wall, the solid adsorbent, and the fluid respectively, c_t, c_s, and c_f represent the respective heat capacities. T_1 and T_2 are the hot upflow and cold downflow temperatures, ρ_f the average fluid density, and n is the number of cycles or half-cycles for the operation under consideration.

In most cases, the duty for heating the tube and contents is roughly twice that for heating the fluid pumped through the column. Moreover, since the duration is only approximately 2 minutes as compared to roughly 20-30 minutes for a typical half cycle time, the <u>rate</u> for heating the tubes and contents could easily be 20 times or more that of the average rate for the entire half cycle. To save the cost of a large heat generating plant (steam boiler), a hot water reservoir could be used to store the heat and the reservoir would be reheated during the cold half cycle.

Cooling requirements during the cold downflow half cycle.

$$q_2 = (w_t c_t + w_s c_s + w_f c_f) Nh \ (T_1 - T_2)_n$$

$$+ Q(1+\phi_B)(\rho_f c_f)(\pi/\omega)(T_{2H} - T_2)n \qquad (77)$$

This equation (III-18) is the same as that for the heating half cycle except for the $(1+\phi_B)$ term (which accounts for the additional column flow needed to supply the bottom product stream on cold downflow) and for the T_{2H} term which accounts for the heat effects of the feed and product streams on the fluid reentering the column. The equation for calculating T_{2H} is derived in Appendix III as Equation (III-14) from heat balances around the top of the column during hot upflow and cold downflow.

For design purposes, it is permissible to substitute T_1 for T_{2H} because T_{2H} is involved only in the portion of the cooling duty pertaining to the fluid flowing down the column during the cold downflow half cycle which is very small compared to the duty during the switchover period from the hot to the cold half-cycles. Furthermore, the substitution of T_1 makes the design more conservative because T_1 is generally higher than T_{2H} due to the cooling effect of the feed stream. For design purposes, Equation III-18 may be modified to the simplified form

$$q_2 = \left[(w_t c_t + w_s c_s + w_f c_f) Nh + Q(1+\phi_B)(\rho_f c_f)(\pi/\omega)\right] (T_1 - T_2) n \quad (78)$$

Finally, in the design, it would be preferable to provide a large cold water reservoir and a relatively small compressor rather than one large compressor for the high initial duty during the switchover period. The system could be regenerated during the hot half-cycle. Most refrigeration systems are designed this way wherever the plant layout provides sufficient space for the reservoir.

Pressure drop of the shellside heat transfer fluid. As derived in Appendix III, the shellside pressure drop is (III-33)

$$\Delta p = \frac{1.525 \times 10^{-4} w^2 (2h-1)}{(0.005732N^{.9474} - 0.001736N)^2} + \frac{2.756 \times 10^{-4} w^{1.8} (0.07117N^{.4737} - 0.0417)(2h)}{(0.03293N^{.4737} - 0.01563)^{1.8}} \quad (79)$$

where N is the number of tubes, w is the water rate in pounds per second, h is the tube length in feed, and Δp is the pressure drop in psi. The equation shown above was derived for water as the shellside fluid for heating or cooling. For other heat transfer media, the pressure

drop can be calculated from Equations (III-23 and III-28) in Appendix III.

Also, Equation (III-33) is for turbulent flow which is correct for most designs using water. For laminar flow, Equations (III-23 and III-29) may be used for fluids in general and Equation (III-34) for water.

The derivations in Appendix III include the complete sets of equations required with no limiting assumptions. The assumptions incorporated in Equation (III-33) are for a 6-inch baffle spacing, 25% baffle cutout, and a 1.375D triangular pitch with D equal to 1/2 inch outside diameter tubes.

The 1/2 inch 18 BWG tubes were chosen because they have approximately the same inside diameter as the packed columns used in research where switchover times were 2 minutes for aqueous systems (Sweed and Gregory, 1971), and 45 seconds for hydrocarbon systems (Sweed, 1969). Since typical half-cycle times are 20-40 minutes, the 0.75-2 minute switchover times are short enough to be considered "instanteous". Should shorter half-cycle times be necessary, smaller diameter tubes can be used and the pressure drop equations easily modified. Conversely, long half cycle times could utilize larger tubes and still operate according to the equilibrium theory, but to do so would extend the

operating time and lower the effective capacity of the equipment.

Pressure drop through the tubes. The basic equation chosen for pressure drop through the packed beds is the Blake-Kozeny equation for laminar flow. In Appendix III, the basic dimensionless form is rearranged to show the relationship between pressure drop and volumetric flow rate as usually expressed for parametric pumping. The equation is also expressed in terms of average column velocity and column length which is the most useful for the design example which follows in the next section. This is (III-20)

$$\Delta p = \frac{150(1-\varepsilon)^2 \mu h v}{D_p^2 \, g_c \varepsilon^3} \qquad (80)$$

where ε, h, v, have been previously defined, D_p is the average particle diameter, μ is the fluid viscosity, and g_c is the gravitational conversion factor.

Equation (III-20) is useful for the design of the parapump column assembly itself and is used for this purpose in the design example in the next section of this chapter. It should be pointed out that this pressure drop is only one of the considerations in the design of the feed and reservoir pumps that supply the necessary

pressure. The design of these pumps is discussed in some detail in Appendix III and also in the description of the parapump equipment later in this chapter.

Process Design Procedure

The n-heptane-toluene-silica gel system was used as an example because this system is a natural extension of previous work. As explained earlier, a binary system is adequate to illustrate the design procedure because the design "sees" only the two key components, regardless of the actual number of components present. The example will be developed in such a way as to show the relationship between capacity (determined as the reservoir rate Q) and the basic parameters of heat transfer and pressure drop. These relationships will be shown in the form of graphs from which the optimum process design can be selected.

The following general assumptions will be made:

1. The insulation is adequate to insure adiabatic operation and restrict the heating and cooling requirements to the process fluid, the adsorbent, and the tube walls.

2. A control system will be used which places the feed and one product stream on flow control. The product and the reservoir streams will be under a back pressure

imposed on the effluent product stream. The entire system will thus be under a constant pressure during both cold downflow and hot upflow half cycles. If liquid thermal expansion is neglected, the minimum pressure imposed will be that calculated for the cold downflow half-cycle.

3. The heat transfer fluid will be water which will be indirectly heated by steam and indirectly cooled by brine or chilled water refrigeration.

4. The heat transfer fluid (water) densities and specific heats, as indicated in Appendix IV, may be assumed equal to one. The viscosity varies from 0.5 to 1.5 over the operating temperature range but, since the viscosity is raised to the 0.2 power, the range is effectively narrowed to 1.08 to 0.88 and the assumption of a uniform value of 1 would be adequate for the present design.

5. A temperature rise of 15.2^{o} F. in the water temperature will be used for design. Fixing this temperature rise automatically ties the heat transfer fluid (water) rate and the water pressure drop to the process reservoir rate Q through a heat balance. Fixing the Δt for the heat transfer fluid is therefore necessary if all the basic design parameters are to be related to the process reservoir rate (capacity parameter).

6. A switchover time of 2 minutes will be assumed for the toluene-heptane system. Sweed (1969) reported an experimental time of 45 seconds and a calculated time of 2 minutes. The two minute time is sufficiently conservative and accurate for engineering purposes.

7. The hot upflow and cold downflow temperatures will be 70° and 5° centigrade respectively.

Column length versus superficial velocity and capacity. In the equation

$$h \geq K'v \tag{72}$$

where

$$K' = \frac{(1+\phi_B)(\pi/\omega)}{(1+m_o)(1+b)(\varepsilon)} \tag{73}$$

and from Chen et al (1972), the values are $\varepsilon = 0.38$, $\phi_B=0.15$, $\pi/\omega = 1200$ seconds or 0.333 hours, $b = 0.22$, $L_2= 0.44$ meters, $h=0.90$ meters, and $m_o= 1.88$. Then $K' = 0.2868$ and (III-9A)

$$h \geq 0.2868v \tag{81}$$

Also, since (from Appendix III, Equation 11)

$$v = (Q/(a_t/N)$$

and since $a_t = 8.81 \times 10^{-4}$ feet, $v = 1135\ (Q/N)$ and

$$h \geq 326\ Q/N \qquad (82)$$

Equation (III-11A) is plotted in the graph, Figure (21) as Q vs. h with lines of constant values of N corresponding to the number of tubes available in various commercial shell sizes.

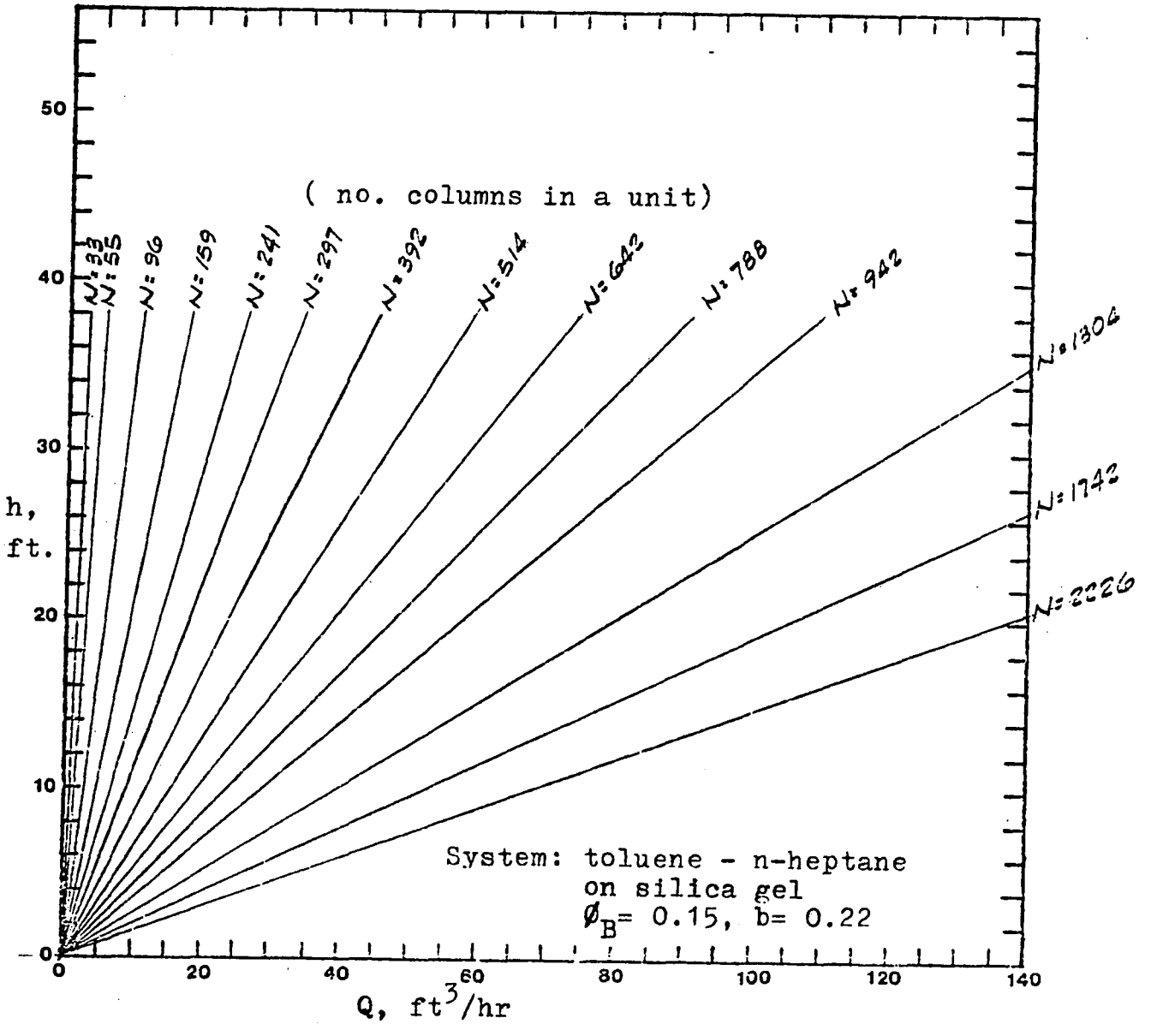

FIGURE (21)

EQUIPMENT SIZE vs RESERVOIR RATE

Column pressure drop. The pressure drop equation is

$$\Delta p = \frac{150(1-\varepsilon)^2 \mu h v}{D_p^2 \varepsilon^3 g_c} \qquad (80)$$

where $\varepsilon = 0.38$, $D_p = 13.2 \times 10^{-4}$ feet, $g_c = 4.17 \times 10^8 lb_m/hr^2/ft$ (ft^2/lb_f), and the viscosity is 0.53 centipoise for a solution of 20% toluene in n-heptane at 5°C and 0.28 cp for the same solution at 70°C. To convert the viscosity to $lb_m/hr/ft$, the required conversion factor is 2.42. The simplified equation is, for cold downflow,

$$\Delta p_2 = 1.855\ hv_2 \qquad (83)$$

If the control system described previously is used, only the cold downflow pressure drop need be considered. The hot upflow pressure drop would be 0.28/0.53 times that of the cold downflow, provided the fluid density is assumed constant and the correct velocity is used.

The pressure drop may also be described in terms of the reservoir flow rate Q. For cold downflow,

$$v_2 = (1+\phi_B)\ v = 1.15v \qquad (84)$$

Since $h = 0.2868v$ (81)

$$v = 1135\ Q/N \qquad (85)$$

then $\Delta p_2 = 2.133\ hv = 0.6118\ v^2 = 7.88 \times 10^5 (Q/N)^2$ (86)

Similarly, for hot upflow

$$v_1 = (1-\phi_B)v = 0.85v \qquad (87)$$

then

$$\Delta p_1 = 1.855(.28/.53)hv_1 = .833hv = .2389v^2 = 3.078x10^5(Q/N)^2 \qquad (88)$$

The pressure drop to be considered for design is that for cold downflow and this pressure would have to be developed by the top reservoir pump as a miminum. This would also be the pressure at the point where the feed enters the column and would have to be developed by the feed pump as a minimum. This subject is discussed at greater length in the next section in this chapter.

Equation (86) is plotted in Figure (22) as the reservoir rate Q vs. the pressure drop in psi with lines of constant values of N corresponding to the number of tubes available in various commercial shell sizes.

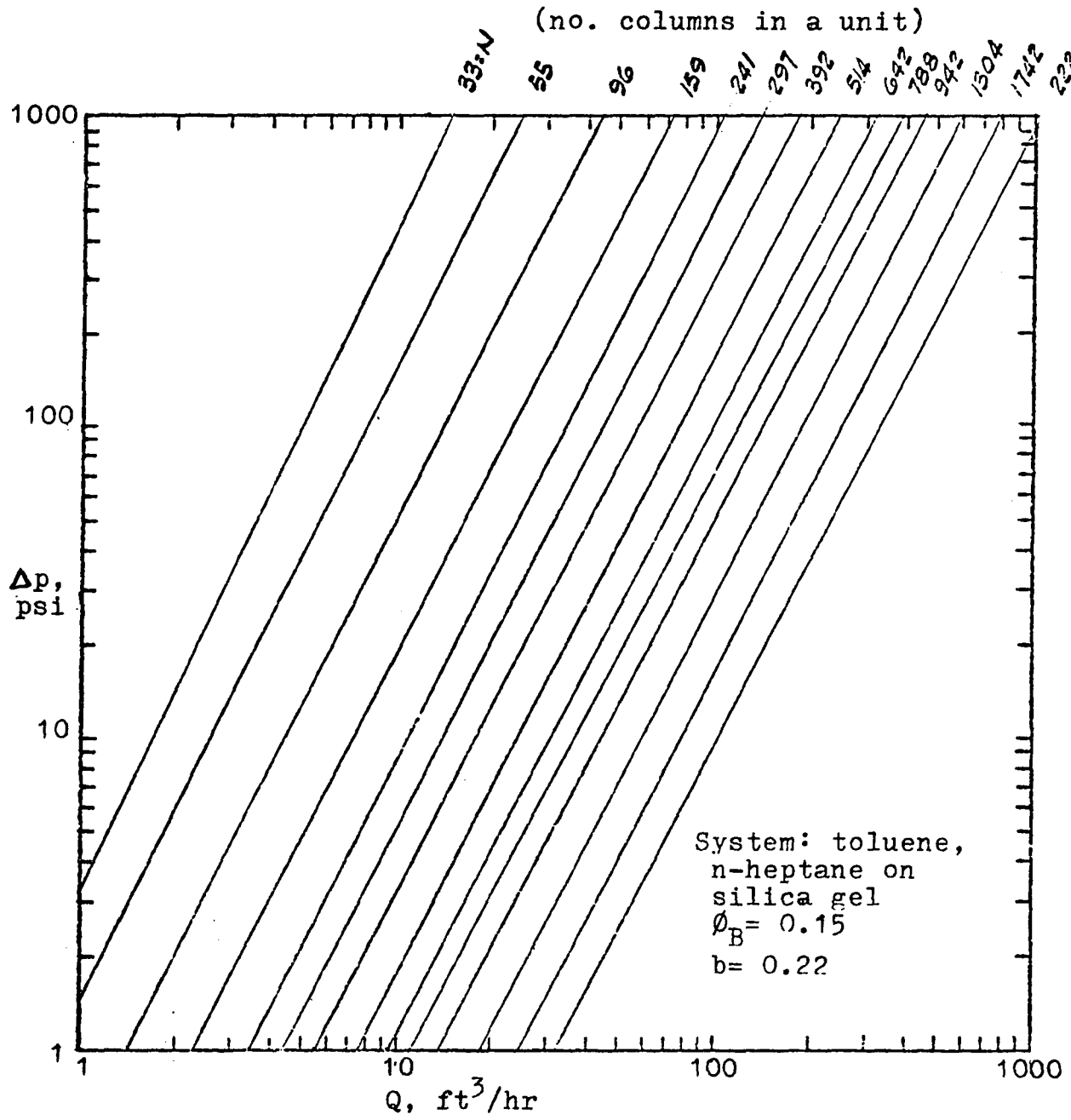

FIGURE (22)

COLUMN PRESSURE DROP vs RESERVOIR RATE

Heat transfer during hot upflow. The basic heat transfer equation given previously is

$$q_1 = \left[(w_t c_t + w_s c_s + w_f c_f) Nh + Q(1-\phi_B)(\rho_f c_f)(\pi/w)\right](T_1 - T_2)n \quad (76)$$

where, from the data in Appendix IV, the quantity $(w_t c_t + w_s c_s + w_f c_f)$ is equal to 0.0874 BTU/^{o}K/ft of tube length, ϕ_B=0.15, ρ_f=0.72x62.3=44.9 lb/ft^3, c_f =0.53 BTU/lb/^{o}F = 0.972 BTU/lb/^{o}K, π/ω =0.333 hr, T_1 = 70^{o}C=343^{o}K, T_2= 5^{o}C = 278 ^{o}K, and n = number of cycles under consideration = 1. Now, substituting these quantities in Equation (76),

$$q_1 = 5.681\ Nh + 803Q$$

or since $Q = vNa_t = 8.81 \times 10^{-4}\ vN$ where v is the average tube velocity,

$$q_1 = 5.681\ Nh + 0.707\ vN$$

or

$$q_1/N = 5.681\ h + 0.707\ v \quad (89)$$

Another way of expressing Equation (89) may be developed by combining it with Equations (82 and 85) to get the expression for q_1 as a minimum

$$q_1/N = 5.681 \times 326\ (Q/N) + 0.707 \times 1135\ (Q/N)$$

or

$$q_1\ (\text{minimum}) = 2651\ Q \quad (90)$$

Now it should be pointed out that, according to Equation (90), the percent of heat transferred during the switchover time is 69.8% of the total and that this heat is transferred in a maximum of two minutes. The rate of heat transfer during the switchover period is therefore

$$\Delta H_1 = 1852Q/(2/60) = 55{,}560\ Q \text{ BTU/hr}$$

This rate is roughly seven times the overall heat transfer rate and this load could be provided by either instantaneous steam heating or by the temperature drop of a large reservoir. In the latter case, the regenerative heat rate would be 7935 BTU/hr, the regeneration occurring during the cold downflow half cycle.

Heat transfer during cold downflow. The basic heat transfer given previously is

$$q_2 = (w_t c_t + w_s c_s + w_f c_f)(Nh)(T_1 - T_2)n + Q(1+\phi_B)(\rho_f c_f)(\pi/\omega)(T_{2H} - T_2)n \qquad (77)$$

As previously explained, T_{2H} may be replaced by T_1 for purposes of design (Equation 78). Substituting the quantities previously given,

$$q_2 = 5.681\ Nh + 1086\ Q$$

The remaining equations are developed in a manner identical to those for hot upflow and they are

$$q_2 = 5.681\ Nh + 0.957vN$$

or

$$q_2/N = 5.681\ h + 0.957v \qquad (91)$$

As was the case for hot upflow, Equation (91) may be combined with Equations (82 and 85) to give the expression for q_2 as a minimum

$$q_2/N = 5.681x326\ (Q/N) + 0.957x1135\ (Q/N)$$

or

$$q_2\ (\text{minimum}) = 2936\ Q \qquad (92)$$

Similar to the case for hot upflow, the percent of heat transferred during the switchover period is 62.9% of the total. Now the switchover rate would still be 55,560 BTU/hr but the regenerative rate would now be 8928 Q due to the higher total duty.

The Equation (92) for cold downflow and also Equation (90) for hot upflow, along with the switchover and regenerative rates are given in Figure (23).

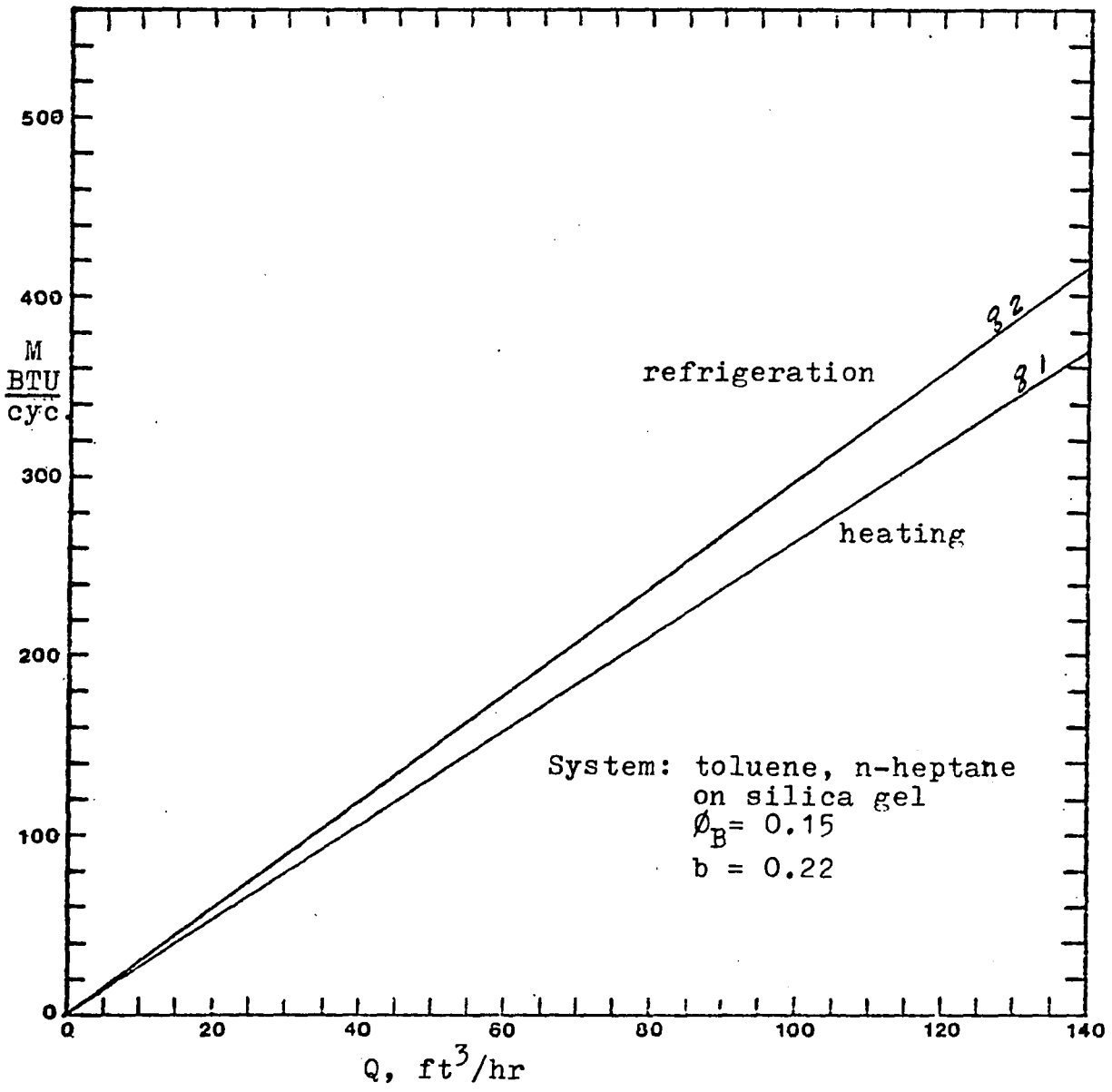

FIGURE (23)

HEAT TRANSFER DUTIES vs RESERVOIR RATE

Heat transfer fluid (water) rate vs. column length and capacity. By definition

$$wc\Delta T + q_t/\tau \qquad (93)$$

where w is the water rate in lb/sec, c is the heat capacity of water equal to 1 BTU/lb/^{o}F, ΔT is the water temperature rise fixed at 15.2^{o}F, q_t is the duty during the switchover period in BTU equal to 5.681 Nh and τ is the time of the switchover period fixed at 120 seconds.

Now rearranging Equation (93) and substituting the quantities,

$$w/N = 3.115 \times 10^{-3} h \qquad (94)$$

The use of q_t was limited to the switchover period because the heat transfer rate is highest during this period.

Also, since $h \geq 326\ (Q/N)$, (82)

$$w(\text{minimum}) = 1.014\ Q \qquad (95)$$

Equation (94) is shown in Figure (24)

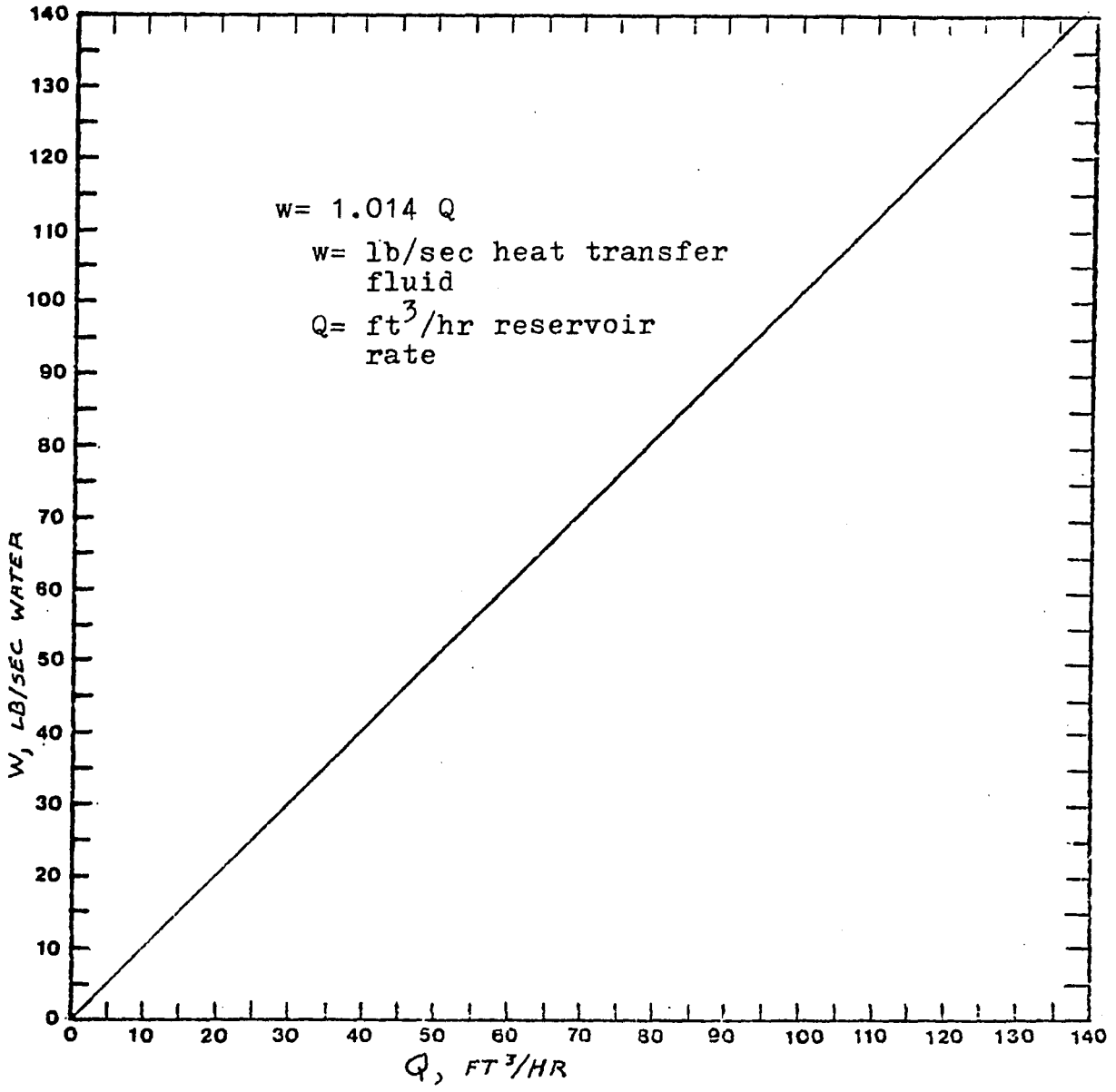

FIGURE (24)

Heat Transfer Fluid Rate vs Reservoir Rate

Shellside (heat transfer fluid) pressure drop. The basic equation previously given is

$$\Delta p = \frac{1.525\times10^{-4} w^2 (2h-1)}{(0.005732N^{.9474}-0.001736N)^2} + \frac{2.756\times10^{-4} w^{1.8}}{(0.03293N^{.4737}-0.01563)^{1.8}} \frac{(0.07117N^{.4737}-0.0417)(2h)}{} \quad (79)$$

In this case it is not possible to get a simple relationship with N, but the equation can be simplified.

$$\Delta p = F_{N1}\, w^2 (2h-1) + F_{N2}\, w^{1.8} (2h) \quad (96)$$

Now since

$$w = 1.014Q \quad (95)$$

and

$$h \geq 326\ Q/N \quad (82)$$

then

$$\Delta p = F_{N1}(670\ Q^3/N - 1.028Q^2) + F_{N2}(670\ Q^{1.8}/N) \quad (97)$$

where F_{N1} and F_{N2} may be obtained from Table (3).

TABLE 3

SHELLSIDE PRESSURE DROP FACTORS

Shell Diam., inches	N (no. tubes)	F_{N1} x 10^6	F_{N2} x 10^4
5	33	15220	25.60
6	55	5967	20.85
8	96	2153	16.72
10	159	856	13.72
12	241	400.8	11.67
14	297	273.9	10.76
16	392	165.2	9.663
18	514	100.9	8.703
20	642	67.36	7.988
22	788	46.43	7.383
24	942	33.58	6.893
28	1304	18.62	6.085
32	1742	11.03	5.446
36	2226	7.077	4.959

An alternative to Equation (96) is a similar equation which includes the term for baffle spacing. This may be useful for very large units where the six inch spacing would lead to unacceptably high pressure drops.

$$\Delta p = F_{N1} w^2 (h/B_s - 1) + F_{N2} (0.5/B_s)^{2.8} (2h) w^{1.8} \tag{98}$$

An examination of the derivations in Appendix III will show that F_{N2} is related to the resistance to the flow across the tube banks and that F_{N1} is related to the resistance through the baffle openings. Generally, as the number of tubes increases, the resistance due to flow through baffle openings remains relatively constant while that across the tube banks increases steadily and, with large numbers of tubes, accounts for practically all the resistance. The significance of this is that for large numbers of tubes, say 800 or more, the effect of dropping the first term of the equation would be small.

The shellside pressure drop with varying tube lengths and numbers of tubes has been calculated, based on water rates corresponding to a 15.2 ^{o}F temperature change. The results are presented in Table (4).

Equation (97) is plotted in Figure (25) as the reservoir rate Q vs. the pressure drop in psi with lines of constant N.

TABLE 4

SHELLSIDE PRESSURE DROPS CORRESPONDING TO A 15.2°F TEMPERATURE CHANGE

h	2	4	6	8	10	12	14	16	18	20
N										
33	.003	.022	.077	.183	.359	.622	.989	1.48	2.10	2.88
55	.003	.028	.096	.227	.443	.763	1.21	1.80	2.56	3.22
96	.005	.040	.134	.314	.606	1.04	1.63	2.42	3.43	4.67
159	.008	.061	.200	.463	.888	1.51	2.36	3.49	4.91	6.68
241	.012	.093	.300	.687	1.31	2.21	3.45	5.07	7.12	9.64
297	.016	.117	.375	.857	1.63	2.74	4.27	6.26	8.78	11.9
392	.022	.162	.516	1.17	2.22	3.73	5.78	8.47	11.8	16.0
514	.031	.226	.716	1.62	3.05	5.13	7.94	11.6	16.2	21.9
642	.042	.300	.946	2.14	4.02	6.74	10.4	15.2	21.2	28.6
788	.055	.392	1.23	2.78	5.22	8.74	13.5	19.8	27.5	37.0
942	.070	.497	1.56	3.51	6.59	11.0	17.0	24.8	34.6	46.6
1304	.109	.770	2.41	5.42	10.2	17.0	26.2	38.1	53.1	71.4
1742	.163	1.15	3.58	8.04	15.0	25.1	38.7	56.4	78.5	106
2226	.230	1.61	5.02	11.3	21.1	35.2	54.2	78.8	110	148

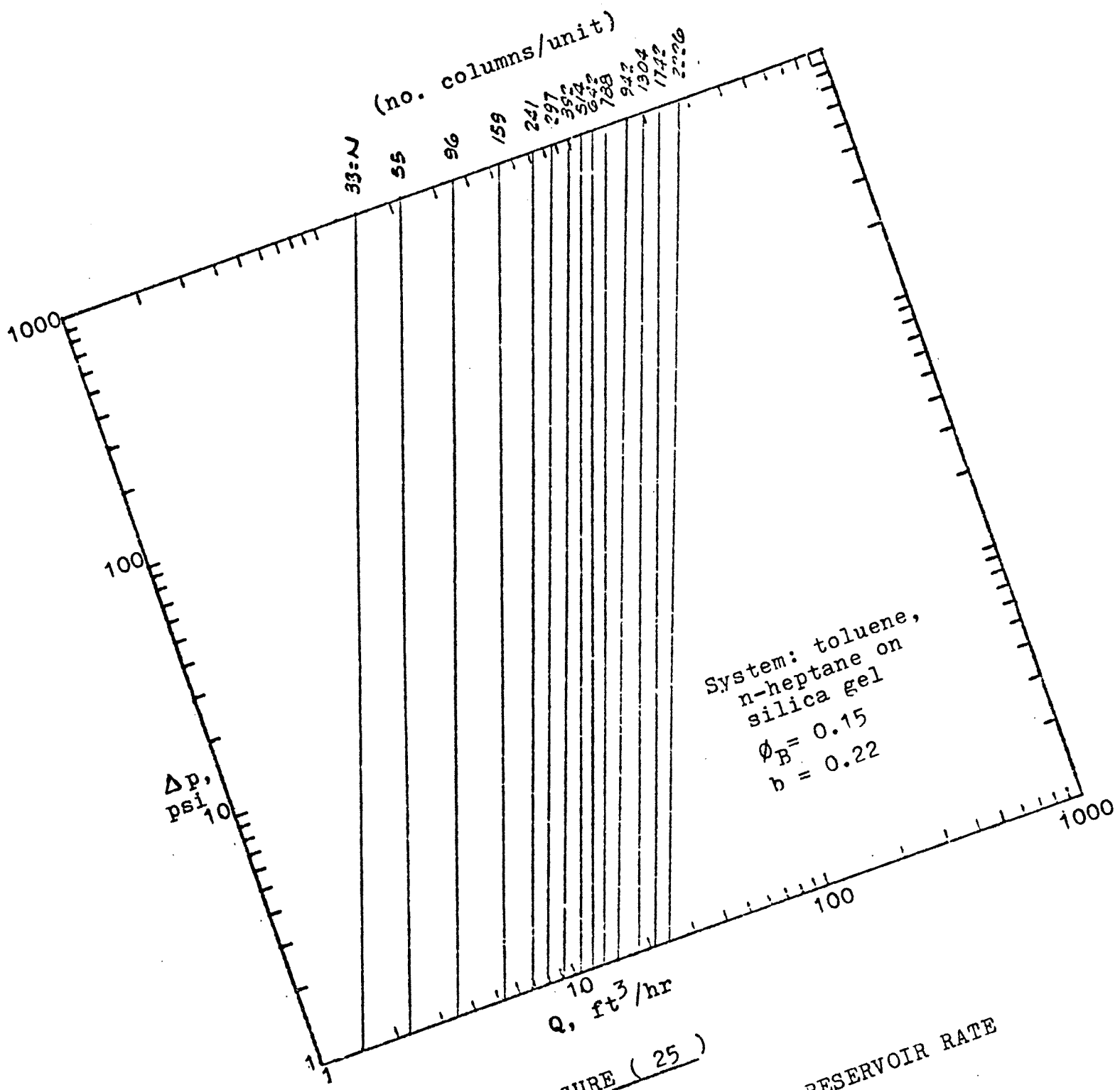

FIGURE (25)

SHELLSIDE PRESSURE DROP vs RESERVOIR RATE

Process design from the tables and graphs. The graphs and tables were developed for the toluene-heptane-silica gel system. Similar charts and graphs could be developed for any other system of interest and could be used to determine the optimum design based on any two parameters of interest.

As can be seen in the equations and graphs, the design parameters are the number of tubes (N), the reservoir rate (Q), the tube length (h), the velocity (v), the column pressure drop, the shellside pressure drop, the heating and cooling capability (q_1,q_2), or the available heat transfer media (water) flow capacity (w). With the selection of any two key parameters, it is possible to determine the remaining parameters and complete the process design. It should be emphasized that this design would be optimum and that safety factors would have to be incorporated into any actual design.

A few typical designs are shown in Table (5). Included in the table is a typical laboratory operation for purposes of comparison. Such a comparison will make it obvious that a practical scale-up design incorporates the use of higher column and shellside pressures as well as larger equipment.

TABLE 5

TYPICAL PARAMETRIC PUMP PROCESS DESIGNS

	Lab Column	Single Tube	Pilot Plant	Plant
Rates, lb./hr. (ρ_f = 44.9 lb./ft.^{3})				
Feed, $Q(\emptyset_T + \emptyset_B)\rho_f$	0.0383	0.767	46.7	1796
Bot. Prod., $Q\emptyset_B\rho_f$	0.0143	0.288	17.5	674
Top Prod., $Q\emptyset_T\rho_f$	0.0240	0.479	29.2	1122
Reservoir, $Q\rho_f$	0.0956	1.917	116.7	4490
Solute conc., y/y_o				
Bot. Prod.	0	0	0	0
Top Prod.	1.6	1.6	1.6	1.6
Cycle time, min.				
Switchover	2	2	2	2
Half cycle, $\P/\omega$	20	20	20	20
Energies, BTU/lb. bottom product				
Heating				
Switchover	412	412	412	412
Half cycle	590	590	590	590
Refrigeration				
Switchover	412	412	412	412
Half cycle	662	662	662	662
Pumping (Total)	0.609	0.609	0.609	0.609
Equipment size				
No. tubes, N	1	1	55	2226
Length, h, ft.	3.28	13.9	15.4	14.8
Heat transfer fluid				
Rate, lb./sec.	0.00216	0.0433	2.64	101.4
Pressure drop, psi				
Column	0.025	10	10	10
Shell	neg'l	neg'l	1.6	60

Energy versus Equipment Size and Productivity

Energy equations relating heating, cooling, and pumping requirements to process parameters were developed in Appendix III from basic equations and from the process design concepts presented in the first two parts of this chapter. These equations relate energy (on a common BTU basis) to the reservoir displacement ($Q\pi/\omega$) for equipment size, to the bottom product/reservoir ratio (ϕ_B) for productivity, to cycle time (π/ω), to reservoir displacement rate (Q), and to N, the number of tubes or columns in a parapump assembly. The length of these tubes (h) is indirectly included in the equations by a separate equation relating it to the column flowrate or tube velocity.

The key parameters are size ($Q\pi/\omega$) and productivity (ϕ_B). The remaining parameters are usually fixed or directly tied to one of these through mathematical expressions. Equipment size ($Q\pi/\omega$) is related to energy on a BTU/cycle basis through Equations (III-45,50,52,57, 62,66, and 70). Productivity (ϕ_B) is related to energy on a BTU/lb of bottom product basis through Equations III-47,51,53,58,63,67, and 71). Both sets of equations, in the case of pumping, were developed via equations for pressure drop and horsepower and these equations are also presented in Appendix III.

All of the equations in Appendix III are presented in full algebraic form and are thus applicable to any system. Since only the toluene-heptane-silica gel system will be discussed in this section, the Appendix III equations will immediately be simplified by assigning the following variables pertinent to the system and to water as the heat transfer fluid.

a_t, tube crossflow area, ft^2/tube	0.000881
b, dimensionless equilibrium parameter	0.22
c_f, process fluid heat capacity, BTU/lb/^oK	0.972
c_{HTF}, heat transfer fluid heat capacity	
BTU/lb/^oK	1.8
BTU/lb/^oR	1.0
D_i, i.d. of the pipelines external to the column, ft	0.0833
D, outside diameter of each column, ft	0.0417
D_p, adsorbent particle diameter, ft	13.2×10^{-4}
g_c, gravitational conversion factor, lb_mxft to lb_fxhr^2	4.17×10^8
m_o, equilibrium constant, dimensionless	1.88
T_1, hot upflow temperature, ^oK	343
T_2, cold downflow temperature, ^oK	278
$(w_t c_t + w_s c_s + w_f c_f)$, heat capacity of column wall, the solid adsorbent, and the fluid calculated from Appendix IV data, BTU/^oK/ft of column height (h)	0.0874

ε, packed bed voidage, dimensionless	0.38
ΔT_w, temperature rise of heat transfer fluid, ^oR	15.2
τ, switchover time, seconds	120
ρ_f, process fluid density, lb/ft^3	44.9
ρ_{HTF}, heat transfer fluid density, lb/ft^3	62.3
μ_1, process fluid viscosity at T_1, $lb_m/hr/ft$	0.678
μ_2, process fluid viscosity at T_2, $lb_m/hr/ft$	1.283
μ_{BP}, bottom product viscosity	$= \mu_2$
μ_{TP}, top product viscosity	$= \mu_1$
μ_F, feed viscosity	$= \mu_1$

From the above data, the value of K_h (Eq. III-48a) was found to be 850, and the value of K_w (Eq. III-54a), 2.65. Most data was from Appendix IV. Values of b, m_o, T_1, T_2, and ε, were given by Chen et al (1972).

The energy equations, simplified by use of the data presented above, are listed below. After each equation is the number of the original equation in Appendix III (to serve as a reference), and the new number of the simplified equation.

Heating duty (steam) (III-45, 47)

$$q_1 = Q\pi/\omega \quad \left[4830(1+\phi_B) + 2837(1-\phi_B)\right] \quad \text{BTU/cycle} \qquad (99)$$

$$\frac{q_i}{P_B(2\pi/\omega)} = 53.78\ \frac{1+\phi_B}{\phi_B} + 31.59\ \frac{1-\phi_B}{\phi_B} \quad \text{BTU/lb BP} \qquad (100)$$

Cooling duty (refrigeration) (III-52, 53)

$$q_2 = 7667\ (Q\pi/\omega)(1+\phi_B) \quad \text{BTU/cycle} \qquad (101)$$

$$\frac{q_2}{P_B(2\pi/\omega)} = 85.4\ \frac{1+\phi_B}{\phi_B} \quad \text{BTU/lb BP} \qquad (102)$$

Heat content of the shellside fluid (III-50, 51)

$$q_s = Q\pi/\omega)\ (1+\phi_B)(27{,}900N^{-0.0526}-8455)\ \text{BTU/cycle} \qquad (103)$$

$$\frac{q_s}{P_B(2\pi/\omega)} = \frac{1+\phi_B}{\phi_B}\ (311N^{-0.0526}-94.2) \quad \text{BTU/lb BP} \qquad (104)$$

Heat transfer fluid pump (III-57, 58, 54b)

$$q_{HTF} = 56.6(Q\pi/\omega)(\pi/\omega)(1+\phi_B)(\Delta p_{HTF}) \quad \text{BTU/cycle} \qquad (105)$$

$$\frac{q_{HTF}}{P_B(2\pi/\omega)} = 0.63\ \frac{1+\phi_B}{\phi_B}\ (\pi/\omega)(\Delta p_{HTF}) \quad \text{BTU/lb BP} \qquad (106)$$

$$\Delta p_{HTF} = Q\frac{\pi}{\omega}^{2}(1+\phi_B)^2\ F_{N1}\left[\frac{11938}{N}\ Q\frac{\pi}{\omega}(1+\phi_B)-7\right] + \left[Q\frac{\pi}{\omega}(1+\phi_B)\right]^{2.8}$$

$$\left(\frac{9824F_{N2}}{N}\right) \qquad (107)$$

Bottom reservoir pump (III-62, 63)

$$q_{BRP} = 1216\ (1-\phi_B)^2(1+\phi_B)(Q/N)^2(Q\pi/\omega)(\pi/\omega)\ \text{BTU/cycle} \quad (108)$$

$$\frac{q_{BRP}}{P_B(2\pi/\omega)} = 13.54\ (1-\phi_B)^2\ \frac{1+\phi_B}{\phi_B}\ (Q/N)^2(\pi/\omega)\ \text{BTU/lb BP} \quad (109)$$

Top reservoir pump (III-66, 67)

$$q_{TRP} = 2302\ (1+\phi_B)^3(Q/N)^2(Q\pi/\omega)(\pi/\omega)\ \text{BTU/cycle} \quad (110)$$

$$\frac{q_{TRP}}{P_B(2\pi/\omega)} = 25.63\ (1+\phi_B)^2\ \frac{1+\phi_B}{\phi_B}\ (Q/N)^2(\pi/\omega)\ \text{BTU/lb BP} \quad (111)$$

Feed pump (III-70, 71)

$$q_{FP} = 3.56\times10^{-4}(Q)(Q\pi/\omega)\left[(\phi_T+\phi_B)^2+\phi_T^2+1.89\phi_B^2\right] + 4594\ (1+\phi_B)^3(Q/N)^2(Q\pi/\omega)(\pi/\omega)\ \text{BTU/cycle} \quad (112)$$

$$\frac{q_{FP}}{P_B(2\pi/\omega)} = 3.96\times10^{-6}(Q/\phi_B)\left[(\phi_T+\phi_B)^2+\phi_T^2+1.89_B^2\right] + 51.2\ (1+\phi_B)^2\ \frac{1+\phi_B}{\phi_B}\ (Q/N)^2(\pi/\omega)\ \text{BTU/lb BP} \quad (113)$$

Relative energy requirements. It is useful to know the relative requirements for steam, refrigeration pumping, and the residual heat content of the shellside fluid. The various utilities can then be ranked as to their energy requirements.

The most convenient method for presenting the relative energy requirements is to use the equations for energy in BTU/lb BP or cycle and reference them to the equation for refrigeration. The equations listed below are therefore in terms of BTU for the utility/BTU for refrigeration:

$$q_1/q_2 = 0.630 + 0.37(1-\phi_B)/(1+\phi_B) \qquad (114)$$

$$q_s/q_2 = 3.64\ N^{-0.0526} - 1.1 \qquad (115)$$

$$q_{HTF}/q_2 = 0.00738\ (\pi/\omega)(\Delta p_{HTF}) \qquad (116)$$

$$q_{BRP}/q_2 = 0.159\ (1-\phi_B)^2 (Q/N)^2 (\pi/\omega) \qquad (117)$$

$$q_{TRP}/q_2 = 0.300\ (1+\phi_B)^2 (Q/N)^2 (\pi/\omega) \qquad (118)$$

$$q_{FP}/q_2 = 4.64 \times 10^{-8}\ Q/(1+\phi_B)\left[(\phi_T+\phi_B)^2+\phi_T^2 + 1.89\phi_B^2\right] + 0.600\ (1+\phi_B)^2 (Q/N)^2 (\pi/\omega) \qquad (119)$$

Now if values are assigned to the variables in Equations (114) to (119), numerical ratios can be given. The values given for the process design example earlier in the chapter were 0.15 for ϕ_B, 0.25 for ϕ_T, and 0.333 hr for π/ω. For the 55 tube unit, values of Q and Δp_{HTF} of 2.6 ft^3/hr and 1.6 psi were given in Table (5) for the process design example. Eq. (107) also gave 1.6 psi. Substitution of these values gives the following numerical ratings:

steam	0.902
heat content of shellside fluid	1.85
heat transfer fluid pump	3.94×10^{-3}
bottom reservoir pump	8.57×10^{-5}
top reservoir pump	2.96×10^{-4}
feed pump	
line resistance	2.78×10^{-8}
column resistance	5.92×10^{-4}

Certain conclusions can be drawn from the ratings. The line resistances for the feed pump can be neglected (for the line sizes and flow rates chosen). The shellside heat transfer fluid must be dumped to the appropriate reservoir at the end of each half cycle (an integral part of the design) or the energy requirements could be roughly tripled. Finally, in overall energy considerations, the pumps consume less than 1 percent of the total.

Energies versus reservoir displacement (equip. size). The equations relating energies to reservoir displacement ($Q\pi/\omega$) (Eq. 99,101,103,105,108,110,112) were used with values of 0.15 for ϕ_B and 0.333 hr for π/ω assigned as in the case of the process design example presented earlier. In the case of the pumping energies, it was necessary to assign a pressure drop of 10 psi for the packed columns during cold downflow. All other pressure drops for pumps would have a lower pressure drop with the possible exception of the heat transfer pump (up to 60 psi for the highest flow) and this can easily be lowered by a small design change (see Eq. 98). Assigning this 10 psi pressure drop allowed the values of Q and the corresponding values of N to be selected from Figure (25). With these values it was possible to include the pumping energies along with those for heating and refrigeration in Fig. (26).

Figures (26) and (27) give the energies and the bottom product concentrations (purities) for any given bottom product volume ($P_B 2\pi/\omega$ ft^3/cycle) and equipment size ($Q\pi/\omega$ ft^3 of reservoir displacement). It is possible to predict the equipment size, the amount of steam, refrigeration, and pumping energies that will be needed to produce a given volume of bottom product at a specified purity.

For example, if a bottom rate of 3 ft^3/cycle and a product purity of $\langle y_{BP} \rangle_\infty / y_o$ of 0.55 is required, then a 10 ft^3 reservoir displacement is needed. The minimum energy requirements per cycle are 88,000 BTU for refrigeration, 80,000 BTU for heating, 3000 BTU equivalents for the heat transfer fluid pump, and 80 BTU equivalents for the feed and reservoir pumps. Now if the product purity must be increased to the maximum ($\langle y_{BP} \rangle_\infty / y_o = 0$), the equipment size must be increased to 13.5 ft^3, and the energies to 120,000 BTU for refrigeration, 110,000 for heating, 6,000 BTU equivalents for the HTF pump and 110 BTU equivalents for the other pumps. Of course, the same purity could be achieved with the original equipment and energy requirements by reducing the product draw-off to 2.2 ft^3/cycle.

Thus the equipment and energy requirements can be predicted by specifying the product rate and purity. Conversely, the performance of existing equipment for a new application can also be predicted. It should be emphasized that the equipment and energy requirements need not be projected beyond the zero $\langle y_{BP} \rangle_\infty / y_o$ level unless it is desired to overspecify the system.

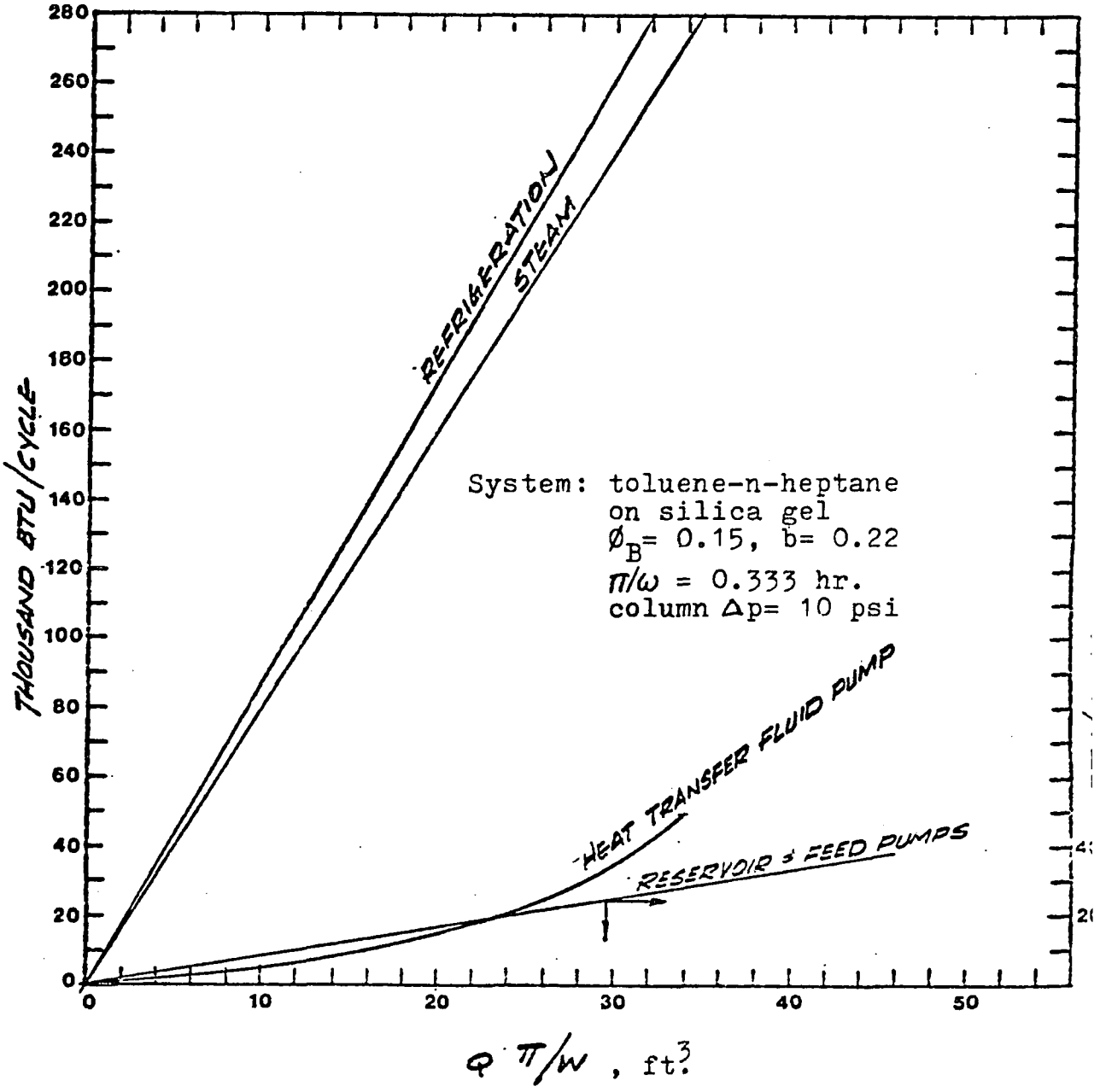

FIGURE (26)

Parametric Pumping Energies vs Reservoir Displacement

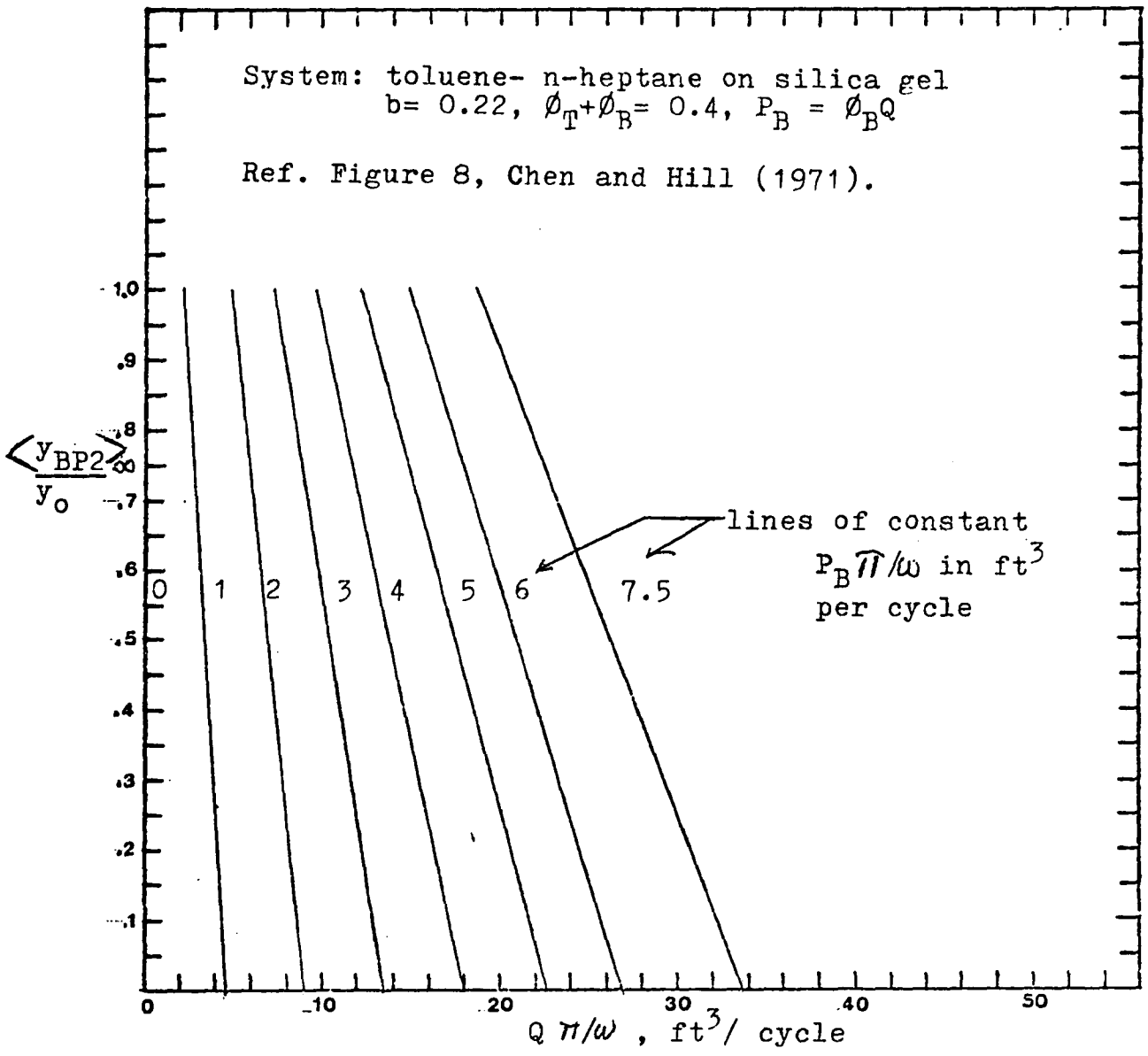

FIGURE (27)

Bottom Product Concentration vs Reservoir Displacement

Energies versus bottom product/reservoir ratio.

The equations in this section (100,102,104,106,109,111, 113) relate the energies per pound of bottom product to the ratio of the bottom product take-off over the reservoir displacement (ϕ_B). As before, the pressure drop in the packed columns was limited to 10 psi which, from Fig.(25) gave Q/N values of 0.0465 over the full range of reservoir displacements. This value of Q/N along with a value of 0.333 hr for π/ω was needed for the pumping energy equations. With these substitutions, the energy equations for the pumps were included in Figure (28), along with the energies for heating and refrigeration.

Figures (28) and (29) show how the key operating variable (ϕ_B) can effect both the product quality and the energy consumption per pound of bottom product. As can be seen in Figure (29), the value of $\langle y_{BP} \rangle_\infty / y_o$ is zero (infinite separation) from a ϕ_B of zero (no bottom product take-off) to a value of 0.22, the value of b for the toluene in n-heptane (Chen et al, 1972). As explained by Chen and his co-workers, the pump is operating in the range of infinite separation when ϕ_B is less than b. When the bottom take-off is increased so that ϕ_B exceeds the value of b, solute appears in the bottom product stream and $\langle y_{BP} \rangle_\infty / y_o$ increases from zero to one as

ϕ_B is increased from 0.22 to 0.4. At 0.4, the volume of the bottom product stream is equal to that of the feed stream and, of course, there is no separation.

Figure (28) shows the corresponding effect on the energies. In the range of ϕ_B from zero to b (0.22), the energies in BTU/lb of bottom product decrease from infinity to finite values. Also, according to Figure (29), the solute separation is complete and there is no benefit derived from the higher energy consumptions. At ϕ_B = 0.22, the consumptions are 490 BTU/lb. of bottom product for refrigeration, 410 for heating, 2.2 BTU equivalents for the heat transfer fluid pump, and 0.5 BTU equivalents for the feed and reservoir pumps.

As the value of ϕ_B continues to increase, the energy consumptions decrease to the lower limits of 300 for refrigeration, 240 for heating, 2.0 for the heat transfer fluid pump, and 0.4 for the feed and reservoir pumps. Of course at this point, the separation is nil and there is no point in operating the column. It is up to the operator to select the operating level between ϕ_B of 0.22 and 0.4 that will give the required separation $\langle y_{BP} \rangle_\infty / y_o$ between zero and one, and to estimate the utility consumptions accordingly.

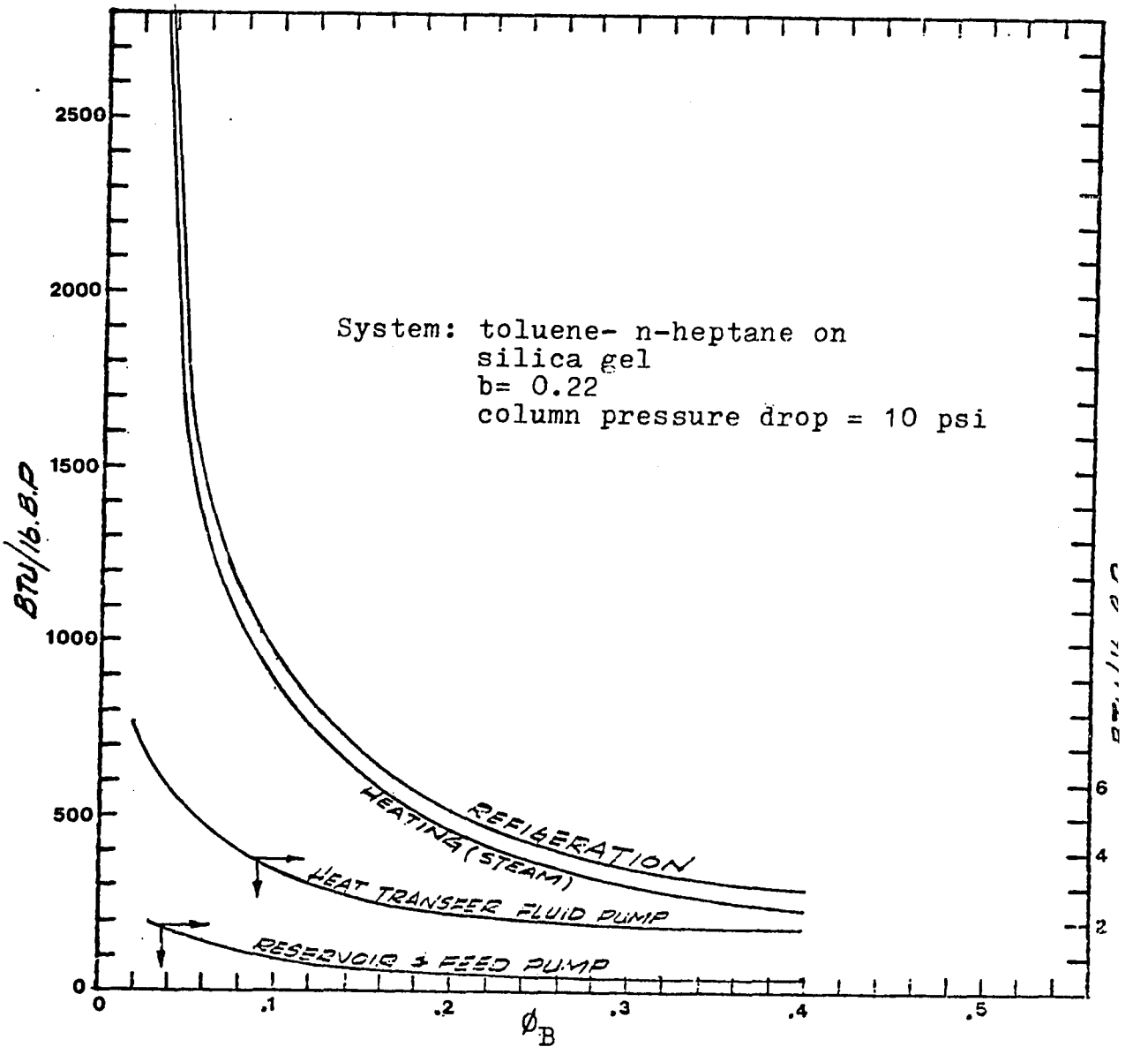

FIGURE (28)

Parametric Pumping Energies vs Bottom Product/ Reservoir Ratio

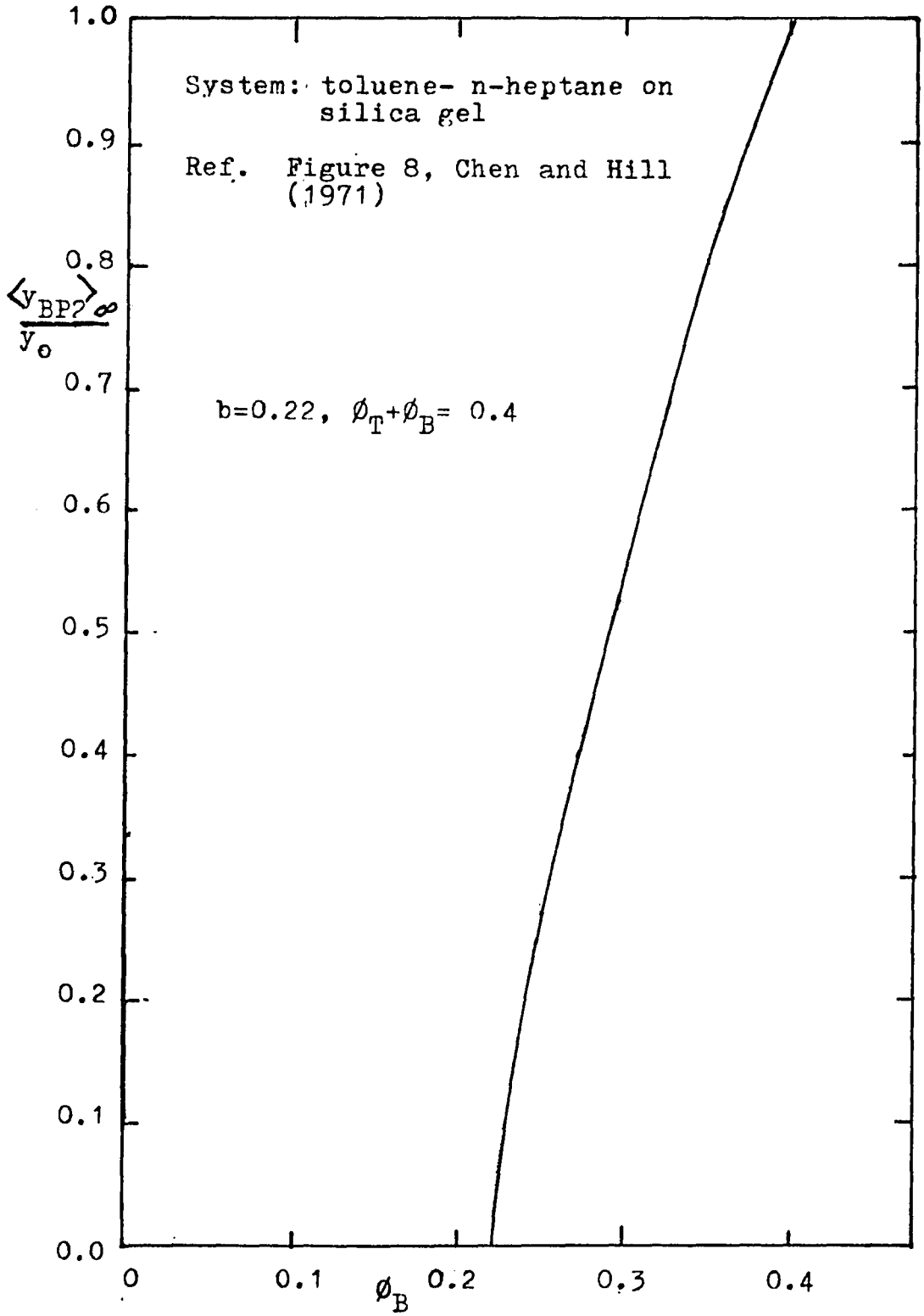

FIGURE (29)

Bottom Product Concentration vs ϕ_B

Comparison of Energies with Distillation Energies. The energy consumption for parametric pumping is the same order of magnitude as other means of separation, such as distillation. If, for simplicity, the sensible heat requirements for distillation are neglected, the total heat requirements for the condenser and reboiler are easily shown to be $2\lambda_v$ (where λ_v is the latent heat of vaporization) BTU/lb of product for a simple stripping column (comparable to a Region 2 type of separation) and $2\lambda_v(R+1)$ for a fractionating column (comparable to a Region 1 separation). Now for parametric pumping, the total heating and cooling requirements are given by summing Equations (100, 103) to give

$$\frac{q}{2P_B\pi/\omega} = \frac{170.8}{\phi_B} + 107.6$$

If toluene is the compound being separated in both cases, then we have in Table 6,

TABLE 6

ENERGIES: PARAMETRIC PUMPING VS. DISTILLATION

	Moderate Separation	Good Separation
Distillation Type	Stripping Column	Fractionator
Condenser, Reboiler, q	$2\lambda v$	$2\lambda_v(R+1)$
Reflux Ratio, R	0	3
Duties, BTU/lb product	311	1246
Parametric Pumping Operation	Region 2	Region 1
Heating and Cooling, q	$170.8/\phi_B+107.6$	$170.8/\phi_B+107.6$
Bottom Product Ratio, ϕ_B	0.35	0.22
Duties, BTU/lb product	596	900

Commercial Scale Parametric Pumping System

The heart of the system is the parapump column assembly described in the first two parts of this chapter. But of course this unit must be augmented by auxiliary tanks, pumps, and other equipment, and the entire system must be instrumented. The design of this auxiliary equipment is standard and not pertinent to this work. Nevertheless, it is useful to briefly describe the operation of this equipment and thus point out what is required for a complete parametric pumping system.

The parametric pumping system may be conveniently divided into four sections: the parapump column assembly; the process reservoir tanks, pumps, and controls; the process feed and product tanks, pumps, and controls; and the heat transfer reservoir tanks, pumps, and controls. The supporting systems for (refrigeration) cooling and (steam) heating are also required but are not described because these systems are usually present as utilities in most large chemical plants.

The equipment is all listed in Table (7) and is shown in the diagram in Figure (30).

TABLE 7

PARAPUMP SYSTEM EQUIPMENT LIST

	Pos. No.	Description
Tanks	T1	Bottom Reservoir
	T2	Top Reservoir
	T3	Hot Heat Transfer Fluid Reservoir
	T4	Cold Heat Transfer Fluid Reservoir
	T5	Feed Tank
	T6	Bottom Product Receiver
	T7	Top Product Receiver
Pumps	P1	Feed Pump
	P2	Bottom Reservoir Pump
	P3	Top Reservoir Pump
	P4	Heat Transfer Fluid Pump
Exchanger	E1	Parapump Column Assembly
Agitators	M1	Bottom Reservoir Mixing Tee
	M2	Top Reservoir Mixing Tee

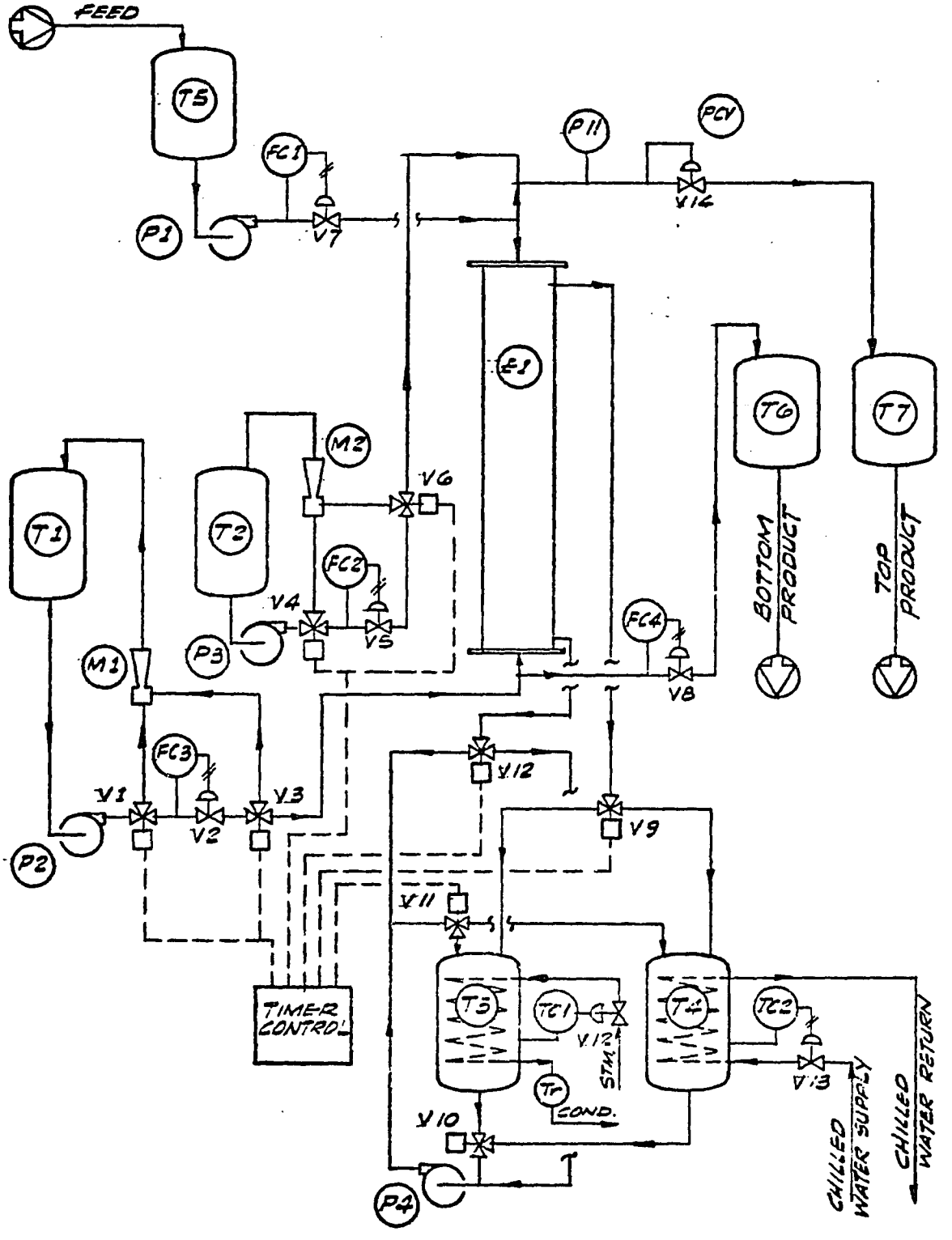

FIGURE (30): Parapump System Diagram

Process description. At the start of the hot upflow half cycle, the timer control switches valves (V1,V3,V4, V6) and the bottom reservoir process fluid is pumped (P2) under flow control (FC3,V2) through the parapump column (E1) and into the top process reservoir (T2) via the mixing tee (M2) where it is thoroughly mixed with top reservoir process fluid pumped (P3) around the recycle loop.

At the same time, valves (V9,V10,V11,V12) are set so the hot water is pumped (P4) from the hot fluid reservoir (T3) into the bottom inlet shellside nozzle of the parapump column (E1). The hot heat transfer fluid leaving the top shellside nozzle (E1) flows through valve (V9) and back into the hot fluid reservoir (T3). Since the water reentering the reservoir has been cooled, the reservoir temperature starts to drop and the temperature controller admits steam to the coil to maintain the hot fluid temperature.

Just prior to the end of the hot half cycle, valves (V10,V11,V12) are switched to divert the flow to the suction side of pump (P4) from the hot fluid reservoir (T3) to the inlet shellside nozzle (E1). Also, the discharge side of pump (P4) is diverted from the inlet shellside

nozzle (E1) to the top of the hot fluid reservoir (T3). Then the hot heat transfer fluid is pumped out of the parapump (E1) shell and back into the reservoir so that it will not mix with the cold heat transfer fluid at the start of the cold downflow half cycle.

Continuously, throughout the hot upflow and cold downflow half cycles, process feed is pumped (P1) from the feed tank (T5) to the top of the parapump column (E1) under flow control (FC1,V7). The top product process fluid leaving the parapump (E1) flows through a back pressure valve (PCV) and into the top product tank (T7). The bottom product flows from the bottom of the parapump column (E1) under flow control (FC4,V8) and into the bottom product tank (T6). By means of this instrumentation scheme, the flow rates of all streams are regulated, the column is kept under a constant back pressure, and air or gas which could affect the adsorption is kept out of the parapump column.

At the start of the cold downflow half cycle, valves (V1,V3,V4,V6) in the process reservoir system are switched. Fluid from the top reservoir (T2) is now pumped (P3) into the top of the parapump column (E1). The effluent from the bottom enters the bottom process reservoir (T2),

being thoroughly mixed with the reservoir contents via the mixing tee (M1) and recycling pump (P2).

At the same time, valves (V9,V10,V11,V12) are switched so the cold water is pumped (P4) from the cold fluid reservoir (T4) into the bottom inlet shellside nozzle of the parapump column (E1). The cold heat transfer fluid leaving the top shellside nozzle (E1) flows through valve (V9) and back to the cold fluid reservoir (T4). Since the water reentering the reservoir has been heated, the reservoir temperature starts to rise and the temperature controller admits chilled water to the coil to maintain the cold fluid temperature.

Just prior to the end of the cold half cycle, valves (V10,V11,V12) are switched and the residual cold water in the shell is pumped back into the cold fluid reservoir in the same manner as previously described for the end of the hot half cycle. At this point, the entire procedure is repeated as described above.

Details of the column assembly. The parapump column assembly is basically a heat exchanger, each tube being a packed column. The columns (or tubes) are 0.5 inch o.d. 18 BWG mounted in an 11/16 inch triangular pitch. The tube size was selected as the equivalent of the

laboratory columns used for parametric pumping in which the 0.402 inch inside diameter equals the approximate 1 centimeter diameter of the laboratory columns.

The number of tubes and their length are related to the fluid velocity or flow rate in the tubes, the relationship having been shown in the design example.

The distribution of the fluid to the tubes is important. The fluid flows into a special flat cylindrical head, through a distributor and into the tubes. The key to good distribution is that the lateral pressure drop between the tubes must be less than one tenth that of the perpendicular pressure drop (in the direction of the tube axis) through the distributor. One way to achieve this is with an orfice plate, the hole diameters being calculated by the usual orfice formulas. Another way would be the use of a sintered filter plate, the pressure drop across the plate being a function of the porosity.

The tubes are held together in a bundle by the shellside baffles and the bundle assemble is contained in a cylindrical shell, usually a pipe of standard nominal size. The relationship between the shell diameter and the number of tubes is shown in Table (3). Since the pressure drop is related to the shell diameter, it is also

related to the number of tubes of a given diameter and spacing (pitch). And since the shellside fluid flows in a particular pattern, the pressure drop is predictable, being a function of the flow rate and number of tubes.

The details of the parapump assembly as described above are illustrated in Figure (31).

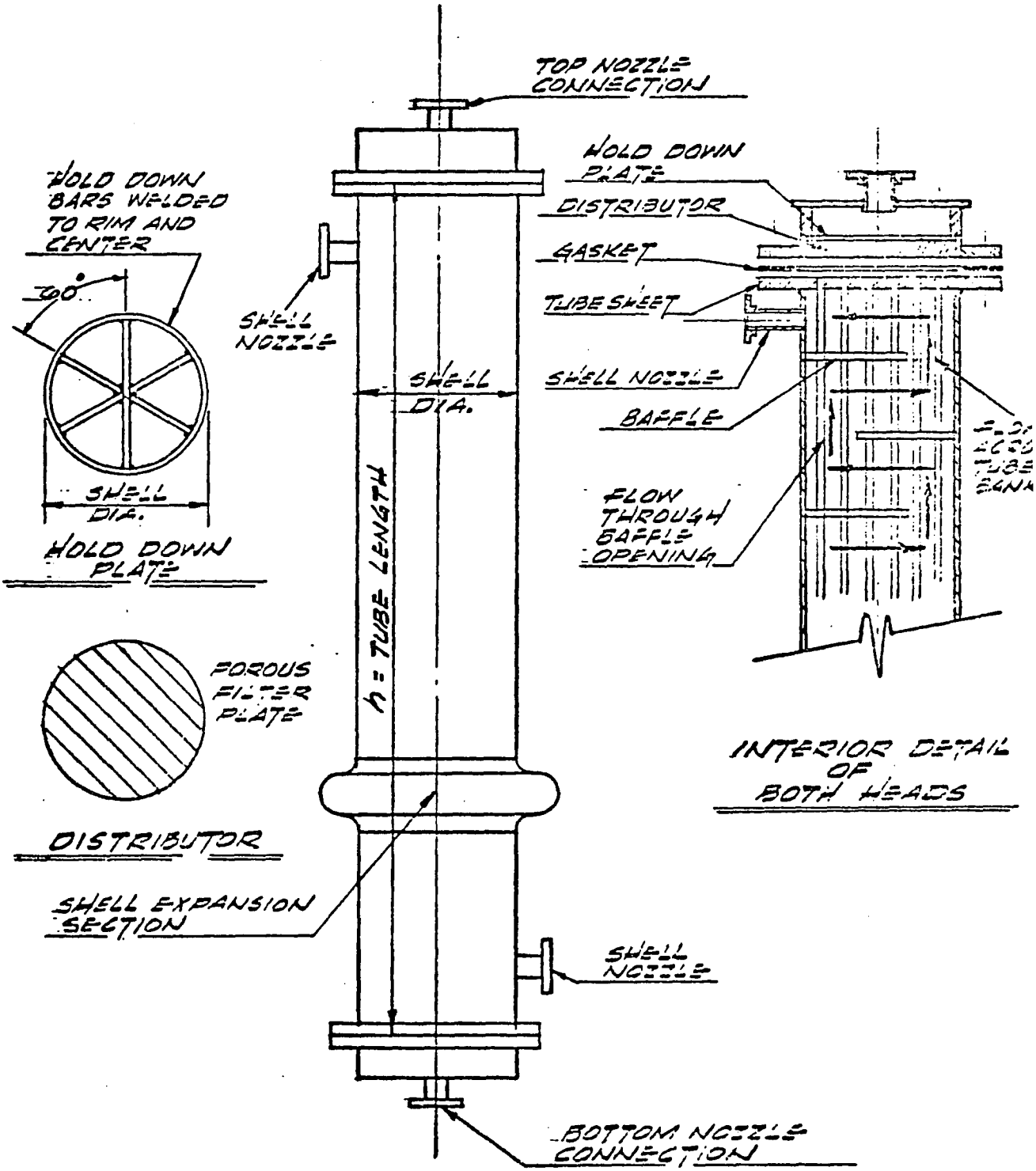

FIGURE (31)

Parapump Column Assembly

Operational and Design Changes

Design criteria review. At the beginning of the chapter it was stated that the basis for designing parametric pumps is the same for multicomponent and binary systems. This design basis can be more easily understood if the key equations (Eq. 74,75) are combined and rearranged to give a dimensionless packed bed volume.

$$\frac{Nha_t\varepsilon}{Q\pi/\omega} \geq \frac{(1+\phi_B)}{(1+b_i)(1+m_{oi})} \qquad (120)$$

which incorporates the principal design parameters. The numerator of the dimensionless volume is equal to the total packed bed void volume and the denominator is equal to the reservoir displacement.

The inequality stems from the criteria (Eq. 23) necessary for complete removal of solute from the bottom product stream. Due to the usual values of ϕ_B (<1), b_i (<1), and m_{oi} (>1), the dimensionless void volume is less than unity and this means that the reservoir volume will be larger than the void volume of the packed bed. Another criteria requires that $\phi_B \leq$ bi, and for the multicomponent system (Eq. 34) this means that

$$b_1 > b_2 > \text{-----} > b_k \geq \phi_B > b_{k+1} \text{-----} > b_s$$

All solute with values of b_i greater than ϕ_B will theoretically be removed from the bottom product stream. In the extreme case where k = s, the bottom stream would consist only of pure solvent. This is the case with the binary system used for the design example except that $b_k = b_s = 0.22$ for toluene and toluene was the only solute. Thus the normal design range of ϕ_B for the multicomponent system would be similar to that of the binary system except that the upper limit would be b_k and the lower limit would not be zero but rather b_{k+1}. For example, if a solute with $b_{k+1} = 0.1$ were added to the toluene-heptane binary, the design criteria for the new system would be identical to the binary--the only difference being that, in actual operation, the bottom product would now contain the new solute as well as the heptane solvent.

Operational changes on an existing system. The equipment designed for a solute split in a multicomponent system could be used for another split in the same general system provided the values of b_k and m_{ok} were both known. The value of ϕ_B would be adjusted so as to keep the dimensionless void volume (Eq. 120) constant. The effect of adjusting ϕ_B on the energies can best be determined by examining the energy equations in Appendix III (Eq. III-45,47,52,53,58,62,63,66,67,70,71). But, simply stated,

if ϕ_B is reduced (smaller bottom product stream), the following energy changes occur. All energies as BTU/lb bottom product increase because of the smaller amount of bottom product withdrawn from the system. However the rate (BTU/hr) of heat supplied for hot upflow and the pumping requirement for hot upflow both increase as a result of the increased volume of flow in the packed bed. Also, the rate of cooling (BTU/hr) and also the reservoir pumping and feed pumping requirements for cold downflow decrease because less fluid is pumped down the packed columns during the cold downflow half cycle.

Now if ϕ_B is increased (instead of reduced) the energy changes are in reverse of those described above to account for the decrease in column flow during hot upflow and the increase during cold downflow.

To summarize, the normal design for a multicomponent system is the same as for the binary--the design value of ϕ_B is equal to or slightly less than the value of b_i immediately above it. If the widest possible range of operation is desired, the lowest values of b_i and m_{oi} should be used for design. Then the pump could be used for the lowest solute split (solute with the lowest value of b_i). Then, with the same equipment, higher

splits could be made by increasing ϕ_B to allow for the higher values of b_i. This would be done at the expense of decreasing ϕ_T (smaller top product stream) until ϕ_T was reduced to zero. Up to this point, the energies would have to be modified to allow for increasing ϕ_B. If ϕ_T were to become zero as a result of increasing ϕ_B, the parapump assembly itself ($Nha_t\varepsilon$) would have to be made larger to allow for the larger $Q\pi/\omega$ due to the need for a larger feed stream.

CHAPTER 6

DISCUSSION AND CONCLUSIONS

In this dissertation, the emphasis has been on the separation of solutes from multicomponent mixtures in both dilute and concentrated solutions, and on the design and scale-up of a multi-tube parametric pump assembly for operation in the direct thermal mode.

Separation of solutes from dilute multicomponent solutions was shown to be predictable from binary information. It was demonstrated that dilute multicomponent solutions could be treated as pairs of pseudo binary systems, each system comprising one solute as one component and the common solvent as the other component. The mathematical model used for predicting separations was obtained by adapting the binary model to multicomponent use. This model consisted of the analytical solutions to the basic mass balance, equilibrium, and rate expressions commonly used for parametric pumping and was based on the equilibrium theory. The calculated product concentration profiles with time were in reasonable agreement with the experimental results for the toluene-aniline-n-heptane-silica gel system.

The separation of solutes from concentrated multicomponent solutions could not be predicted by simple

analytical solutions to the basic mass balance, equilibrium, and rate expressions. It was necessary to resort to computer calculations and numerical solutions via the method of characteristics. The computed concentration profiles agreed reasonably well with the experimental results. The basic parameters affecting the separations were the bottom product rate, the cycle time, and, of course, the solute concentrations in the feed. The separation of solute(s) from the bottom product stream was significantly increased by decreasing the bottom product rate and increasing the cycle time. The column became saturated and the separation capability dropped off sharply as the total solute concentrations reached 40 volume percent.

Significantly, the mathematical model for the separation from concentrated solutions dealt with the mass transfer and equilibria of individual solutes. Equilibrium expressions dealing with the interplay of all the solutes were not successfully incorporated into the model. Apparently, in the case of the toluene-acetophenone-n-heptane-silica gel system used for the work with concentrated solutions, the effect of the concentration of the individual solutes was more significant then the interplay between solutes.

Separation of solutes from multicomponent systems on a commercial scale has often been mentioned in connection with parametric pumping. To this end, design equations based on the analytical equations of the dilute solution theory were developed and presented. The pilot plant and commercial systems described take the form of multi-tube units in a heat exchanger configuration to permit operation via direct thermal mode where rapid temperature changes between the hot and cold half-cycles are essential. Construction of these units is probably feasible as described, and the energies (steam, refrigeration, electrical) required were shown to be of the same order of magnitude as other separation techniques such as distillation. Energy consumption was also shown to vary with separation efficiency. The practical operating range of solute separations from 50-100% required 590-900 BTU per lb. of product for the system studied as compared to 310 to 1,250 for distillation.

In addition to the design of the parametric pumping assembly itself, a description of a complete system including auxilliary equipment (tanks, pumps) and instrumentation is shown along with a process description of the operation.

APPENDIX I

PARAMETRIC PUMPING RUNS FOR SOLUTE CONCENTRATION EFFECT EXPERIMENTAL DATA

Run No. 1

Run No. 1 was a short test run to test the parametric pumping equipment. The duration was four 40-minute cycles, each hot upflow and cold downflow half cycle (π/ω) lasting 20 minutes. The feed concentration (y_o) was 2.5 volume % toluene in n-heptane. The ratio of bottom product to reservoir displacement (ϕ_B) was 0.15. The ratio of feed to reservoir displacement ($\phi_T+\phi_B$) was 0.40. The reservoir displacement ($Q\pi/\omega$) was 20 cc. The hot half cycle temperature (T_1) was 70°C. and the cold half cycle temperature (T_2) was 25°C.

Run No. 2

Conditions: Binary system- dilute.

π/ω = 20 min.; $Q\pi/\omega$ = 35 cc.

y_o = 2.5 vol. % acetophenone in n-heptane

ϕ_B = 0.1; $\phi_T+\phi_B$ = 0.40

T_1 = 70°C.; T_2 = 25°C.

Run No. 2 was generally successful and lasted for 16 cycles. The sample containers, however, were not solvent tight and the analyses were unacceptable. The sample containers (snap-on type) were replaced with screw-cap type vials and the run was repeated (see Run No. 4).

Run No. 3

Conditions: Binary system- dilute n-heptane solution

y_{o1} (toluene) = 2.5 vol. %; y_{o2} (acetophenone) = 0

π/ω = 20 min.; $Q\pi/\omega$ = 35 cc

ϕ_B = 0.035; $\phi_B+\phi_T$ = 0.400

T_1 = 70°C; T_2 = 25°C

Cycle	Temp.	Feed	Top Product			Bottom Product		
No.	°C	cc	cc	y_1/y_{o1}	y_2/y_{o2}	cc	y_1/y_{o1}	y_2/y_{o2}
1	71	14	6.8	-	-	1.5	-	-
1	23	14	6.4	0.663	0	1.1	0.949	0
2	70.5	14	7.2	-	-	1.6	-	-
2	24	14	6.8	0.989	0	1.2	0.731	0
3	70.5	14	7.4	-	-	1.4	-	-
3	25	14	6.8	1.214	0	1.0	0.436	0
4	71	14	10.0	-	-	1.4	-	-
4	25	14	6.2	1.241	0	1.3	0.381	0
5	71	14	10.8	-	-	1.3	-	-
5	25	14	8.0	1.171	0	1.0	0.215	0
6	71	14	8.8	-	-	1.0	-	-
6	24	14	9.0	1.581	0	1.2	0.144	0
7	71	14	10.5	-	-	1.2	-	-
7	25	14	10.8	1.519	0	1.6	0.0967	0
8	70.5	14	12.2	-	-	1.1	-	-
8	24.5	14	8.0	1.567	0	1.5	0.0711	0
9	71	14	14.5	-	-	1.2	-	-
9	25	14	12.0	1.696	0	1.3	0.0515	0
10	70.5	14	7.5	-	-	1.0	-	-
10	24.5	14	9.1	1.291	0	1.0	-	0

Run No. 4

Conditions: Binary system- dilute n-heptane solution

y_{o1} (toluene) = 0; y_{o2} (acetophenone) = 2.5 vol. %

π/ω = 20 min.; $Q\pi/\omega$ = 35 cc

ϕ_B = 0.035; $\phi_T+\phi_B$ = 0.400

T_1 = 70°C; T_2 = 25°C

Cycle	Temp.	Feed	Top Product			Bottom Product		
No.	°C	cc	cc	y_1/y_{o1}	y_2/y_{o2}	cc	y_1/y_{o1}	y_2/y_{o2}
1	70	14	5.4	-	-	1.1	-	-
1	25	14	6.2	0	0.337	1.2	0	0.893
2	71	14	9.3	-	-	1.2	-	-
2	25	14	9.6	0	0.468	1.2	0	0.420
3	70	14	10.8	-	-	1.2	-	-
3	25	14	6.8	0	0.707	1.1	0	0.128
4	70	14	13.7	-	-	1.3	-	-
4	25	14	9.0	0	0.823	1.1	0	0.108
5	70	14	12.8	-	-	1.4	-	-
5	25	14	10.8	0	0.822	1.2	0	0.037
6	71	14	9.2	-	-	1.0	-	-
6	25	14	8.6	0	0.991	2.0	0	0.028
7	71	14	12.2	-	-	1.2	-	-
7	25	14	9.2	0	0.853	1.2	0	0.038
8	71	14	11.0	-	-	2.4	-	-
8	25	14	11.2	0	0.872	0.6	0	0.009
9	71	14	10.0	-	-	1.0	-	-
9	25	14	8.6	0	1.060	1.0	0	0.008
10	71	14	13.7	-	-	1.2	-	-
10	25	14	9.6	0	0.885	1.1	0	0.004
11	71	14	16.0	-	-	1.1	-	-
11	25	14	10.8	0	0.800	1.2	0	0.002
12	70	14	12.0	-	-	1.2	-	-
12	25	14	11.2	0	0.983	1.0	0	0.001
13	70	14	14.8	-	-	1.3	-	-
13	25	14	11.0	0	1.040	1.2	0	0.0007
14	70	14	11.8	-	-	1.4	-	-
14	25.5	14	7.0	0	0.980	1.3	0	0
15	71	14	16.0	-	-	1.3	-	-
15	25	14	12.2	0	1.040	1.1	0	0
16	71.2	14	12.8	-	-	1.2	-	-
16	26	14	10.4	0	0.880	1.1	0	0

Run No. 5

Conditions: Ternary system- conc. n-heptane solution

y_{o1} (toluene) = 10; y_{o2} (acetophenone) = 10 vol. %

π/ω = 20 min.; $Q\pi/\omega$ = 25 cc

ϕ_B = 0.25; $\phi_T+\phi_B$ = 0.40

T_1 = 70°C; T_2 = 25°C

Cycle	Temp.	Feed	Top Product			Bottom Product		
No.	°C	cc	cc	y_1/y_{o1}	y_2/y_{o2}	cc	y_1/y_{o1}	y_2/y_{o2}
1	71	10	1.6	-	-	1.5	-	-
1	25	10	1.4	1.03	0.790	3.0	1.01	0.514
2	71	10	3.4	-	-	6.25	-	-
2	25	10	2.0	1.18	0.839	5.7	0.594	0.219
3	71	10	3.65	-	-	6.1	-	-
3	25	10	1.3	1.17	0.911	6.0	0.487	0.117
4	71	10	4.9	-	-	6.5	-	-
4	25	10	0.7	1.49	0.875	5.9	0.647	0.0443
5	71.2	10	3.6	-	-	6.1	-	-
5	25	10	1.3	1.19	1.140	5.8	1.02	0.0400
6	71	10	4.1	-	-	6.3	-	-
6	25.5	10	2.0	1.14	1.27	6.2	1.22	0.0265
7	71.1	10	4.0	-	-	6.2	-	-
7	25.5	10	2.1	1.03	1.31	6.2	1.35	0.0167
8	71	10	2.8	-	-	6.2	-	-
8	25	10	1.6	0.896	1.19	6.1	1.36	0.0129
9	71.1	10	3.7	-	-	6.2	-	-
9	24.5	10	1.3	0.893	1.39	6.2	1.30	0.0449
10	71	10	4.1	-	-	6.2	-	-
10	24.5	10	1.8	0.957	1.45	6.2	1.22	0.240
11	71	10	4.8	-	-	6.3	-	-
11	25	10	1.2	0.957	1.49	6.4	1.18	0.383
12	71	10	4.5	-	-	6.3	-	-
12	25	10	2.3	0.958	1.46	5.9	1.12	0.477
13	71.2	10	5.2	-	-	6.2	-	-
13	25.1	10	1.6	0.957	1.51	6.0	1.10	0.719
14	71	10	4.2	-	-	6.25	-	-
14	25	10	1.3	0.950	1.52	6.25	1.08	0.615
15	71	10	3.8	-	-	6.2	-	-
15	25	10	1.7	0.978	1.44	5.95	1.05	0.684
16	71	10	3.7	-	-	6.2	-	-
16	25.3	10	1.1	0.956	1.56	6.1	1.03	0.777

Run No. 6

Conditions: Ternary system- dilute n-heptane solution

y_{o1} (toluene) - 2.5; y_{o2} (acetophenone) - 2.5 vol. %

π/ω = 20 min.; $Q\pi/\omega$ = 25 cc

ϕ_B = 0.25; $\phi_T+\phi_B$ = 0.40

T_1 = 70°C; T_2 = 25°C

Cycle	Temp.	Feed	Top Product			Bottom Product		
No.	°C	cc	cc	y_1/y_{o1}	y_2/y_{o2}	cc	y_1/y_{o1}	y_2/y_{o2}
1	71	10	2.4	-	-	4.2	-	-
1	25	10	1.0	0.997	0.881	5.2	0.746	0.416
2	71	10	5.0	-	-	6.25	-	-
2	26	10	1.0	1.23	0.696	6.1	0.478	0.126
3	71	10	3.7	-	-	6.2	-	-
3	24	10	1.4	1.34	0.953	5.8	0.377	0.100
4	71.1	10	3.6	-	-	6.2	-	-
4	25	10	1.5	1.36	1.27	6.2	0.288	0.040
5	71	10	3.6	-	-	6.2	-	-
5	25	10	1.0	1.25	1.69	6.0	0.246	0.035
6	71	10	2.0	-	-	6.3	-	-
6	25.1	10	2.1	1.48	1.46	5.8	0.219	0.024
7	71	10	5.0	-	-	6.3	-	-
7	25	10	2.0	1.29	1.52	6.1	0.124	0.010
8	71	10	1.0	-	-	5.8	-	-
8	25.1	10	0.8	1.65	1.43	6.2	0.133	0.007
9	71	10	3.7	-	-	6.2	-	-
9	25	10	1.0	1.47	1.90	7.2	0.189	0.007
10	71	10	3.8	-	-	5.6	-	-
10	24.9	10	2.3	1.30	1.63	5.8	0.253	0.005
11	71.5	10	3.1	-	-	6.4	-	-
11	25	10	1.4	1.30	2.11	6.2	0.349	0.005
12	71	10	5.2	-	-	6.2	-	-
12	25	10	1.6	1.56	1.77	6.1	0.435	0.005
13	71	10	4.7	-	-	6.25	-	-
13	25	10	1.7	1.54	1.84	6.0	0.481	0.002
14	71.2	10	4.2	-	-	6.4	-	-
14	24.9	10	3.5	1.43	1.90	6.2	0.587	0.001
15	71	10	3.5	-	-	6.2	-	-
15	25	10	2.1	1.35	1.97	6.2	0.709	0.001
16	71.2	10	3.8	-	-	7.0	-	-
16	24.9	10	1.3	1.35	1.94	5.7	0.739	0

Run No. 7

Conditions: Ternary system- conc. n-heptane solution

y_{o1} (toluene) = 10; y_{o2} (acetophenone) = 10 vol. %

π/ω = 20 min.; $Q\pi/\omega$ = 25 cc

ϕ_B = 0.035; $\phi_T+\phi_B$ = 0.400

T_1 = 70°C; T_2 = 25°C

Cycle	Temp.	Feed	Top Product			Bottom Product		
No.	°C	cc	cc	y_1/y_{o1}	y_2/y_{o2}	cc	y_1/y_{o1}	y_2/y_{o1}
1	71.1	10	7.8	-	-	1.0	-	-
1	24.1	10	4.0	0.959	0.567	0.8	1.00	0.542
2	71	10	11.0	-	-	0.8	-	-
2	24	10	7.5	1.00	0.636	0.8	0.804	0.286
3	71.2	10	11.0	-	-	1.0	-	-
3	23	10	7.0	1.04	0.775	0.9	0.685	0.178
4	71	10	9.5	-	-	0.8	-	-
4	25	10	6.9	1.14	0.825	0.9	0.673	0.098
5	71	10	11.0	-	-	0.9	-	-
5	24	10	6.5	1.26	0.888	0.9	0.611	0.0617
6	71.1	10	11.0	-	-	0.85	-	-
6	25	10	7.6	1.10	0.682	0.8	0.505	0.0382
7	71	10	10.7	-	-	0.9	-	-
7	24.8	10	7.5	1.12	0.924	0.9	0.527	0.0493
8	71	10	11.0	-	-	0.9	-	-
8	25	10	6.8	1.10	0.885	0.8	0.425	0.0221
9	71	10	11.0	-	-	0.8	-	-
9	25	10	6.4	1.18	0.956	0.95	0.435	0.0227
10	71.1	10	9.8	-	-	0.8	-	-
10	25	10	6.7	1.04	0.997	1.0	0.415	0.0162
11	71	10	9.6	-	-	1.0	-	-
11	25	10	7.4	1.06	1.55	1.1	0.459	0.0292
12	71	10	11.4	-	-	0.85	-	-
12	24.9	10	6.4	1.03	1.05	1.0	0.452	0.0126
13	71.1	10	9.6	-	-	0.8	-	-
13	25	10	6.4	1.12	1.06	0.9	0.428	0.0164
14	70	10	9.8	-	-	1.1	-	-
14	24.9	10	6.0	1.03	1.11	0.85	0.412	0.0111
15	71	10	9.9	-	-	0.85	-	-
15	25	10	6.2	1.03	1.07	0.9	0.396	0.0078
16	71.1	10	11.0	-	-	0.9	-	-
16	25	10	6.1	1.03	1.13	0.9	0.376	0.0064

Run No. 7 (continued)

Cycle	Temp.	Feed	Top Product			Bottom Product		
No.	°C	cc	cc	y_1/y_{o1}	y_2/y_{o2}	cc	y_1/y_{o1}	y_2/y_{o2}
17	71	10	8.5	-	-	0.9	-	-
17	25	10	6.0	1.03	1.15	0.8	0.440	0.0281
18	71	10	11.0	-	-	1.0	-	-
18	25	10	5.9	1.08	1.16	1.0	0.439	0.0169
19	70.9	10	11.1	-	-	0.8	-	-
19	24.9	10	7.0	1.08	1.14	0.85	0.455	0.0090
20	71	10	9.8	-	-	0.95	-	-
20	24	10	6.9	1.03	1.15	0.9	0.362	0.0030
21	71	10	11.7	-	-	0.9	-	-
21	25	10	7.6	1.05	1.09	0.85	0.383	0.0023
22	71.1	10	11.3	-	-	0.95	-	-
22	24.9	10	7.1	1.08	1.08	0.95	0.413	0.0015
23	71	10	9.7	-	-	1.0	-	-
23	25	10	6.1	1.21	1.08	0.95	0.446	0.0011
24	70.9	10	11.2	-	-	1.0	-	-
24	25.2	10	6.7	1.10	1.05	0.8	0.434	-
25	71.1	10	11.7	-	-	0.8	-	-
25	25	10	7.7	1.12	1.07	0.8	0.324	0.0006
26	71	10	11.0	-	-	0.8	-	-
26	25	10	7.0	1.10	1.11	0.8	0.324	0.0003
27	71	10	11.3	-	-	0.8	-	-
27	25.1	10	6.8	1.08	1.16	0.9	0.311	0
28	71	10	11.4	-	-	0.95	-	-
28	25	10	7.5	1.16	1.10	0.8	0.301	0.0003
29	71.1	10	10.8	-	-	0.9	-	-
29	24.9	10	6.2	1.06	1.05	0.9	0.267	0.0003
30	71	10	11.3	-	-	1.0	-	-
30	25	10	7.3	1.12	1.04	0.9	0.330	0
31	71	10	11.2	-	-	0.95	-	-
31	25	10	6.2	1.11	0.961	0.8	0.213	0
32	71	10	9.7	-	-	0.9	-	-
32	25	10	6.3	1.14	1.05	0.8	0.201	0

Run No. 8

Conditions: Ternary system- conc. n-heptane solution

y_{o1} (toluene) = 10; y_{o2} (acetophenone) = 10 vol. %

π/ω = 10 min.; $Q\pi/\omega$ = 25 cc

ϕ_B = 0.035; $\phi_T+\phi_B$ = 0.400

T_1 = 70°C; T_2 = 25°C

Cycle	Temp.	Feed	Top Product			Bottom Product		
No.	°C	cc	cc	y_1/y_{o1}	y_2/y_{o2}	cc	y_1/y_{o1}	y_2/y_{o2}
1	71	10	5.8	-	-	0.8	-	-
1	25	10	6.2	1.01	0.635	0.8	0.710	0.325
2	71.1	10	9.9	-	-	0.9	-	-
2	24.9	10	4.5	1.05	0.570	0.8	0.662	0.185
3	71.2	10	10.2	-	-	0.9	-	-
3	25	10	7.1	1.09	0.811	0.8	0.620	0.111
4	71.1	10	10.2	-	-	0.9	-	-
4	25.1	10	6.6	1.64	0.886	0.8	0.548	0.056
5	71	10	11.3	-	-	0.9	-	-
5	24.9	10	7.2	1.12	0.958	0.8	0.674	0.0315
6	70.9	10	11.4	-	-	0.9	-	-
6	25	10	7.7	1.08	1.02	0.9	0.502	0.0187
7	71	10	10.4	-	-	1.0	-	-
7	25	10	7.0	1.12	0.979	0.8	0.548	0.0199
8	71	10	10.9	-	-	0.8	-	-
8	25	10	6.8	1.25	1.03	0.85	0.530	0.0139
9	70.8	10	11.0	-	-	0.9	-	-
9	26.1	10	7.0	1.07	1.06	0.85	0.517	0.0088
10	71	10	10.0	-	-	0.8	-	-
10	26	10	6.5	1.12	1.02	0.95	0.477	0.0091
11	71	10	11.6	-	-	0.8	-	-
11	25	10	6.2	1.08	1.04	0.8	0.499	0.0070
12	71	10	11.4	-	-	0.85	-	-
12	25	10	7.5	1.05	1.01	1.1	0.497	0.0051
13	71	10	11.2	-	-	0.9	-	-
13	26	10	7.2	1.03	1.02	0.9	1.008	0.0041
14	71	10	11.1	-	-	1.0	-	-
14	25	10	6.7	1.04	1.06	0.9	0.465	0.0040
15	71	10	11.3	-	-	1.0	-	-
15	25	10	6.6	1.04	1.11	1.0	0.448	0.0032
16	71	10	10.8	-	-	0.8	-	-
16	25	10	6.9	1.03	1.04	0.9	0.507	0.0026

Run No. 8 (continued)

Cycle	Temp.	Feed	Top Product			Bottom Product		
No.	°C	cc	cc	Y_1/Y_{o1}	Y_2/Y_{o2}	cc	Y_1/Y_{o1}	Y_2/Y_{o2}
17	71	10	11.4	-	-	1.0	-	-
17	25	10	6.6	1.00	1.07	0.9	0.479	0.0026
18	71	10	11.7	-	-	0.8	-	-
18	25	10	6.9	1.05	1.08	0.8	0.435	0.00306
19	71.2	10	10.6	-	-	0.85	-	-
19	25	10	6.8	1.04	1.11	0.85	0.436	0.00181
20	71	10	11.4	-	-	0.9	-	-
20	25	10	6.7	1.03	1.02	0.8	0.794	0.00181
21	71	10	4.2	-	-	0.8	-	-
21	25	10	5.6	0.818	1.14	0.8	0.964	0.00411
22	71	10	10.1	-	-	0.85	-	-
22	25	10	7.3	0.847	1.13	0.8	0.964	0.00257
23	71.1	10	10.0	-	-	0.8	-	-
23	25	10	7.3	1.31	1.19	0.8	0.891	0.459
24	71	10	11.1	-	-	0.9	-	-
24	26	10	7.0	1.07	1.14	0.9	0.729	0.00154
25	71	10	11.0	-	-	0.9	-	-
25	26	10	6.7	0.808	1.20	0.85	0.795	0.00103
26	71	10	11.6	-	-	1.0	-	-
26	25.5	10	7.9	0.653	1.17	0.8	0.787	0.00154
27	71.1	10	10.7	-	-	0.9	-	-
27	25	10	7.5	0.890	1.19	0.8	0.886	0.00103
28	71	10	10.4	-	-	1.05	-	-
28	24.9	10	7.8	0.907	1.23	1.0	0.591	0.00041

Run No. 9

Conditions: Ternary system- Conc. n-heptane solution

y_{o1} (toluene) = 10; y_{o2} (acetophenone) = 10 vol. %

π/ω = 5 min.; $Q\pi/\omega$ = 25 cc

ϕ_B = 0.035; $\phi_T+\phi_B$ = 0.400

T_1 = 70°C; T_2 = 25°C

Cycle	Temp.	Feed	Top Product			Bottom Product		
No.	°C	cc	cc	y_1/y_{o1}	y_2/y_{o2}	cc	y_1/y_{o1}	y_2/y_{o2}
1	71	10	2.0	-	-	0.4	-	-
1	25	10	5.1	0.896	0.744	1.0	0.778	0.398
2	71	10	11.1	-	-	0.8	-	-
2	25	10	7.5	0.741	0.708	0.9	0.957	0.293
3	71	10	10.6	-	-	0.95	-	-
3	25	10	7.5	0.932	0.744	0.9	0.690	0.267
4	71	10	11.5	-	-	0.8	-	-
4	27	10	7.4	0.848	0.849	1.1	0.782	0.172
5	71	10	11.0	-	-	0.8	-	-
5	26	10	6.9	0.906	0.891	0.9	0.980	0.989
6	71	10	11.2	-	-	0.8	-	-
6	26	10	6.8	0.726	0.943	0.8	0.850	0.0716
7	71	10	11.5	-	-	0.8	-	-
7	26	10	6.7	1.04	1.01	1.0	0.692	0.508
8	71	10	11.2	-	-	0.8	-	-
8	26.2	10	6.9	0.916	1.06	0.8	0.712	0.0423
9	71	10	10.9	-	-	0.8	-	-
9	25	10	6.5	0.972	0.998	0.8	1.08	0.0378
10	71	10	12.0	-	-	0.8	-	-
10	25	10	7.1	0.927	0.958	0.8	0.720	0.0289
11	71.1	10	11.2	-	-	0.8	-	-
11	25	10	6.9	1.04	1.09	1.0	1.03	0.0208
12	71	10	10.3	-	-	0.8	-	-
12	25	10	8.7	0.929	1.11	1.0	0.691	0.0212
13	71	10	10.4	-	-	0.8	-	-
13	26	10	7.7	0.909	1.09	1.0	0.678	0.0189
14	71	10	10.7	-	-	0.8	-	-
14	25	10	6.5	1.21	1.12	0.8	0.884	0.0131
15	71	10	11.5	-	-	0.8	-	-
15	25	10	7.5	0.879	1.17	0.8	0.604	0.0090
16	71	10	11.1	-	-	0.8	-	-
16	25	10	6.8	0.976	1.09	0.8	1.18	0.0148

Run No. 9 (continued)

Cycle	Temp.	Feed	Top Product			Bottom Product		
No.	°C	cc	cc	y_1/y_{o1}	y_2/y_{o2}	cc	y_1/y_{o1}	y_2/y_{o2}
17	71	10	9.0	-	-	0.8	-	-
17	23	10	6.0	1.24	1.14	0.9	1.06	0.0667
18	71	10	11.7	-	-	0.8	-	-
18	25	10	6.7	1.27	1.21	0.8	1.00	0.0145
19	69	10	11.7	-	-	1.2	-	-
19	26	10	6.9	1.26	1.18	0.8	0.996	0.0111
20	71	10	11.8	-	-	0.8	-	-
20	25	10	6.8	1.25	1.18	0.8	1.015	0.0074
21	71	10	11.5	-	-	0.9	-	-
21	25	10	7.6	1.26	1.19	0.8	1.018	0.0045
22	71	10	11.3	-	-	0.8	-	-
22	26	10	7.0	1.25	1.20	0.8	1.032	0.0037

Run No. 10

Conditions: Ternary system- conc. n-heptane solution

y_{o1} (toluene) = 20; y_{o2} (acetophenone) = 20 vol. %

π/ω = 10 min.; $Q\pi/\omega$ = 25 cc

ϕ_B = 0.035; $\phi_T+\phi_B$ = 0.400

T_1 = 70°C; T_2 = 25°C

Cycle	Temp.	Feed	Top Product			Bottom Product		
No.	°C	cc	cc	y_1/y_{o1}	y_2/y_{o2}	cc	y_1/y_{o1}	y_2/y_{o2}
1	71	10	1.3	-	-	0.4	-	-
1	25	10	2.0	1.02	0.637	0.8	1.01	1.03
2	71	10	9.0	-	-	0.8	-	-
2	25	10	6.0	1.06	0.833	0.8	0.997	0.430
3	71	10	10.5	-	-	0.8	-	-
3	25	10	6.5	1.03	0.946	0.8	1.05	0.382
4	71	10	11.4	-	-	0.8	-	-
4	25	10	6.2	1.03	1.04	0.8	1.08	0.308
5	71	10	11.3	-	-	0.8	-	-
5	25	10	6.3	1.12	1.06	1.0	1.09	0.273
6	70.9	10	11.1	-	-	0.9	-	-
6	24.9	10	7.9	1.01	1.01	0.8	1.10	0.252
7	71	10	10.5	-	-	0.9	-	-
7	25	10	6.6	0.986	1.09	1.0	1.12	0.212
8	71	10	11.2	-	-	0.8	-	-
8	24.9	10	6.8	0.986	1.10	0.8	1.11	0.243
9	70.9	10	10.6	-	-	0.9	-	-
9	25	10	7.0	1.00	1.09	0.8	1.33	0.207
10	71.1	10	11.2	-	-	0.9	-	-
10	24.9	10	7.0	1.00	1.11	0.9	1.11	0.209
11	71	10	11.3	-	-	0.85	-	-
11	25	10	7.7	0.997	1.10	0.9	1.12	0.174
12	71	10	10.2	-	-	1.2	-	-
12	25	10	7.3	0.999	1.10	0.7	1.12	0.193
13	69.9	10	10.7	-	-	0.8	-	-
13	24.9	10	7.6	0.986	1.08	0.8	1.13	0.163
14	71	10	11.2	-	-	0.8	-	-
14	25	10	7.0	0.985	1.10	0.8	1.12	0.150
15	71	10	11.3	-	-	0.8	-	-
15	24.9	10	7.0	0.917	1.11	1.0	1.15	0.152
16	71	10	11.7	-	-	0.8	-	-
16	25	10	6.9	0.991	1.10	0.9	1.12	0.146

Run No. 10 (continued)

Cycle	Temp.	Feed	Top Product			Bottom Product		
No.	°C	cc	cc	y_1/y_{o1}	y_2/y_{o2}	cc	y_1/y_{o1}	y_2/y_{o2}
17	71	10	12.1	-	-	1.0	-	-
17	25	10	6.6	0.979	1.081	0.8	1.13	0.128
18	71	10	11.2	-	-	0.8	-	-
18	25	10	7.1	0.982	1.10	0.8	1.15	0.230
19	71	10	11.4	-	-	1.2	-	-
19	25	10	7.1	0.996	1.08	0.8	1.20	0.105
20	71.1	10	11.4	-	-	0.9	-	-
20	25.5	10	6.7	0.994	1.10	0.8	1.12	0.107

Run No. 11

Conditions: Ternary system- conc. n-heptane solution

y_{oi}(toluene) = 20 vol. %; y_{o2}(acetophenone) = 10 vol.

π/ω = 10 min.; $Q\pi/\omega$ = 25 cc

ϕ_B = 0.035; $\phi_T+\phi_B$ = 0.400

T_1 = 70°C; T_2 = 25°C

Cycle	Temp.	Feed	Top Product			Bottom Product		
No.	°C	cc	cc	y_1/y_{o1}	y_2/y_{o2}	cc	y_1/y_{o1}	y_2/y_{o2}
1	71	10	8.7	-	-	0.9	-	-
1	25	10	1.8	1.03	0.755	0.8	0.918	0.656
2	71	10	11.4	-	-	0.85	-	-
2	24.9	10	6.9	1.05	0.854	0.8	1.23	0.296
3	71.1	10	10.9	-	-	0.9	-	-
3	24	10	6.3	1.02	0.918	0.8	0.915	0.187
4	71	10	12.0	-	-	0.8	-	-
4	25	10	6.7	1.02	1.00	0.8	0.951	0.110
5	71	10	11.0	-	-	0.9	-	-
5	25	10	6.9	1.00	1.05	0.8	0.925	0.0654
6	71	10	11.5	-	-	0.8	-	-
6	25	10	7.1	1.01	1.13	0.8	0.905	0.0389
7	71	10	11.2	-	-	0.8	-	-
7	25	10	7.1	1.01	1.10	0.9	0.924	0.0321
8	71	10	11.0	-	-	0.8	-	-
8	25	10	7.7	0.996	1.10	0.8	0.901	0.0218
9	71.1	10	11.1	-	-	0.9	-	-
9	25.5	10	8.1	0.992	1.11	1.2	0.893	0.0200
10	70.9	10	11.6	-	-	0.8	-	-
10	24.9	10	6.8	1.01	1.13	0.8	0.885	0.0148
11	71	10	11.5	-	-	0.8	-	-
11	25	10	11.7	1.22	1.08	0.9	0.906	0.0148
12	71	10	11.3	-	-	1.0	-	-
12	25	10	7.6	1.00	1.15	0.8	0.876	0.0121
13	71	10	11.3	-	-	0.8	-	-
13	24.9	10	7.5	1.00	1.15	0.8	0.900	0.0082
14	71	10	11.4	-	-	0.9	-	-
14	25	10	7.0	1.00	1.17	0.9	0.892	0.0090
15	71	10	10.9	-	-	0.9	-	-
15	25	10	8.2	1.01	1.16	0.8	0.909	0.0087
16	71	10	11.0	-	-	0.8	-	-
16	25	10	7.7	0.995	1.08	0.8	0.871	0.0109

Run No. 11 (continued)

Cycle	Temp.	Feed	Top Product			Bottom Product		
No.	°C	cc	cc	y_1/y_{o1}	y_2/y_{o2}	cc	y_1/y_{o1}	y_2/y_{o2}
17	71	10	10.8	-	-	0.9	-	-
17	25	10	6.8	0.999	1.120	0.8	0.877	0.0070
18	69.8	10	11.3	-	-	0.8	-	-
18	25	10	6.5	1.01	1.13	0.9	0.865	0.0104
19	71	10	11.6	-	-	0.8	-	-
19	25	10	4.0	1.02	1.10	0.8	0.868	0.0092
20	71	10	10.0	-	-	0.8	-	-
20	25	10	8.0	1.02	1.10	0.8	0.890	0.0047

Run No. 12

Conditions: Binary system- conc. n-heptane solution

y_{o1}(toluene) - 0; y_{o2}(acetophenone) = 10 vol. %

π/ω = 20 min. $Q\pi/\omega$ = 35 cc

ϕ_B = 0.035; $\phi_T+\phi_B$ = 0.400

T_1 - 70°C; T_2 = 25°C

Cycle	Temp	Feed	Top Product			Bottom Product		
No.	°C	cc	cc	y_1/y_{o1}	y_2/y_{o2}	cc	y_1/y_{o1}	y_2/y_{o2}
1	71	14	11.0	-	-	1.2	-	-
1	24.5	14	10.0	0	0.268	1.2	0	0.912
2	70	14	15.2	-	-	1.2	-	-
2	23	14	10.7	0	0.715	1.2	0	0.662
3	70.5	14	15.6	-	-	1.2	-	-
3	24.9	14	11.2	0	0.938	1.2	0	0.362
4	70.5	14	14.8	-	-	1.2	-	-
4	24.5	14	11.1	-	0.895	1.2	0	0.221
5	71	14	15.7	-	-	1.2	-	-
5	24.5	14	8.7	0	1.114	1.2	0	0.180
6	71	14	15.5	-	-	1.2	-	-
6	25	14	9.4	0	1.097	1.4	-	0.148
7	71.1	14	14.3	-	-	1.4	-	-
7	25.2	14	10.8	-	1.194	1.2	-	0.074
8	71	14	16.2	-	-	1.2	-	-
8	25.1	14	9.7	0	1.227	1.2	0	0.040
9	70.9	14	14.8	-	-	1.2	-	-
9	25.1	14	10.5	0	1.073	1.2	0	0.031
10	71.1	14	15.5	-	-	1.3	-	-
10	25.0	14	10.6	0	1.061	1.2	0	0.016
11	71.1	14	16.1	-	-	1.2	-	-
11	25.0	14	9.8	-	1.141	1.2	0	0.013
12	71.1	14	14.4	-	-	1.2	-	-
12	25.1	14	10.1	-	1.361	1.2	0	0.008
13	71	14	13.8	-	-	1.2	-	-
13	25.0	14	10.5	0	1.253	1.2	0	0.012
14	71	14	15.9	-	-	1.2	-	-
14	25.1	14	10.2	0	0.946	1.3	0	0.008

APPENDIX II

COMPUTER PROGRAM

NOMENCLATURE

```
      PROGRAM KIM
C     PARAMETRIC PUMPING CALCULATION        CHONG YONG KIM
C     SYMBOL                  DISCRIPTION                          DIMENSIO
C     VISA1=VISCOSITY OF HEPTANE IN HOT TEMPERATURE                G/CM MIN
C     VISA2=VISCOSITY OF HEPTANE IN COLD TEMPERATURE               G/CM MIN
C     VISB1=VISCOSITY OF TOLUENE IN HOT TEMPERATURE                G/CM MIN
C     VISB2=VISCOSITY OF TOLUENE IN COLD TEMPERATURE               G/CM MIN
C     VISC1=VISCOSITY OF ACETOPHENONE IN HOT TEMPERATURE           G/CM MIN
C     VISC2=VISCOSITY OF ACETOPHENONE IN COLD TEMPERATURE          G/CM MIN
C     H=HEIGHT OF COLUMN                                           CM
C     TIME=HALF CYCLE TIME                                         MIN
C     YA=INITIAL CONCENTRATION OF HEPTANE                          G MOLE/CC
C     YBO=INITIAL CONCENTRATION OF TOLUENE                         G-MOLE/CC
C     YCO=INITIAL CONCENTRATION OF ACETOPHENONE                    G-MOLE/CC
C     Q=DISPLACEMENT                                               CC
C     VT=DEAD VOLUME OF TOP RESERVOIR                              CC
C     VB=DEAD VOLUME OF BOTTOM RESERVOIR .                         CC
C     VOID=VOID VOLUME
C     DENS=DENSITY OF SOLID                                        G-SOLID/CC
C     ERR=ERROR
C     A=CROSSSECTIONAL AREA                                        SQ. CM
C     AP=SURFACE AREA OF SOLID PER GRAM OF SOLID                   SQ. CM/G-SOLI
C     DENB=DENSITY OF TOLUENE                                      G-MOLE/CC
C     DENC=DENSITY OF ACETOPHENONE                                 G-MOLE/CC
C     DB,DC=CONSTANTS IN MODIFIED LANGMUIR ISOTHERM                CC PORE/G
C     DP=SOLID PARTICLE DIAMETER                                   CM
C     TEM1=TEMPERATURE OF HOT CYCLE                                DEGREE K
C     TEM2=TEMPERATURE OF COLD CYCLE                               DEGREE K
C     VMB=MOLAR VOLUME OF TOLUENE                                  DE
C     VMB=MOLAR VOLUME OF TOLUENE                                  CC/MOLE
C     VMC=MOLAR VOLUME OF ACETOPHENONE                             CC/MOLE
C     AMW=MOLECULAR WEIGHT OF HEPTANE                              G/G-MOLE
C     BMW=MOLECULAR WEIGHT OF TOLUENE                              G/G-MOLE
C     CMW=MOLECULAR WEIGHT OF ACETOPHENONE                         G/G-MOLE
C     NOMENCLATURES OF SYMBOLS THAT ARE USED IN THIS PROGRAM
C     N=NUMBER OF CYCLES
C     NNZ=NUMBER OF INTERVALS
C     NCASE=NUMBER OF CASES OF PHOB(I)
C     NITER=NUMBER OF ITERATIONS
C     PB1,QB1=EQUILIBRIUM CONSTANTS OF TOLUENE IN HOT TEMPERATURE
C     PB2,QB2=EQUILIBRIUM CONSTANTS OF TOLUENE IN COLD TEMPERATURE
C     PC1,QC1=EQUILIBRIUM CONSTANTS OF ACETOPHENONE IN HOT TEMPERATURE
C     PC2,QC2=EQUILIBRIUM CONSTANTS OF ACETOPHENONE IN COLD TEMPERATURE
      DIMENSION PHOT(10),PFOB(10),XBP(500),XC2(500),YBTP2(500)
     1 ,YCTP2(500),YB2(500),YC2(500),YBBP2(500),YCBP2(500),XXB2(500),
     2 XXC(500),YYB(500),YYC(500),XBT(500),XCT(500),XXBS(500),XXCS(500),
     3 YYBS(500),YYCS(500),NTR(500),XXC2(500),YYB2(500),XXB(500),
     4 YYC2(500),YYB2BS(500),YYC2BS(500),YYB2ES(500),YYC2ES(500),
     5 RATB(500),RATC(500),RABB(500),RABC(500)
      READ 10,N,NNZ,NCASE,NITER
```

PROGRAM

```
      PROGRAM KIM
C       PARAMETRIC PUMPING CALCULATION       CHONG YONG KIM
        DIMENSION PHOT(10),PHOB(10),XB2(500),XC2(500),YBTP2(500)
     1 ,YCTP2(500),YB2(500),YC2(500),YBBP2(500),YCBP2(500),XXB2(500),
     2 XXC(500),YYB(500),YYC(500),XBT(500),XCT(500),XXBS(500),YXCS(500),
     3 YYBS(500),YYCS(500),NTR(500),XXC2(500),YYB2(500),XXB(500),
     4 YYC2(500),YYB2EQ(500),YYC2EQ(500),YYB2ES(500),YYC2ES(500),
     5 RATB(500),RATC(500),RABP(500),RABC(500)
        READ 10,N,NNZ,NCASE,NITER
   10 FORMAT(4I10)
        READ 12,PB1,PB2,PC1,PC2
   12 FORMAT(4F20.2)
        READ 13,QB1,QB2,QC1,QC2
   13 FORMAT(4F20.2)
        READ 14,VISA1,VISA2,VISB1,VISB2,VISC1,VISC2
   14 FORMAT(6F12.6)
        READ 15,H,TIME,YA,YBO,YCO,Q,VT,VB,VOID,DENS,ERR,A
   15 FORMAT(8F10.5)
        READ 16,AP,DENB,DENC,LB,DC,DP
   16 FORMAT(6F12.6)
        READ 17,TEM1,TEM2,VMB,VMC
   17 FORMAT(4F10.2)
        READ 18,AMW,BMW,CMW
   18 FORMAT(3F10.4)
        READ 20,(PHOT(I),PHOB(I), I=1,NCASE)
   20 FORMAT(2F10.4)
        DO 600 I=1,NCASE
 2020 FORMAT( '1' )
   11 FORMAT(///)
        PRINT 2020
        PRINT3030
 3030 FORMAT(9X,'N',8X,'NNZ',5X,'NCASE',5X,'NITER'//)
        PRINT 10,N,NNZ,NCASE,NITER
        PRINT 11
        PRINT 3040
 3040 FORMAT(10X,'PB1',10X,'PB2',10X,'PC1',10X,'PC2'//)
        PRINT 12,PB1,PB2,PC1,PC2
        PRINT 11
        PRINT 3050
 3050 FORMAT(10X,'QB1',10X,'QB2',10X,'QC1',10X,'QC2'//)
        PRINT 13,QB1,QB2,QC1,QC2
        PRINT 11
        PRINT 3060
 3060 FORMAT(7X,'VISA1',7X,'VISA2',7X'VISB1',7X,'VISB2',7X,'VISC1',7X,
     1 'VISC2')
        PRINT 14,VISA1,VISA2,VISB1,VISB2,VISC1,VISC2
        PRINT 11
        PRINT 3070
 3070 FORMAT(5X,'H',5X,'TIME',5X,'YA',5X,'YBO',5X,'YCO',5X,'Q',5X,
     1 'VT',5X,'VB')
```

```
FORTRAN IV (VER 45 ) SOURCE LISTING: KIM      PROGRAM

      51          PRINT 15,H,TIME,YA,YBC,YCC,Q,VT,VB
      52          PRINT 11
      53          PRINT 3080
      54 3080     FORMAT(7X,'VOID',7X,'DENS',7X,'ERR',7X,'A'//)
      55          PRINT 15,VOID,DENS,ERR,A
      56          PRINT 11
      57          PRINT3090
      58 3090     FORMAT(10X,'AP',10X,'DENB',10X,'DENC',10X,'DB',10X,'DC',10X,'DP')
      59          PRINT 16,AP,DENB,DENC,DB,DC,DP
      60          PRINT 11
      61          PRINT 4010
      62 4010     FORMAT(10X,'TEM1',10X,'TEM2',10X,'VMB',10X,'VMC'//)
      63          PRINT 17,TEM1,TEM2,VME,VMC
      64          PRINT 11
      65          PRINT 4020
      66 4020     FORMAT(10X,'AMW',10X,'BMW',10X,'CMW'///)
      67          PRINT 18,AMW,BMW,CMW
      68          PRINT 11
      69          PRINT 7070
      70 7070     FORMAT(6X,'PHOT',6X,'PHOB'//)
      71          PRINT 20,PHOT(I),PHOB(I)
      72          PRINT 2020
      73          V1=(1.-PHOB(I))*Q/(A*VOID*TIME)
      74          V2=(1.+PHOB(I))*Q/(A*VOID*TIME)
      75          DT1= H/(NNZ*V1)
      76          DT2= H/(NNZ*V2)
      77          PRINT 111,V1,V2,DT1,DT2
      78 111      FORMAT(15X,'V1',19X,'V2',15X,'DT1',15X,'DT2'//4(10X,F10.5))
      79          NZ= NNZ+1
      80          YBT1= YBO
      81          YCT1= YCO
      82          DO 30      J=1,NZ
      83          YB2(J)= YBO
      84          YC2(J)= YCO
      85 30       CALL EQYTOX(PB1,PC1,QE1,QC1,DB,DC,YB2(J),YC2(J),DENB,DENC,XB2(J),
      86         1 XC2(J))
      87          M= 1
      88          IF(M-1) 31,31,32
      89 31       YBTP22=YBO
      90          YCTP22=YCO
      91          GO TO 33
      92 32       YBTP22=YBTP2(M-1)
      93          YCTP22=YCTP2(M-1)
      94 33       YBTP1=((PHOT(I)+PHOB(I))*YBO+(1.-PHOB(I))*YBT1)/(1.+PHOT(I))
      95          YCTP1=((PHOT(I)+PHOB(I))*YCO+(1.-PHOB(I))*YCT1)/(1.+PHOT(I))
      96          IND=2
      97          YBTP2(M)=(Q*YBTP1+VT*YBTP22)/(VT+Q)
      98          YCTP2(M)=(Q*YCTP1+VT*YCTP22)/(VT+Q)
      99          YBT2=((PHOT(I)+PHOB(I))*YBO+(1.-PHOT(I))*YBTP2(M))/(1.+PHOB(I))
     100          YCT2=((PHOT(I)+PHOB(I))*YCO+(1.-PHOT(I))*YCTP2(M))/(1.+PHOB(I))
```

FORTRAN IV (VER 45) SOURCE LISTING: KIM PROGRAM

```
      YBIN=YBT2
      YCIN=YCT2
C
      PRINT 222,YBTP1,YCTP1,YBT2,YCT2
  222 FORMAT('-',5X,'YBTP1',E20.5,5X,'YCTP1',E20.5,5X,'YBT2',E20.5,5X,
     1 'YCT2',E20.5///)
      CALL XYCAL(VOID,DENS,VISA1,VISA2,VISB1,VISB2,VISC1,VISC2,
     1 TEM1,PB1,PB2,QB1,GB2,PC1,PC2,GC1,GC2,V1,V2,IND,DT1,DT2,NITER,XB2,
     2 XC2,YB2,YC2,YBIN,YCIN,TIME,NZ,XXB,XXC,YYB,YYC,YBB,YCB,M,ERR,DENB,
     3 DENC,TEM2,VMB ,VMC ,DB,DC,AMW,BMW,CMW,DP,AP,YA)
      YBBP2(M)=YBB
      YCBP2(M)=YCB
      PRINT 800,M,YBTP2(M),YCTP2(M),YBBP2(M),YCBP2(M)
  800 FORMAT(3X,'M',I10, 5X,'YBTP2',E15.5, 5X,'YCTP2',E15.5, 5X,
     1 'YBBP2',E15.5, 5X,'YCBP2',E15.5///)
      RATB(M)=YBTP2(M)/YBC
      RATC(M)=YCTP2(M)/YCC
      RABB(M)=YBBP2(M)/YBC
      RABC(M)=YCBP2(M)/YCC
      PRINT 900,RATB(M),RATC(M),RABB(M),RABC(M)
  900 FORMAT(5X,'RATB',E15.5,5X,'RATC',E15.5,5X,'RABB',E15.5,5X,
     1 'RABC',E15.5//)
      IF(M-N) 50,500,500
   50 IF(M-1) 51,51,52
   51 YBBP22=YB0
      YCBP22=YC0
      GO TO 53
   52 YBBP22=YBBP1
      YCBP22=YCBP1
   53 YBBP1=(Q*YBBP2(M)+VB*YBBP22)/(Q+VB)
      YCBP1=(Q*YCBP2(M)+VB*YCBP22)/(Q+VB)
      PRINT 333,YBBP1,YCBP1
  333 FORMAT(5X,'YBBP1',E20.5,5X,'YCBP1',E20.5//)
      M=M+1
      YBIN=YBBP1
      YCIN=YCBP1
      DO 60  L=1,NZ
      LL=L-1
      XB2(L)=XXB(NZ-LL)
      XC2(L)=XXC(NZ-LL)
      YB2(L)=YYB(NZ-LL)
   60 YC2(L)=YYC(NZ-LL)
      IND=1
C
      CALL XYCAL(VOID,DENS,VISA1,VISA2,VISB1,VISB2,VISC1,VISC2,
     1 TEM1,PB1,PB2,QB1,GB2,PC1,PC2,GC1,GC2,V1,V2,IND,DT1,DT2,NITER,XB2,
     2 XC2,YB2,YC2,YBIN,YCIN,TIME,NZ,XXB,XXC,YYB,YYC,YBT1,YCT1,M,ERR,
     3 DENB,DENC,TEM2,VMB ,VMC ,DB,DC,AMW,BMW,CMW,DP,AP,YA)
      DO 70  L=1,NZ
      LL=L-1
```

```
FORTRAN IV (VER 45 ) SOURCE LISTING: KIM      PROGRAM

      XP2(L)=XXB(NZ-LL)
      XC2(L)=XXC(NZ-LL)
      YB2(L)=YYB(NZ-LL)
   70 YC2(L)=YYC(NZ-LL)
      GO TO 32
  500 PRINT 510,(M,YBTP2(M),YCTP2(M),YBBP2(M),YCBP2(M),M=1,N)
  510 FORMAT('-',3X,'M',5X,'YBTP2',5X,'YCTP2',5X,'YCBP2',5X,'YCBP2'//
     1 (5X,I5,4E15.5))
      PRINT 520,(M,RATB(M),RATC(M),RABB(M),RABC(M), M=1,N)
  520 FORMAT('-',3X,'M',5X,'RATB',5X,'RATC',5X,'RABB',5X,'RABC'//
     1 (5X,I5,4E15.5))
  600 CONTINUE
      STOP
      END
```

FORTRAN IV (VER 45) SOURCE LISTING: XYCAL SUBROUTINE

```
      1         SUBROUTINE XYCAL(VOID,DENS,VISA1,VISA2,VISB1,VISB2,VISC1,VISC2,
      2        1 TEM1,PB1,PB2,QB1,QB2,PC1,PC2,QC1,QC2,V1,V2,IND,DT1,DT2,NITER,XB2,
      3        2 XC2,YB2,YC2,YBIN,YCIN,TIME,NZ,XXB,XXC,YYB,YYC,YYCAV,YYCAV,M,ERR,
      4        3 DENB,DENC,TEM2,VMB ,VMC ,DB,DC,AMW,BMW,CMW,DP,AP,YA)
      5         DIMENSION XB2(500),XC2(500),YB2(500),YC2(500),XXB2(500),
      6        1 XXC(500),YYB(500),YYC(500),XBT(500),XCT(500),YYBS(500),XXCS(500),
      7        2 YYBS(500),YYCS(500),NIR(500),XXC2(500),YYB2(500),XXB(500),
      8        3 YYC2(500),YYB2EQ(500),YYC2EC(500),YYB2ES(500),YYC2ES(500)
      9         SUMB=YB2(NZ)
     10         SUMC=YC2(NZ)
     11         IF((-1)**IND) 20,10,10
     12   10    VISA=VISA2
     13         VISB=VISB2
     14         VISC=VISC2
     15         V=V2
     16         PB=PB2
     17         PC=PC2
     18         QB=QB2
     19         QC=QC2
     20         DT=DT2
     21         TEM=TEM2
     22         GO TO 30
     23   20    VISA=VISA1
     24         VISB=VISB1
     25         VISC=VISC1
     26         V=V1
     27         PB=PB1
     28         PC=PC1
     29         QB=QB1
     30         QC=QC1
     31         DT=DT1
     32         TEM=TEM1
     33   30    CNSTB=-(1.-VOID)*DENS/VOID
     34         CNSTC=-(1.-VOID)*DENS/VOID
     35         XBT(1)=XB2(1)
     36         XCT(1)=XC2(1)
     37         DO 22  L=1,NZ
     38         XXB2(L)=XB2(L)
     39         XXC2(L)=XC2(L)
     40         YYB2(L)=YB2(L)
     41   22    YYC2(L)=YC2(L)
     42         K=1
     43  155    CNK=K
     44         TT=DT*CNK
     45         YYB(1)=YBIN
     46         YYC(1)=YCIN
     47         CALL EQXTOY (PB,PC,QB,QC,DB,DC,YBEQI,YCEQI,DENB,DENC,XXB2(1),
     48        1 XXC2(1))
     49         CALL RK(YYB2(1),YYC2(1),YBEQI,YCEQI,XXB2(1),XXC2(1),PB,PC,QB,QC,
     50        1 DB,DC,DENB,DENC,XB,XC,DT,YA,AMW,BMW,CMW,VISA,VISB,VISC,DP,VOID,
```

FORTRAN IV (VER 45) SOURCE LISTING: XYCAL SUBROUTINE

```
      2 VMB,VMC,V,AP,TEM)
        XBT(K+1)=XB
        XCT(K+1)=XC
        XXB(1)=XBI(K+1)
        XXC(1)=XCT(K+1)
        I=2
C
 85     ITER=1
        NTR(1)=1
        YYB2EQ(1)=YBEQI
        YYC2EQ(1)=YCEQI
        CALL CMSS(YA,YYB2(I-1),YYC2(I-1),AMW,BMW,CMW,VISA,VISB,VISC,DF,
      1 VOID,AP,VMB,VMC,CLB,CLC,V,TEM)
        YYBS(I)=YYB2(I-1)+CONSTB*CLB*DT*(YYB2(I-1)-YYB2EQ(I-1))
        YYCS(I)=YYC2(I-1)+CONSTC*CLC*DT*(YYC2(I-1)-YYC2EQ(I-1))
        CALL EQXIDY(PB,PC,QB,QC,DB,DC,YYB2EQ(I),YYC2EQ(I),DENB,DENC,
      1 XXB2(I),XXC2(I))
        XXBS(I)=XXB2(I)+CLB*DT*(YYB2(I)-YYB2EQ(I))
        XXCS(I)=XXC2(I)+CLC*DT*(YYC2(I)-YYC2EQ(I))
 101    CALL EQXIDY(PB,PC,QB,QC,DB,DC,YYB2ES(I),YYC2ES(I),DENB,DENC,
      1 XXBS(I),XXCS(I))
        YYB(I)=YYB2(I-1)+(DT/2.)*CONSTB*CLB*(YYBS(I)+YYB2(I-1)-YYB2ES(I)-
      1 YYB2EQ(I-1))
        YYC(I)=YYC2(I-1)+(DT/2.)*CONSTC*CLC*(YYCS(I)+YYC2(I-1)-YYC2ES(I)-
      1 YYC2EQ(I-1))
        XXB(I)=XXB2(I)+(CLB*DT/2.)*(YYBS(I)+YYB2(I)-YYB2ES(I)-YYB2EQ(I))
        XXC(I)=XXC2(I)+(CLC*DT/2.)*(YYCS(I)+YYC2(I)-YYC2ES(I)-YYC2EQ(I))
        DEVYB=(YYB(I)-YYBS(I))/YYBS(I)
        DEVYC=(YYC(I)-YYCS(I))/YYCS(I)
        IF(ABS(DEVYB)-ERR) 50,50,60
 50     IF(ABS(DEVYC)-ERR) 70,70,60
 70     DEVXB=(XXB(I)-XXBS(I))/XXBS(I)
        DEVXC=(XXC(I)-XXCS(I))/XXCS(I)
        IF(ABS(DEVXB)-ERR) 80,80,60
 80     IF(ABS(DEVXC)-ERR) 71,71,60
 60     IF(ITER-NITER) 81,71,71
 81     YYBS(I)=YYB(I)
        YYCS(I)=YYC(I)
        XXBS(I)=XXB(I)
        XXCS(I)=XXC(I)
        ITER=ITER+1
        GO TO 101
 71     NTR(I)=ITER
        IF(I-NZ) 82,90,90
 82     I=I+1
        GO TO 85
 90     SUMB=SUMB+YYB(NZ)
        SUMC=SUMC+YYC(NZ)
        IF(TT-TIME) 150,200,200
150     DO 151 L=1,NZ
```

FORTRAN IV (V21 45) SOURCE LISTING: YYCAL SUBROUTINE

```
  101          YYB2(L)=YYB(L)
  102          YYC2(L)=YYC(L)
  103          XXB2(L)=XXB(L)
  104 151      XXC2(L)=XXC(L)
  105          K=K+1
  106          GO TO 155
  107 200      TOTK=K+1
  108          YYBAV=SUMB2/TOTK
  109          YYCAV=SUMC2/TOTK
  110          RETURN
  111          END
```

FORTRAN IV (VER 45) SOURCE LISTING: RK SUBROUTINE

```
      1     SUBROUTINE RK(YBI,YCI,YBEQI,YCEQI,XBI,XCI,PB,PC,QB,QC,
      2    1 DC,TC,DENB,DENC,XB,XC,TT,YA,AMW,BMW,CMW,VISA,VISB,VISC,DP,VOID,
      3    2 VMB,VMC,V,AP,TEM)
      4     CALL CMSS(YA,YBI,YCI,AMW,BMW,CMW,VISA,VISB,VISC,DP,VOID,AP,V/B,
      5    1 VMC,CLB,CLC,V,TEM)
      6     AKB1=CLB*(YBI-YBEQI)*TT
      7     AKC1=CLC*(YCI-YCEQI)*TT
      8     X2B=XBI+(AKB1/2.)
      9     X2C=XCI+(AKC1/2.)
     10     CALL EQXTJY(PB,PC,QB,QC,DB,DC,YBEQ,YCEQ,DENB,DENC,X2B,X2C)
     11     AKB2=CLB*(YBI-YBEQ)*TT
     12     AKC2=CLC*(YCI-YCEQ)*TT
     13     X3B=XBI+(AKB2/2.)
     14     X3C=XCI+(AKC2/2.)
     15     CALL EQXTJY(PB,PC,QB,QC,DB,DC,YBEQ,YCEQ,DENB,DENC,X3B,X3C)
     16     AKB3=CLB*(YBI-YBEQ)*TT
     17     AKC3=CLC*(YCI-YCEQ)*TT
     18     X4B=XBI+AKB3
     19     X4C=XCI+AKC3
     20     CALL EQXTJY(PB,PC,QB,QC,DB,DC,YBEQ,YCEQ,DENB,DENC,X4B,X4C)
     21     AKB4=CLB*(YBI-YBEQ)*TT
     22     AKC4=CLC*(YCI-YCEQ)*TT
     23     DXB=(AKB1+2.*AKB2+2.*AKB3+AKB4)/6.
     24     DXC=(AKC1+2.*AKC2+2.*AKC3+AKC4)/6.
     25     XB=XBI+DXB
     26     XC=XCI+DXC
     27     RETURN
     28     END
```

FORTRAN IV (VER 45) SOURCE LISTING: CMSS SUBROUTINE

```
      1       SUBROUTINE CMSS(YA,YB,YC,AMW,BMW,CMW,VISA,VISB,VISC,DP,VOID,AP,
      2     1 VMB,VMC,CLB,CLC,J,TEM)
      3       ALPHB=0.0.5*EXP(-YB/0.00045)
      4       ZC=YC/0.0005
      5       ALPHC=0.005-0.002*ZC+0.000925*ZC**2-0.000103*ZC**3
      6       DEN=YA*AMW+YB*BMW+YC*CMW
      7       VIS=(VISA*YA+VISB*YB+VISC*YC)/(YA+YB+YC)
      8       FACT=(DP**3*VOID**8*DEN)/(VIS*(1.-VOID))
      9       FJB=ALPHB*(FACT**(-0.75))
     10       FJC=ALPHC*(FACT**(-0.75))
     11       DCONST=(7.4*10.**(-8.0))*60.*(AMW**(0.5))
     12       DBA=DCONST*TEM/(VIS*VMB**(0.6))
     13       DCA=DCONST*TEM/(VIS*VMC**(0.6))
     14       CLB=AP*FJB*V*VOID**((DEN*DBA/VIS)**(2./3.))
     15       CLC=AP*FJC*V*VOID**((DEN*DCA/VIS)**(2./3.))
     16       RETURN
     17       END
```

FORTRAN IV (VER 45) SOURCE LISTING: EQYTCX SUBROUTINE

```
      1     SUBROUTINE EQYTCX(PB,PC,QB,QC,DB,DC,YB,YC,DENB,DENC,XB,XC)
      2     XB=PB*YB/(1.+QB*YB/(DENB))+DB*YB
      3     XC=PC*YC/(1.+QC*YC/(DENC))+DC*YC
      4     RETURN
      5     END
```

FORTRAN IV (VER 45) SOURCE LISTING: FOXTOY SUBROUTINE

```
      1     SUBROUTINE FOXTOY(PB,PC,QB,QC,DB,DC,YB,YC,DENB,DENC,XB,XC)
      2     CONSRB=(PB+DB)*QB*XB-QB*XB
      3     YB=(-CONSRB+SQRT(CONSRB**2+4.*QB*DB*XB*DENB))/(2.*QB*DB)
      4     CONSRC=(PC+DC)*QC*XC-QC*XC
      5     YC=(-CONSRC+SQRT(CONSRC**2+4.*QC*DC*XC*DENC))/(2.*QC*DC)
      6     RETURN
      7     END
```

APPENDIX III

DEVELOPMENT OF SCALE-UP AND DESIGN EQUATIONS

Capacity and Column Diameter

In most ion exchange and adsorption applications, column diameters of three feet or more are not uncommon, and, at first, it would appear that the same would be true with parametric pumping columns. In the latter case however, heat transfer is an important consideration--especially if the system obeys the equilibrium theory of Pigford et al (1969) where instantaneous temperature change between the hot upflow and cold downflow half-cycles is a prime requisite. The longer the switchover time (downtime), the longer the overall cycle time, and the lower the capacity for a given installation.

The duration of the switchover time depends on the speed of heat penetration into the column which, in turn, depends on the tube diameter. Sweed (1969) used an equation derived from Carslaw and Jaeger (1959) and applied it to laboratory scale parametric pumping.

$$t_{90} = 0.5\ r^2/k \qquad \text{(III-1)}$$

The time t_{90} for the axis temperature to reach 90% of its ultimate value is directly proportional to the

square of the column radius r, and inversely proportional to the thermal diffusivity k. This equation taken from Carslaw and Jaeger (1959) is basically the same one developed by other workers and shown in the textbook by Bird, Stewart, and Lightfoot (1960). The equation is one solution of the general equation for unsteady state heat conduction,

$$\frac{\partial T}{\partial t} = \alpha \nabla^2 T$$

where α is the thermal diffusivity of the solid. In applying this equation to a packed column an "effective" thermal diffusivity may be used.

This general equation has been solved for practically all conceivable sizes and shapes and the results plotted as constant dimensionless times where, in the case of a cylinder,

$Y = \frac{T-T_0}{T_1-T_0}$, dimensionless temperature or ordinant

and

$X = \frac{r}{R}$, dimensionless radius or abscissa, against which are plotted the dimensionless time curves, $\alpha t/R^2$. In these equations, T is the temperature at the point in question, T_0 is the initial cylinder temperature, T_1

is the surface temperature for all $t > 0$, r is the distance from the center of the cylinder, and R is the radius of the cylinder.

Since the point of interest is only the axis (r=0), the relationship is simplified to one of dimensionless temperature and dimensionless time--the equivalent of reading the ordinant at the intersections of the dimensionless time curves. At the point on the ordinant where the dimensionless temperature is 0.9, the column axis temperature is 90% of the ultimate temperature and $\alpha t/R^2 = 0.5$. This is the equation used by Sweed (1969) and is shown here as Equation (III-1).

Using the thermal diffusivity value of 0.001 $cm^2/sec.$ for the hydrocarbon system toluene-heptane, Sweed calculated two minutes switchover time for the laboratory column. The actual measured time was only 0.75 minutes (which corresponded to a diffusivity of 0.003). In any case, the time was short enough so that the switchover time could be considered "instantaneous" as compared to the half-cycle time of 20 minutes.

Now consider the case where several small tubes are used with the same total cross section area as one large tube. Then, applying Equation (III-1) to both the large

tube (subscript 1) and the small tubes (subscript 2),

$$t_1/t_2 = r_1^2/r_2^2 = d_1^2/d_2^2 \qquad \text{(III-2)}$$

because, after dividing the two equations, the 0.5 factor and the k (thermal diffusivity) cancel out. Moreover if N is equal to the number of tubes and N (area of one small tube) equals the area of one large tube of $Na_2 = a_1$ where a_1 and a_2 are the cross section areas of the large and the small tubes respectively, then $1/N = (d_2/d_1)^2$ and

$$t_1/t_2 = N \qquad \text{(III-3)}$$

Therefore the time required for the temperature switchover in the case of the single tube is N times that for N small tubes. For example, the time required for a normal 45 second switchover for one large tube compared to only 26 small tubes would be 20 minutes--the entire time for a typical half cycle. And, since a production scale unit could require as many as 2226 tubes in a single 3 foot diameter shell heat exchanger configuration, we are talking about a switchover time for a single tube equivalent unit of nearly 28 hours idle time between 20 minute half cycles.

Clearly, if the direct thermal mode (heating and cooling through the walls of the tubes) is to be used

in commercial units, the only way to scale up is by means of multitube parametric pumps in a shell and tube "heat exchanger" configuration.

Capacity and Column Length

In addition to increasing capacity by increasing the number of columns, it is also possible to increase capacity by increasing the fluid velocity through each column. The latter procedure will involve both an increase in pressure drop which will be discussed later, and an effect on the axial adsorption penetration distance which will be discussed in this section.

Chen and Hill (1971) clearly defined one of the fundamental principles of parametric pumping systems obeying the equilibrium theory, the relationship of column length versus capacity. Three distinct regions of operation were described, the boundaries of which were outlined by the relationship of column length and the wave front penetration distances on the hot upflow and cold downflow half-cycles.

Of particular interest in design was their region I and the corresponding equations which defined the limitations of pump operation necessary to insure high separation capabilities. The basic requirement was that

the penetration distance on cold downflow must be less than or equal to the penetration distance on hot upflow or the height of the column. That is

$$L_2/L_1 \leq 1 \text{ and } L_2 \leq h \qquad \text{(III-4)}$$

where L_1 and L_2 are the wave front penetration distances on hot upflow and cold downflow respectively and h is the height or length of the column.

Chen et al (1972) conveniently defined L_1 and L_2 for the continuous parametric pump as

$$L_2 = \frac{v_o(1+\phi_B)}{(1+b)(1+m_o)} \quad \frac{\pi}{\omega} \qquad \text{(III-5)}$$

and

$$L_2/L_1 = \frac{1+\phi_B}{1-\phi_B} \quad \frac{1+b}{1-b} \qquad \text{(III-6)}$$

And, as shown by Chen at al (1974) these equations are converted to a multicomponent system by simply adding the subscript i to L_1, L_2, m_o, and b. L_1 and L_2 were previously defined while m_o and b are dimensionless equilibrium constant parameters. ϕ_B, v_o, and π/ω are general terms, and represent the bottom product/reservoir rate, interstitial velocity and the half-cycle time

respectively. It should be pointed out that b (or b_i) and the other parameters that bear the subscript i refer to a particular component in relation to the common solvent whether the system is a binary or multicomponent. For the present design purposes, once the key component has been selected and the values assigned, the subscript i may be dropped. This will be done in the equations that follow.

As pointed out by Chen et al (1972)(1974), ϕ_B must be set at a value less than b, a condition for the operation of the column such that the component i, at steady state, does not appear in the bottom product stream. Also, as a condition for design, $L_2 = h$, which means that as a design limit for maximum separation

$$h \geq L_2 = \frac{(1+\phi_B)\ \frac{\pi}{\omega}}{(1+b)\,(1+m_o)} \cdot v_o \qquad \text{(III-7)}$$

so that if the operating conditions of the bottom product rate ratio, ϕ_B, the half-cycle time, π/ω, are set for a given system (fixed b and m_o), then as a limit

$$h \geq (\text{constant})\ v_o \qquad \text{(III-8)}$$

or, in terms of the superficial velocity, v,

$$h \geq K\ v/\varepsilon = K'v \qquad \text{(III-9)}$$

where $K' = (1+\phi_B)(\pi/\omega) / [(1+b)(1+m_o)\varepsilon]$ (III-10)

h, the column length, may be related to column capacity since

$$v = Q/a_t N \quad \text{(III-11)}$$

where Q is the reservoir displacement rate, a_t is the cross section area of one tube, and N is the number of tubes.

Therefore

$$h \geq K'Q/a_t N = K''Q/N \quad \text{(III-12)}$$

where

$$K'' = \frac{(1+\phi_B)(\pi/\omega)}{(1+b)(1+m_o)\varepsilon a_t} \quad \text{(III-13)}$$

so that, for a given system, product rate, and tube size, there is a direct relationship between tube length and capacity.

Heat and Material Balances Around the Top of the Column

The heat and material balances around the top of the column are required to calculate the true temperature of the fluid re-entering the column on cold downflow. This temperature value is required for an accurate estimate of the cooling requirements for the cold downflow

half-cycle. Heat and material balances for both the hot upflow and cold downflow half-cycles must be considered. In all cases, the reference temperature will be $0^{o}K$.

Hot Upflow Balance

Heat Input from the Feed = $(\phi_T+\phi_B)Q\rho_F c_F(T_F-0)$

Heat Input from the Column = $(1-\phi_B)Q\rho_{T1}c_{T1}(T_1-0)$

Heat Output to Top Product= $\phi_T Q\rho_{TP1}c_{TP1}(T_{TP1}-0)$

Heat Output to Reservoir = $Q\rho_{TP1}c_{TP1}(T_{TP1}-0)$

$$(\phi_T+\phi_B)Q\rho_F c_F T_F+(1-\phi_B)Q\rho_{T1}c_{T1}T_1=Q(1+\phi_T)\rho_{TP1}c_{TP1}T_{TP1}$$

Cold Downflow Balance

Heat Input from the Feed = $(\phi_T+0_B)Q\rho_F c_F(T_F-0)$

Heat Input from Reservoir = $Q\rho_{TP1}c_{TP1}(T_{TP1}-0)$

Heat Output to Top Product= $\phi_T Q\rho_{TP2}c_{TP2}(T_{TP2}-0)$

Heat Output to the Column = $Q(1+\phi_B)\rho_{T2H}(T_{2H}-0)c_{2H}$

$$(\phi_T+\phi_B)Q\rho_F c_F T_F+Q\rho_{TP1}c_{TP1}T_{TP1}=Q\phi_T\rho_{TP2}c_{TP2}T_{TP2}+Q(1+\phi_B)\rho_{T2H}c_{T2H}T_{2H}$$

Combining the two heat balances:

$$2(\phi_T+\phi_B)\rho_F c_F T_F+(1-\phi_B)\rho_{T1}c_{T1}T_1-\phi_T\rho_{TP1}c_{TP1}T_{TP1}-\phi_T\rho_{TP2}c_{TP2}T_{TP2}-(1+\phi_B)\rho_{T2H}c_{T2H}T_{2H}=0 \quad .$$

and

$$T_{2H}=\frac{2(\phi_T+\phi_B)\rho_F c_F T_F+(1-\phi_B)\rho_{T1}c_{T1}T_1-\phi_T\rho_{TP1}T_{TP1}-\phi_{TP2}c_{TP2}T_{TP2}}{(1+\phi_B)\rho_{T2H}c_{T2H}} \qquad \text{(III-14)}$$

The overall effect is to lower the temperature of the stream (T_{2H}) re-entering the column. It is twice lowered by the feed stream and lowered by heat removed in the top product stream during both the hot upflow and cold downflow half cycles.

The effect of the heat removed can be neglected if it is assumed that the feed enters the top of the column at the same temperature as the fluid leaving the column during the hot half cycle. In this case the operation would be isothermal in both the hot upflow and cold downflow half cycles and the temperature in all cases would be T_1, the hot upflow temperature of the fluid leaving the column.

This assumption of a relatively hot feed temperature is not unreasonable because, in many real cases, the feed could come from an exothermic reaction and any excess enthalpy could be usefully "siphoned" off via a heat exchanger external to the parametric pumping process.

Also in those cases where the feed temperature is normally lower than T_1, it could be increased by heat exchange with the slightly warmer product stream. In any actual case, the temperature differences of the streams around the top of the column would be small, and, for purposes of this usage, could be considered isothermal.

Heating and Cooling Requirements

Heat is provided by a recirculating liquid system heated indirectly by steam. The total duty is the sum of the duty for heating the tubes and tube contents from the cold to the hot temperature plus the duty for heating the fresh fluid as it is pumped into the column during the hot half cycle. Duty required to heat the exchanger shell, tubesheets, and external piping can be neglected for rough estimates if it is assumed that these equipment sections are insulated. The duty for heating or cooling the residual heat transfer fluid left in the shell is not included because this fluid is dumped to the appropriate reservoir prior to starting the next half cycle. The heat that is saved by this procedure is estimated by Equation (III-50).

The duty for heating the tubes and tube contents is:

$$q_t = (w_t c_t + w_s c_s + w_f c_f)(T_1 - T_2)(N)(h) \quad \text{(III-15)}$$

where w and c are the mass per unit length and heat capacity at constant pressure of the tubes, the solid adsorbent, and the fluid phase surrounding the adsorbent. T_1 and T_2 are the hot upflow and cold downflow column temperatures respectively, N is the number of tubes in the exchanger, and h is the height (length) of the exchanger tubes.

The duty for heating the process fluid being pumped through the tubes during the hot half cycle is:

$$q_1' = Q(1-\phi_B)(\rho_1)(T_1-T_2)(\pi/\omega)(c_1) \qquad \text{(III-16)}$$

where $Q(1-\phi_B)$ is the volumetric flow rate in the column, ρ_1 is the fluid density at T_1, π/ω is the half cycle time duration, and c_1 is the specific heat of the incoming fluid.

Now if n is the number of half cycles (or cycles) for any time period under consideration, the total heating duty for that time period is:

$$q_1 = \left[(w_t c_t + w_s c_s + w_f c_f)(N)(h) + Q(1-\phi_B)(\rho_1)(c_1)(\pi/\omega)\right](T_1-T_2)(n) \qquad \text{(III-17)}$$

The cooling duty estimation is slightly complicated by the fact that the effluent leaving the top of the column is contacted by the feed and is heated (or cooled) by the incoming feed. Also, some heat is removed by the effluent top product stream. The same is true during the cold downflow half cycle when the top reservoir effluent is again heated or cooled by contact with the feed, and more heat is removed by the top product stream. In this situation, the temperature of the fluid (T_{2H}) would be

different for each design and its value can be estimated from the equation derived previously.

$$T_{2H} = \frac{2(\emptyset_B+\emptyset_T)(\rho cT)_F + (1-\emptyset_B)(\rho cT)_1 - \emptyset_T(\rho cT)_{TP1} - \emptyset_T(\rho cT)_{TP2}}{(1+\emptyset_B)(\rho c)_{T2H}} \qquad \text{(III-14)}$$

In this equation, the reservoir volumetric term Q, being common to all the streams in the heat balance cancels out, leaving the terms $\emptyset_T$ and $\emptyset_B$, the ratios of the top and bottom product stream flow rates to the reservoir flow rate. Similarly, the terms $(\emptyset_T+\emptyset_B)$, $(1-\emptyset_B)$, and $(1+\emptyset_B)$ refer to the feed, the column upflow, and column downflow rates, respectively. The subscripts F, 1, TP1, and T2H refer to the feed, hot upflow column effluent, top product during column up and downflow half cycles, and to the stream re-entering the column during cold downflow.

The overall cooling duty is therefore:

$$q_2 = (w_t c_t + w_s c_s + w_f c_f)(N)(h)(T_1-T_2)(n)$$

$$+ (1+\emptyset_B)(\rho_2)(c_2)(\pi/\omega)(T_{2H}-T_2)(n) \qquad \text{(III-18)}$$

This equation is quite similar to the equation for the heating half cycle except for the T_{2H} and $(1+\emptyset_B)$ terms. For rough estimations, it would not be unreasonable to assume that the feed enters at the same temperature

as the hot upflow column effluent. This could easily be the case if the feed were the product of an exothermic reaction. If adiabatic operation around the top of the column were also assumed, then the common temperature T_1 would apply to all the streams and $T_{2H} = T_1$.

Column Pressure Drop

The total pressure drop includes, in addition to the drop through the column, the pressure drop in the lines, static drop, expansion and contraction losses, etc. With careful design and attention to layout, these incidential losses can be considered negligable compared to the drop through the columns. Also, the amount of dead volume (volume of the reservoir, pump, and lines in excess of the column displacement) can be accounted for by the theory, and only the drop through the column itself need be considered.

The pressure drop in the packed bed may be expressed by the dimensionless Blake-Kozeny equation for laminar flow:

$$\frac{\Delta p g_c \rho}{G^2} \quad \frac{D_P}{h} \quad \frac{\varepsilon^3}{1-\varepsilon} = \frac{150\ (1-\varepsilon)}{D_p G/\mu} \qquad \text{(III-19)}$$

where Δp is the pressure drop in lb_f/ft^2

G is the rate in $lb/hr/ft^2 = v\rho$

μ is the viscosity in $lb_m/hr/ft$

Rearranging and substituting,

$$\Delta p = \frac{150\ (1-\varepsilon)^2}{D_p^2\ g_c \varepsilon^3}\ (\mu)(h)(v) \qquad \text{(III-20)}$$

where v = velocity = $Q/A(1-\phi_B)$ for hot upflow and

$Q/A(1+\phi_B)$ for cold downflow in ft/hr

g_c = conversion factor = $4.17 \times 10^8 = (lb_m/hr^2/ft)(ft^2/lb_f)$

Q = reservoir flow rate in ft^3/hr

A = total crossflow area = flow area/tube x no. of tubes

$= a_t N$

Now if the static head, $(h\rho)$ is to be handled separately as a part of the overall pumping system layout,

$$\Delta p = \frac{150(1-\varepsilon)^2}{D_p^2\ g_c \varepsilon^3}\ \frac{\mu h}{a_t N}\ Q(1 \mp \phi_B) \qquad \text{(III-20)}$$

for hot upflow and cold downflow respectively.

Now the rate of flow is $Q(1-\phi_B)$ for hot upflow and $Q(1+\phi_B)$ for cold downflow.

The hydraulic horsepower for the pump is easily calculated as follows:

$$(\Delta p)\,(lb_f/ft^2)\,(Q(1\mp\phi_B)\,(ft^3/hr)\,(Hp\text{-}hr/1.98x10^6 ft\text{-}lb_f)$$

$$Hp_1 = \frac{150(1-\varepsilon)^2}{D_p^2\, g_c \varepsilon^3}\ \frac{h}{a_t N}\ Q^2\ \mu_1 (1-\phi_B)^2\ (1.98x10^6)^{-1} \qquad \text{(III-21)}$$

$$Hp_2 = \Delta p_2 (Q)\,(1+\phi_B)\,(1.98x10^6)^{-1} \qquad \text{(III-22)}$$

It should be noted that the viscosity could be roughly estimated from the equation from Bird, Stewart and Lightfoot (1960)

$$\mu = 9.65x10^{-3}\rho/M \exp\ (3.8T_B/T)\ lb_m ft^{-1} hr^{-1}$$

Substitution of this equation would eliminate the viscosity variable. However, the accuracy would be poor and would not allow for the concentration effect.

Heat Transfer Fluid Pressure Drop

The equations used in this derivation are based on those presented by Donohue (1955). The pressure drop through the shellside of a heat exchanger may be divided into two main parts, the drop through the baffle openings and the drop across the rows of tubes between the baffles.

The pressure drop through each baffle opening is:

$$\Delta p_b' = 3.76\ G_b^2/(s.g.x10^6) \qquad \text{Donohue (1955)}$$

where $G_b = w/A_b$ = mass flow rate/area = lb/sec/ft^2

and $A_b = 3.14/4\ (d^2-ND^2)\ B_c$

in which A_b = area through the baffle opening

d = i.d. shell, ft.

D = o.d. tubes, ft.

B_c = baffle cutout fraction

N = no. tubes in the shell

s.g. = specific gravity of the fluid

Now the number of baffle openings in h/B_s-1

where h = tube length, ft.

and B_s = baffle spacing, ft.

Therefore the total pressure drop through all the baffle openings is:

$$\Delta P_b = 6.10\text{x}10^{-6} w^2 B_c^{-2}\ (d^2-ND^2)^{-2}(h/B_s-1) \quad \text{(III-23)}$$

The pressure drop across each tube bank for turbulent flow is: $\Delta p_c' = 1.98\text{x}10^{-6}(G_c)^{1.8}(\mu^{.2}/\text{s.g.})(N')(P-D)^{-0.2}$

Donohue (1955)

where $G_c = w/A_c$ = mass flow rate/area = lb/sec/ft^2

and $A_c = (d-N_cD)(B_s)$

where N_c = number of crossflow tubes = 1 + (outer diameter tube bundle-tube diameter)/(space between tubes). The outer tube bundle diameter (for the case of a triangular pitch (equal to 1.375D and the flow perpendicular to the apex) was calculated for 5,6,8,10,12, and 36 inch

shells and was found to range from 92-96% of the shell i.d. so that OTL = 0.94d ± 2%. Furthermore, for this configuration, the space between the tubes is equal to the pitch so that:

$$N_c = 1 + (0.94d - D)/1.375D = (0.94d + 0.375D)/1.375D$$

$$N_c D = (0.94d + .375D)/1.375 \qquad \text{(III-24)}$$

$$\text{and } A_c = \left[(0.435d - 0.375D)/1.375\right](B_s) \qquad \text{(III-25)}$$

$$\text{Therefore } G_c = 1.375w/(0.435d - 0.375D)/B_s \qquad \text{(III-26)}$$

Now N' = number of tube rows in the direction of flow which are covered by one baffle

$$N' = (1-B_c)(OTL-D)/0.866P = (1-B_c)(0.94d-D)/1.191D$$

$$P-D = 1.375D - D = 0.375D = 4.5D \text{ where D is in ft.}$$

$$\text{and } \Delta p'_c = \frac{2.183\times10^{-6}(w)^{1.8}(\mu)^{0.2}(1-B_c)(0.94d-D)}{(0.435d-0.375D)^{1.8}(B_s)^{1.8}(s.g.)(D)^{1.2}} \qquad \text{(III-27)}$$

Now the number of tube rows crossed is h/B_s.

Therefore, for turbulent flow:

$$\Delta p_c = \frac{2.183\times10^{-6}(w)^{1.8}(u)^{0.2}(1-B_c)(0.94d-D)(h)}{(0.435d-0.375D)^{1.8}(B_s)^{2.8}(s.g.)(D)^{1.2}} \qquad \text{(III-28)}$$

In the case of laminar flow:

$$\Delta p'_c = 8.37 \times 10^{-7}\ N's.g.^{-1} (G'_c)(\mu)/\bar{P}\text{-}D) \qquad \text{Donohue (1955)}$$

$$\Delta p_c = \frac{2.147 \times 10^{-7} (1-B_c)(0.94d-D)(w)(\mu)(h)}{(s.g.)(0.435d-0.375D)(B_s)^2 (D)^2} \qquad \text{(III-29)}$$

The total pressure drop through the exchanger shell is:

$\Delta p = \Delta p_b + \Delta p_c$ and the drop can be calculated accurately from the equations derived. However, if some simplifying assumptions are made, e.g.:

$B_c = 0.2$ A 25% cutout for baffles is a common design

Bs = 0.5 ft. A 6 inch baffle spacing may be assumed

D = 0.5/12 ft. 1/2 inch tubes approximate lab columns

$s.g. \tilde{=} 1$ Assume the fluid is water

$\mu^{.2} \tilde{=} 1$ This is reasonable even for water at high temp.

For turbulent flow, the simplified total pressure drop is:

$$\Delta p = \frac{1.525 \times 10^{-4} (w)^2 (2h-1)}{(d^2-0.001736N)^2} + \frac{2.756 \times 10^{-4} (w)^{1.8} (.94d-.0417) 2h}{(0.435d-0.01563)^{1.8}} \qquad \text{(III-30)}$$

For laminar flow, the simplified total pressure drop is:

$$\Delta p = \frac{1.525x10^{-4}(w)^2(2h-1)}{(d^2 - 0.001736N)^2} + \frac{1.979x10^{-4}(.94d-.0417)2w\mu h}{(0.435d - .01563)}$$

(III-31)

As shown in Figure (32) for the configuration described,

$$d = 0.07571N^{0.4734} \text{ and } d^2 = 0.005732^{0.9474}$$

(III-32)

Therefore, for turbulent flow:

$$\Delta p = \frac{1.525x10^{-4}(w)^2(2h-1)}{(0.005732N^{.9474}-0.001736N)^2} + \frac{2.756x10^{-4}(w)^{1.8}(.07117N^{.4737}-.0417)2h}{(.03293N^{.4737}- .01563)^{1.8}}$$

(III-33)

And for laminar flow:

$$\Delta p = \frac{1.525x10^{-4}(w)^2(2h-1)}{(0.005732N^{.9474}-0.001736N)^2} + \frac{1.979x10^{-4}(.07117N^{.4737}-.0417)2w\mu h}{(.03293N^{.4737} - .01563)}$$

(III-34)

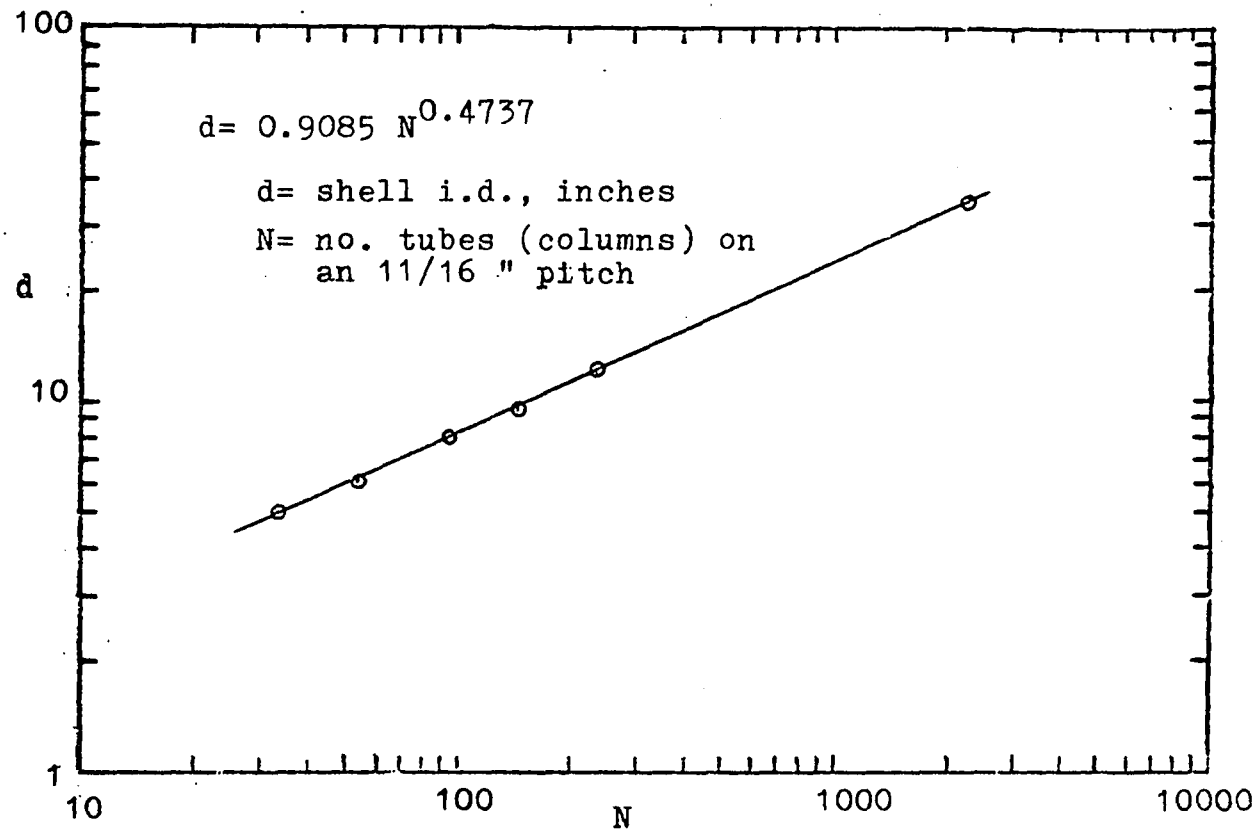

FIGURE (32)

Heat Exchanger: No. Tubes vs Shell Diameter

where w = fluid (water) rate in lbs/second

h = length of the exchanger tubes, ft.

Δp= pressure drop in psi

N = number of tubes in the exchanger. This must be the full number of tubes that will fill a given shell diameter. Otherwise, "dummy" tubes must be used or the pressure drop calculated will not apply. Also, the tubes must be arranged in a triangular pitch with the flow directed perpendicular to the apex, and the pitch must be 1.375x tube diameter. Finally, it was also assumed that the baffle cutout was 20% (25% area) and that the baffle spacing was 0.5 ft. Most of these assumptions are typical for design, and even the baffle spacing is quite reasonable for the present purpose. However, if it is required, the complete equation with only the first four assumptions, including the 1.375 D pitch, is available in the Appendix.

Also, for the case of laminar flow, the viscosity, μ, is included in the equation. In the case of turbulent flow, the viscosity term was raised to the 0.2 power and, as such could be neglected.

The hydraulic horsepower for the pump is easily calculated from the pressure drop as follows:

$$Hp = \Delta p,\ lb_f/in^2\,(144\ in^2/ft^2)\,(w\ lb_m/sec)\,(3600\ sec/hr)$$

$$(ft^3/62.3\ lb_m)\,(Hp\text{-}hr/1.98\times10^6\ ft\text{-}lb_f)$$

$$Hp = 0.00420\Delta p(w) \qquad \text{(III-35)}$$

Feed and Product Pressure Drop

The feed pump must overcome the line resistance to the column, the pressure developed in the column due to the action of the hot upflow and cold downflow reservoir pumps, and the resistance in the lines to the top and bottom product receivers. During the hot upflow half cycle, the column back pressure is almost nil because the pressure exerted by the hot upflow reservoir pump is spent as the effluent leaves the column. However, the back pressure during the cold downflow half cycle is, for all practical purposes, equal to the full pressure developed by the cold downflow reservoir pump. Therefore, if a positive displacement pump is used for feeding the column, the pressure and the power required is much less during the hot upflow half cycle than during the cold downflow half cycle.

However, if a centrifugal pump is used, the feed rate must be kept at a constant value by means of a flow rate controller and valve. In this case, the feed pump develops full pressure during both hot upflow and cold

downflow half cycles. During the cold downflow half cycle, the back pressure is high and the control valve compensates by assuming a wide open position. During the hot upflow half cycle, the pressure is low and the control valve must exert the missing back pressure in order to maintain a constant flow rate to the column. Therefore, during both the hot upflow and cold downflow half cycles, a centrifugal type feed pump would deliver a constant pressure and would consume a constant amount of power.

The pressure required to overcome the resistance in the top and bottom product lines must be developed by all three pumps (feed, hot upflow reservoir, and cold downflow reservoir pumps) because these lines eminate from the two common high pressure points at the top and bottom of the column. One way of assuring constant flow rates and sufficient pressure to overcome the resistance in the lines would be to install a back-pressure valve in the top product line and a flow controller and control valve in the bottom product line. Exact control of the bottom product rate is desirable because this value is critical to the process. Flow control of the top product stream is thus obtained indirectly because the feed stream is also controlled.

As previously discussed, the pressure drop during the hot upflow half cycle is, essentially, the line pressure drop. Since the flow rates are very low, the equations for laminar flow would apply:

$$\Delta p = \frac{4fl}{D_i} \quad \frac{v^2\rho}{2g_c}$$

$$f = \frac{16}{Re} = \frac{16\mu}{D_i v\rho}$$

$$\Delta p = \frac{64\mu l}{D_i^2 v\rho} \quad \frac{v^2\rho}{2g_c} = \frac{32\mu lv}{D_i^2\, g_c}$$

where μ = viscosity $lb_m/hr/ft$

l = line length, ft.

v = velocity, ft/hr

ρ = fluid density lb_m/ft^3

g_c = conversion factor = $4.17 \times 10^8 = (lb_m/hr^2/ft)(ft^2/lb_f)$

D_i = inside diameter conduit, ft.

$\Delta p = lb_f/ft^2$

now if $v_F = (\phi_T + \phi_B)Q/.785\ D_i^2$ for the feed (III-36)

$v_{TP} = \phi_T Q/\ .785 D_i^2$ for the top product (III-37)

$v_{BP} = \phi_B Q/\ .785 D_i^2$ for the bottom product (III-38)

then the total pressure drop for the hot upflow half cycle is:

$$\Delta p = \frac{32Q}{.785D_i^4 g_c}\left[\mu_F l_F(\phi_T+\phi_B) + \mu_{TP} l_{TP}\phi_T + \mu_{BP} l_{BP}\phi_B\right] + \Delta p_v \qquad \text{(III-39)}$$

where Δp_v = pressure drop for the control valve.

For the case where a positive displacement pump is used,

$$\Delta p_v = 0$$

For the case where a centrifugal pump is used, Δp_v is the full pressure drop developed by the reservoir pump. This was previously derived and the equation is:

$$\Delta p_v = \frac{150(1-\varepsilon)^2}{D_p^2 g_c \varepsilon^3}\ \frac{\mu h}{a_t N}\ Q(1+\phi_B) \qquad \text{(III-20)}$$

It should be pointed out that this pressure drop was that derived for the cold downflow. The equation derived for hot upflow would not be applicable because it represents the pressure developed at the discharge of the hot upflow reservoir pump at the bottom of the column whereas the feed input is at the top of the column.

The overall equation for the feed pump pressure drop for the cold downflow half cycle for both the centrifugal and positive displacement pumps is:

$$\Delta p_F = \frac{32Q}{.785D_i^4 g_c}\left[\mu_F l_F(\phi_T+\phi_B) + \mu_{TP} l_{TP}\phi_T + \mu_{BP} l_{BP}\phi_B\right]$$

$$+ \frac{150(1-\varepsilon)^2}{D_p^2 g_c \varepsilon^3}\ \frac{\mu h}{a_t N}\ Q(1+\phi_B) \qquad \text{(III-40)}$$

This is also the pressure drop equation for the centrifugal pump for the hot upflow half cycle. As previously discussed, due to the action of the control valve, the pressure drops for both the hot upflow and cold downflow half cycles are the same.

The hydraulic horsepower is easily calculated for the cold downflow half cycle for both the centrifugal and P.D. pumps:

$$Hp_F = \Delta p\ lb_f/ft^2 (\text{rate, } ft^3/hr)(Hp\text{-}hr/1.98\text{x}10^6 ft\text{-}lb_f)$$

$$Hp_{F2} = \frac{2.059\text{x}10^{-5}\ Q^2}{D_i^4 g_c}\left[\mu_F l_F(\phi_T+\phi_B)^2 + \mu_{TP} l_{TP}\phi_T^2 + \mu_{BP} l_{BP}\phi_B^2\right]$$

$$+ \frac{7.576\text{x}10^{-5}(1-\varepsilon)^2}{D_p^2 g_c \varepsilon^3}\ \frac{\mu h}{a_t N}\ Q^2(1+\phi_B)^2 \qquad \text{(III-41)}$$

For the hot upflow half cycle, the equations are:

For the centrifugal pump:

$$Hp_{Fl} = \frac{2.059x10^{-5}Q^2}{D_i^4 g_c}\left[\mu_F l_F(\phi_T+\phi_B)^2+\mu_{TP}l_{TP}\phi_T^2+\mu_{BP}l_{BP}\phi_B^2\right]$$

$$+ \frac{7.576x10^{-5}(1-\varepsilon)^2}{D_p^2 g_c \varepsilon^3}\ \frac{\mu h}{a_t N}\ Q^2(1+\phi_B)(1-\phi_B) \qquad \text{(III-42)}$$

For the positive displacement (P.D.) pump:

$$Hp_{Fl} = \frac{2.059x10^{-5}Q^2}{D_i^4 g_c}\left[\mu_F l_F(\phi_T+\phi_B)^2+\mu_{TP}l_{TP}\phi_T^2+\mu_{BP}l_{BP}\phi_B^2\right] \qquad \text{(III-43)}$$

Utility Cost Equations

The cost of operating the parametric pumping system is a useful criteria on which to base the choice of a feed material. Certainly, the value of the products from separation would have to equal, as a bare minimum, the cost of the utilities. In any real design, the costs of depreciation, labor, and overhead would also have to be met. But these costs can vary widely depending on the materials of construction, the use of new or existing equipment, the labor costs in particular area, the degree of automatic control adopted, and other factors. For the present case, the purpose is mainly to provide a basic yardstick against which to measure the feasibility of

attempting the separation at all. The other factors can be readily taken into account once the actual basic cost of operating the equipment has been established.

The utility operating costs can best be estimated on a yearly basis. In the case of pumping, the design equations were developed for the hydraulic horsepower for the hot up and cold downflow half cycles. To obtain the yearly costs, it is necessary to multiply the hydraulic horsepower by the duration of the half cycles, (π/ω), the number of half cycles per year (n), the reciprocal of the pump efficiency (1/E), the conversion factor (0.746 kw-hr./Hp-hr.), and the cost of electricity in \$/kw-hr (C_{EL}).

For the heating and cooling requirements, the duties were developed as equations for the duration of the hot upflow and cold downflow half cycles. The cost of heating may be taken as the cost of the steam used during all the hot upflow half cycles during the year and the cost of cooling may be taken as the cost of brine refrigeration consumed during the cold downflow half cycles. Therefore, if (n) is taken as the number of cycles (or half cycles) per year, the cost

of heating may be estimated by multiplying the appropriate equation by the reciprocal of the heating value of a pound of steam (roughly 1/1000) and by the cost of a pound of steam (C_{ST}).

The cost of cooling (refrigeration) would be estimated by multiplying the appropriate equation by the conversion factor (ton-hr/12000 BTU) and by the cost of the brine in dollars per ton-hr (C_{BR}).

The overall cost of the utilities for operating the plant would be as follows:

$$C_O = \left[(w_t c_t + w_s c_s + w_f c_f)(N)(h) + Q(1-\phi_B)(\rho_1)(c_1)(\pi/\omega)\right]$$

$$(T_1 - T_2)(n)(C_{ST}/1000)$$

$$+ \left[(w_t c_t + w_s c_s + w_f c_f(N)(h) + Q(1+\phi_B)(\rho_2)(c_2)(\pi/\omega)\right]$$

$$(T_2 - T_{2H})(n)(C_{BR}/12000)$$

$$+\ 0.00420(n)(2\pi/\omega)(0.746/E)(C_{EL})$$

$$\left[\frac{1.525\times10^{-4}(w)^{3}(2h-1)}{(0.005732N^{0.9474}-0.001736N)^{2}}\right.$$

$$\left.+\ \frac{2.756\times10^{-4}(w)^{2.8}(0.07117N^{0.4737}-0.04117)(2h)}{(0.03293N^{0.4737}-0.01563)^{1.8}}\right]$$

$$+(1.98\times10^{6})^{-1}(\pi/\omega)(n)(0.746/E)(C_{EL})$$

$$\left[\frac{150(1-\varepsilon)^{2}}{D_p^2 g_c \varepsilon^3}\quad\frac{\mu h}{a_t N}(Q^2)\right]\left[\mu_1(1-\phi_B)^2+\mu_2(1+\phi_B)^2\right]$$

$$+\ (1.98\times10^{6})^{-1}(\pi/\omega)(n)(0.746/E)C_{EL})$$

$$\left\{\frac{2\ \times\ 32\ Q^2}{0.785D_i^4\ g_c}\quad\left[\mu_F l_F(\phi_B+\phi_T)^2+\mu_{TP}l_{TP}\phi_T^2+\mu_{BP}l_{BP}\phi_B^2\right]\right.$$

$$\left.+\ \frac{150\ (1-\varepsilon)^2}{D_p^2\ g_c\varepsilon^3}\quad\frac{\mu_2 hQ^2}{a_t N}\left[(1+\phi_B)^2+(1+\phi_B)(1-\phi_B)\right]\right\}$$

(III-44)

These equations apply to the conditions of turbulent flow in the parapump assembly shell, laminar flow in the feed and product lines, and the use of a centrifugal type feed pump. Equations have been derived for alternate conditions and are presented in the design equation sections and in the Appendix. However, the equations used in the cost equation represent the most likely conditions to be met in any actual design.

Energy Equations

In this section the energy equations for steam, refrigeration, and electrical pumping power are developed as functions of the key parameters of reservoir displacement ($Q\pi/\omega$), the bottom product/reservoir ratio (ϕ_B), the reservoir displacement rate (Q), the cycle time (π/ω), and the number of tubes (n) in the multicolumn parapump assembly.

To put the energy equations on a common basis, the electrical energies will be converted to their equivalents in BTU/cycle. Then all energy equations will also be presented as BTU/lb of bottom product.

Steam heating. The duty in BTU/cycle is obtained by combining Equations (III-12, 13) with Equation (III-17)

$$q_1 = \left[\frac{(w_t c_t + w_s c_s + w_f c_f)(T_1 - T_2)}{(1+m_o)(1+b)(\varepsilon)(a_t)}\right](Q\pi/\omega)(1+\phi_B) + \rho_f c_f (T_1 - T_2)(Q\pi/\omega)(1-\phi_B) \qquad \text{(III-45)}$$

Now since the pounds of bottom product per cycle is

$$P_B(2\pi/\omega) = Q\phi_B\rho_f(2\pi/\omega) = 2\rho_f(Q\pi/\omega)\phi_B \qquad \text{(III-46)}$$

the duty per pound of bottom product is

$$\frac{q_1}{P_B(2\pi/\omega)} = \left[\frac{(w_t c_t + w_s c_s + w_f c_f)(T_1 - T_2)}{(1+m_o)(1+b)(\varepsilon)(a_t)(2\rho_f)}\right]\frac{(1+\phi_B)}{\phi_B} + \left[\frac{c_f(T_1 - T_2)}{2}\right]\frac{(1-\phi_B)}{\phi_B} \qquad \text{(III-47)}$$

Heat transfer fluid. If the parapump system design is correct, heat transfer fluid left in the shell at the end of a hot or cold half cycle should normally be displaced to the reservoir servicing the column during that half cycle. The heat saved by this procedure can be a substantial portion of the total. This heat content is

$$q_s = V_s \rho_{HTF} c_{HTF} (T_1 - T_2)$$

where V_s is the volume of the shellside fluid, and

$$V_s = .785h(d^2 - D^2N) \qquad \text{(III-48)}$$

Now, from Equations (III-12,13),

$$h \geq \left[\frac{1}{(1+b)(1+m_o)\varepsilon(a_t)}\right] \left(Q\frac{\pi}{\omega}\right)\left(\frac{1+\phi_B}{N}\right) = K_h \left(Q\frac{\pi}{\omega}\right) \frac{1+\phi_B}{N} \qquad \text{(III-48a)}$$

and

$$d = 0.07571\ N^{0.4737} \qquad \text{(III-32)}$$

Then

$$V_s = \frac{(1+\phi_B)(Q\pi/\omega)}{(1+b)(1+m_o)\varepsilon(a_t)} \quad (0.0045N^{-0.0526} - 0.785D^2) \qquad \text{(III-49)}$$

and

$$q_s = \frac{(1+\phi_B)(Q\pi/\omega)(\rho c)_{HTF}(T_1 - T_2)}{(1+b)(1+m_o)(\varepsilon)(a_t)} \quad \left[\frac{0.0045}{N^{0.0526}} - .785D^2\right] \qquad \text{(III-50)}$$

Now Equation (III-50) represents the heat content of the heat transfer fluid surrounding the tubes at the end of each half cycle and is ordinarily ignored in bench scale operations. However, even in this case, there is occasionally some difficulty in restoring the hot and cold operating temperatures of the baths during the recuperation periods when there is no direct process heat or cooling load.

If the design or the operation is poor and the shellside heat transfer fluid is, at the end of the cold half cycle, dumped into the hot fluid reservoir, then the temperature of the reservoir must be raised above the normal operating level to provide the sensible heat needed to cope with the instantaneous load represented by Equation (III-50) in addition to the instantaneous load due to the temperature switchover of the tubes (Equation III-15). The same duties apply to the cold fluid reservoir and the refrigeration load.

Therefore, Equation (III-50) is a potential maximum additional duty for both steam and refrigeration in units of BTU/cycle. In BTU per pound of bottom product,

$$\frac{q_s}{P_B(2\pi/\omega)} = \frac{(\rho_{HTF})(c_{HTF})(T_1-T_2)}{(1+b)(1+m_o)(\varepsilon)(a_t)(2\rho_f)} \left[\frac{0.0045}{N^{0.0526}} - .785D^2\right] \frac{1+\phi_I}{\phi_B}$$

(III-51)

Refrigeration cooling. The equations for cooling are almost identical to those for heating. Combining Equations (III-12, 13 and III-18), the BTU/cycle

$$q_2 = \left[\left[\frac{(w_t c_t + w_s c_s + w_f c_f)}{(1+m_o)(1+b)(\varepsilon)(a_t)} + \rho_f c_f\right] (T_1-T_2)\right] Q\pi/\omega)(1+\phi_B)$$

(III-52)

and the duty per pound of bottom product is

$$\frac{q_2}{P_B(2\pi/\omega)} = \left[\left[\frac{(w_t c_t + w_s c_s + w_f c_f)}{(1+m_o)(1+b)(\varepsilon)(a_t)(2\rho_f)} + \frac{c_f}{2}\right](T_1-T_2)\right] \frac{(1+\phi_B)}{\phi_B}$$

(III-53)

Heat transfer fluid pump. The power for heat transfer fluid pumping depends first on the heat transfer during the switchover period, which, by combining Equations (III-15) and (III-12, 13) is, in BTU/switchover,

$$q_t = \left[\frac{(w_t c_t + w_s c_s + w_f c_f)(T_1 - T_2)}{(1+m_o)(1+b)(\varepsilon)(a_t)}\right] (Q\pi/\omega)(1+\phi_B) \qquad \text{(III-54)}$$

The time for the switchover, as discussed in Chapter 5 and Appendix III in general, and specifically in the assumptions for the Chapter 5 process design example, is short (τ = 120 seconds). The switchover heat transfer rate (q_t/τ) is then, as shown in Figure (23) typically 18 to 20 times the overall rate for either the heating or cooling half cycle. The pumping rate for the heat transfer fluid (water) is then obtained from a heat balance (Eq. 93) combined with Eq. (III-54) to give

$$w = \left[\frac{(w_t c_t + w_s c_s + w_f c_f)(T_1 - T_2)}{(1+m_o)(1+b)(\varepsilon)(a_t)(\tau)(c_{HTF})(\Delta T_w)}\right] Q\frac{\pi}{\omega} (1+\phi_B)$$

$$= (K_w)(Q\pi/\omega)(1+\phi_B) \qquad \text{(III-54a)}$$

The temperature rise (ΔT_w), as discussed under the general assumptions for the Chapter 5 process design example, may be taken as 15.2°R, and c_{HTF} is 1 BTU/lb/$^{\circ}$R.

The pressure drop for the heat transfer fluid was given by Equation (III-33) which, in a simpler form, is

$$\Delta p_{HTF} = F_{N1} w^2 (2h-1) + F_{N2} (2h) w^{1.8} \qquad (96)$$

where F_{N1} and F_{N2} are functions of the number of columns or tubes in the parapump assembly and are listed in Table (3) for different values of N. The water rate (w) in pounds per second was given above and the tube length (h) may be taken from Equation (III-48a). Combining (III-48a, 54a, and 96) gives

$$\Delta P_{HTF} = (2F_{N1}K_w^2K_h)(Q\pi/\omega)^3(1+\phi_B)^3/N - (F_{N1}K_w^2)(Q\pi/\omega)^2(1+\phi_B)^2 + (2F_{N2}K_w^{1.8}K_h)(Q\pi/\omega)^{2.8}(1+\phi_B)^{2.8}/N \qquad \text{(III-54b)}$$

The hydraulic horsepower for the heat transfer fluid is obtained by combining Equations (III-35), (93), and (III-54) to give

$$Hp_{HTF} = 0.0042\left[\frac{(w_tc_t+w_sc_s+w_fc_f)(T_1-T_2)(\Delta p_{HTF})}{(1+m_o)(1+b)(\varepsilon)(a_t)(\tau)(c_{HTF})(\Delta T_w)}\right] Q\frac{\pi}{\omega}(1+\phi_B) \qquad \text{(III-55)}$$

The BTU/cycle equivalent of the horsepower is

$$q_{HTF} = HP_{HTF}(2\pi/\omega \text{ hr/cycle})(2546 \text{ BTU/Hp-hr}) \qquad \text{(III-56)}$$

or

$$q_{HTF} = \left[\frac{21.4(w_tc_t+w_sc_s+w_fc_f)(T_1-T_2)(\Delta p_{HTF})}{(1+m_o)(1+b)(\varepsilon)(a_t)(\tau)(c_{HTF})(\Delta T_w)}\right] Q\frac{\pi}{\omega}(1+\phi_B)\left(\frac{\pi}{\omega}\right) \qquad \text{(III-57)}$$

And the equation for the BTU/lb of bottom product is a combination of Equations (III-57) and (III-50).

$$\frac{q_{HTF}}{P_B(2\pi/\omega)} = \left[\frac{10.7(w_t c_t + w_s c_s + w_f c_f)(T_1 - T_2)(\Delta p_{HTF})}{(1+m_o)(1+b)(\varepsilon)(a_t)(\tau)(c_{HTF}\Delta T_w)(\rho_f)}\right]\left[\frac{1+\phi_B}{\phi_B}\right]\frac{\pi}{\omega} \tag{III-58}$$

Bottom reservoir pump. The pressure drop for the bottom reservoir pump is given by combining Equations (III-20) and (III-12, 13) to give

$$\Delta p_{BRP} = \left[\frac{150(1-\varepsilon)^2(\mu_1)}{D_p^2(g_c)(\varepsilon)^4(a_t)^2(1+m_o)(1+b)}\right]\left(\frac{Q}{N}\right)^2 (1-\phi_B^2)\frac{\pi}{\omega} \tag{III-59}$$

The horsepower for the bottom reservoir pump is

$$Hp_{BRP} = \Delta p_{BRP}\,(Q)(1-\phi_B)(\text{Hp-hr}/1.98 \times 10^6 \text{ft-lb}_f) \tag{III-60}$$

where the pressure drop is in lb_f/ft^2 and the rate term is in ft^3/hr. In more exact terms,

$$Hp_{BRP} = \left[\frac{150\,(1-\varepsilon)^2(\mu_1)(1.98\times10^6)^{-1}}{D_p^2(g_c)(\varepsilon)^4(a_t)^2(1+m_o)(1+b)}\right]\left(\frac{Q}{N}\right)^2 (1-\phi_B)^2(1+\phi_B)\;Q\frac{\pi}{\omega} \tag{III-61}$$

The BTU/cycle equivalent to Equation (III-61) is obtained by multiplying by the factor 2546 BTU/Hp-hr and the hours per cycle of operation (π/ω). The result is

$$q_{BRP} = \left[\frac{0.193(1-\varepsilon)^2(\mu_1)}{D_p^2(g_c)(\varepsilon)^4(a_t)^2(1+m_o)(1+b)}\right]\left(\frac{Q}{N}\right)^2 (1-\phi_B)^2(1+\phi_B)Q\left(\frac{\pi}{\omega}\right)^2 \quad \text{(III-62)}$$

The heat transfer in BTU/lb of bottom product is

$$\frac{q_{BRP}}{P_B(2\pi/\omega)} = \left[\frac{0.193(1-\varepsilon)^2(\mu_1)(2\rho_f)^{-1}}{D_p^2(g_c)(\varepsilon)^4(a_t)^2(1+m_o)(1+b)}\right]\left(\frac{Q}{N}\right)^2 (1-\phi_B)^2\frac{(1+\phi_B)}{\phi_B}\left(\frac{\pi}{\omega}\right) \quad \text{(III-63)}$$

Top reservoir pump. The pressure drop for the top reservoir pump is obtained by combining Equations (III-20) and (III-12, 13) to give

$$\Delta p_{TRP} = \left[\frac{150\ (1-\varepsilon)^2(\mu_2)}{D_p^2(g_c)(\varepsilon)^4(a_t)^2(1+m_o)(1+b)}\right]\left(\frac{Q}{N}\right)^2 (1+\phi_B)^2\left(\frac{\pi}{\omega}\right) \quad \text{(III-64)}$$

The horsepower for the top reservoir pump is obtained, as before, by multiplying the pressure drop by the flow rate $Q(1+\phi_B)$ and by the factor $(\text{Hp-hr}/1.98\text{x}10^6\ \text{ft-lb}_f)$.

$$Hp_{TRP} = \left[\frac{150\ (1-\varepsilon)^2(\mu_2)(1.98\text{x}10^6)^{-1}}{D_p^2(g_c)(\varepsilon)^4(a_t)^2(1+m_o)(1+b)}\right]\left(\frac{Q}{N}\right)^2(1+\phi_B)^3(Q\pi/\omega) \quad \text{(III-65)}$$

The BTU/cycle equivalent to Equation (III-65) is obtained by multiplying by the factor 2546 BTU/Hp-hr and the hours per cycle (π/ω) of operation. The result is

$$q_{TRP} = \left[\frac{0.193(1-\varepsilon)^2(\mu_2)}{D_p^2(g_c)(\varepsilon)^4(a_t)^2(1+m_o)(1+b)}\right]\left(\frac{Q}{N}\right)^2 (1+\phi_B)^3 (Q\pi/\omega)\ \frac{\pi}{\omega}$$

(III-66)

The heat transfer in BTU/lb of bottom product is

$$\frac{q_{TRP}}{P_B(2\pi/\omega)} = \left[\frac{0.193(1-\varepsilon)^2(\mu_2)(2\rho_f)^{-1}}{D_p^2(g_c)(\varepsilon)^4(a_t)^2(1+m_o)(1+b)}\right]\left(\frac{Q}{N}\right)^2 \frac{(1+\phi_B)^3}{\phi_B}\left(\frac{\pi}{\omega}\right)$$

(III-67)

Feed pump. The pressure drop for the feed pump is in two parts, the resistance of the lines and the resistance due to the column. This was discussed at length (see pages 198 to 203). The equation for the pressure drop is obtained by combining Equations (III-40) and (III-12, 13).

$$\Delta P_{FP} = \frac{32Q}{.785_i^4 g_c}\left[\mu_F l_F(\phi_T+\phi_B)+\mu_{TP}l_{TP}\phi_T+\mu_{BP}l_{BP}\phi_B\right]$$
$$+ \frac{150(1-\varepsilon)^2(\mu_2)}{D_p^2(g_c)(\varepsilon)^4(a_t)^2(1+m_o)(1+b)}\left(\frac{Q}{N}\right)^2 (1+\phi_B)^2\left(\frac{\pi}{\omega}\right)$$

(III-68)

It will be noticed that the second half of the equation is identical to Equation (III-64) for the top reservoir pump. This, as was discussed previously, is due to the fact that the feed pump must exceed the maximum pressure imposed on the column which is at the point of entry during cold downflow.

The hydraulic horsepower for the feed pump is obtained by multiplying each half of Equation (III-68) by the respective flow rates and by the factor (Hp-hr/1.98×10^{6}).

$$Hp_{FP} = \frac{20.6\times10^{-6}Q^2}{D_i^4\ g_c}\left[\mu_F l_F(\phi_T+\phi_B)^2+\mu_{TP}l_{TP}\phi_T^2+\mu_{BP}l_{BP}\phi_B^2\right] + \left[\frac{150(1-\varepsilon)^2(\mu_2)(1.98\times10^{6})^{-1}}{D_p^2(g_c)(\varepsilon)^4(a_t)^2(1+m_o)(1+b)}\right]\left(\frac{Q}{N}\right)^2 (1+\phi_B)^3(Q\pi/\omega) \qquad \text{(III-69)}$$

The BTU/cycle equivalent to Equation (III-69) is obtained by multiplying by the factor 2546BTU/Hp-hr and the hours of operation per cycle ($2\pi/\omega$). The result is

$$q_{FP} = \frac{0.105Q^2\pi/\omega}{D_i^4\ g_c}\left[\mu_F l_F(\phi_T+\phi_B)^2+\mu_{TP}l_{TP}\phi_T^2+\mu_{BP}l_{BP}\phi_B^2\right] + \frac{0.385(1-\varepsilon)^2(\mu_2)}{D_p^2(g_c)(\varepsilon)^4(a_t)^2(1+m_o)(1+b)}\left(\frac{Q}{N}\right)^2 (1+\phi_B)^3(Q\pi/\omega)\frac{\pi}{\omega} \qquad \text{(III-70)}$$

The heat transfer in BTU/lb of bottom product is

$$\frac{q_{FP}}{P_B(2\pi/\omega)} = \frac{0.0525}{\rho_f D_i^4 g_c}\left(\frac{Q}{\phi_B}\right)\left[\mu_F l_F(\phi_T+\phi_B)^2+\mu_{TP}l_{TP}\phi_T^2+\mu_{BP}l_{BP}\phi_B^2\right] + \frac{0.385(1-\varepsilon)^2(\mu_2)(2\rho_f)^{-1}}{D_p^2(g_c)(\varepsilon)^4(a_t)^2(1+m_o)(1+b)}\left(\frac{Q}{N}\right)^2 \frac{(1+\phi_B)^3}{\phi_B}\frac{\pi}{\omega} \qquad \text{(III-71)}$$

APPENDIX IV

PHYSICAL AND THERMODYNAMIC DATA

The data presented in this section are used in the process design example for the toluene-heptane-silica gel system in Chapter 5 and also for the salt-water-resin system in Appendix V. The two systems, insofar as engineering and physical properties are concerned, are representative of two general types--an aqueous system with an ion-exchange resin, and an organic anhydrous system with a solid adsorbent. The data appear in the following tables and graphs:

TABLE 8

Properties of Adsorbents and Column Materials

Silica Gel (Fisher Scientific Co.)	
Specific heat, calories/gram/^{o}C	0.316
Void fraction, ε	0.38
Specific gravity	2.2
Packing density, grams/cm^3	0.722
Pore volume, cm^3/gm dry adsorbent	0.43
Moisture, weight %	0
Particle size--range, microns	250-550
average, feet	13.2×10^{-4}
Ion Exchange Resin (Bio Rad AG 11 A8)	
Specific heat, calories/gram/^{o}C	0.65
Void fraction, ε	0.38
Density, gm dry resin/cm^3 wet resin	0.766
Packing density, gm dry resin per cm^3 of bed volume	0.475
Pore volume, cm^3/gm dry resin	0.522
Moisture, weight %	36.8-40.3
Particle size, microns	149
feet	4.89×10^{-4}
Column Materials	
Specific heat, calories/gm/^{o}C	
borosilicate glass	0.20
stainless steel	0.12
Specific gravity, grams/cm^3	
borosilicate glass	2.24
stainless steel	8.02

TABLE 9

Viscosities of Toluene-n-Heptane Mixtures, Centipoise

Temp., ^{o}C	n-Heptane	Toluene	20% Toluene	10% Toluene
80	.25	.33	.26	.26
70	.27	.36	.28	.28
60	.29	.40	.31	.30
50	.33	.45	.35	.34
40	.37	.49	.39	.38
30	.40	.54	.42	.41
20	.44	.60	.46	.45
10	.48	.67	.51	.49
5	.50	.70	.53	.51
0	.54	.75	.57	.56

Source: Perry's Chemical Engineers' Handbook, 4th ed., Figure 3-43

Mixture viscosities calculated from the Kern equation

$1/\mu_{Lm} = w_1/\mu_1 + w_2/\mu_2$ where w = wt. fract.

TABLE 10

Properties of Dilute $NaNO_3$ Solutions

Temp., °C	Sp. Gr.	Visc., cp	Sp. Heat
Water			
0	0.99987	1.7938	1.0087
25	0.99707	0.8954	0.9977
50	0.98807	0.5492	0.9983
75	0.97489	0.3807	1.0016
100	0.95838	0.2839	1.0065
5% $NaNO_3$			
0	1.0322*	1.9** $_{20^\circ}$	0.9706***
25	1.0293*	1.0713	0.9608***
50	1.0200*	0.65**	0.9619***
75	1.0064*	0.48**	0.9656***
100	0.9894*	0.32**	0.9708***
10% $NaNO_3$			
0	1.0673*	2.05** $_{20^\circ}$	0.9325***
25	1.0643*	1.1279	0.9239***
50	1.0547*	0.75**	0.9255***
75	1.0406*	0.50**	0.9295***
100	1.0230	0.38**	0.9352***

Notes:

* Calculated from the specific gravity at 20/4°C for 5% $NaNO_3$ (1.0323) and 10% $NaNO_3$ (1.0674).

** Estimated from the viscosity data at 20°C and the generalized chart, Fig. 3-61, Perry, 4th ed.

*** Calculated from the values for water and for solid $NaNO_3$ (0.247 at 0° and 0.270 at 50°C).

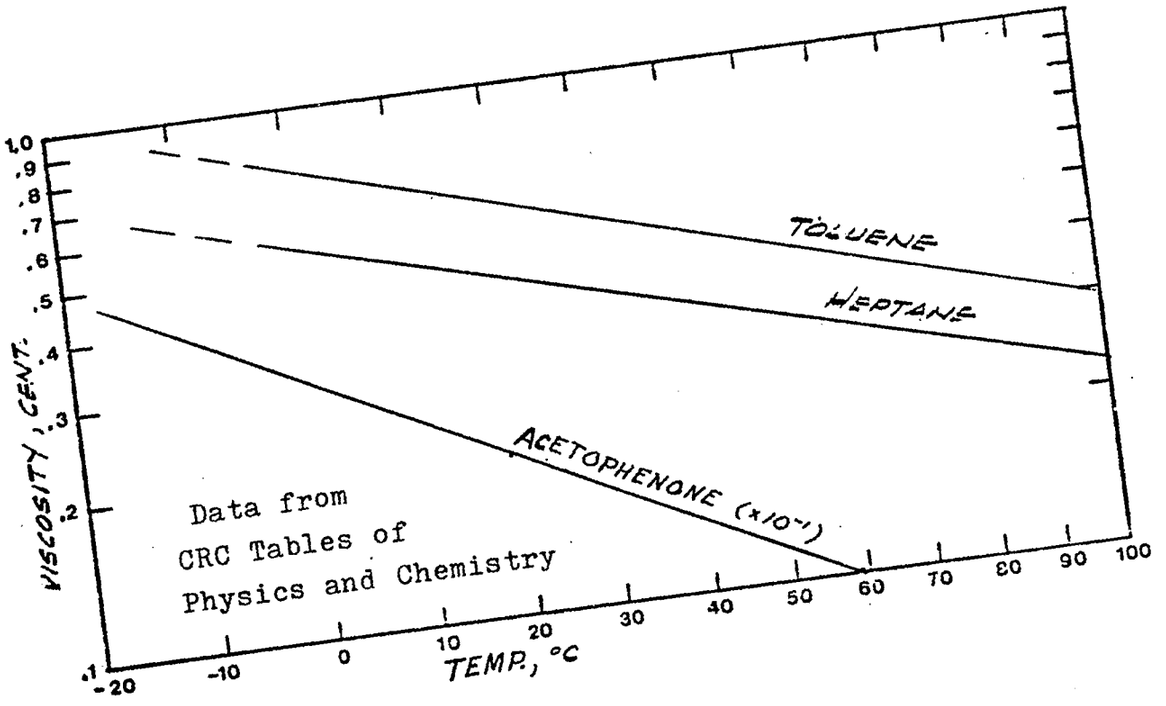

FIGURE (33)

Viscosities of Toluene, n-Heptane, and Acetophenone

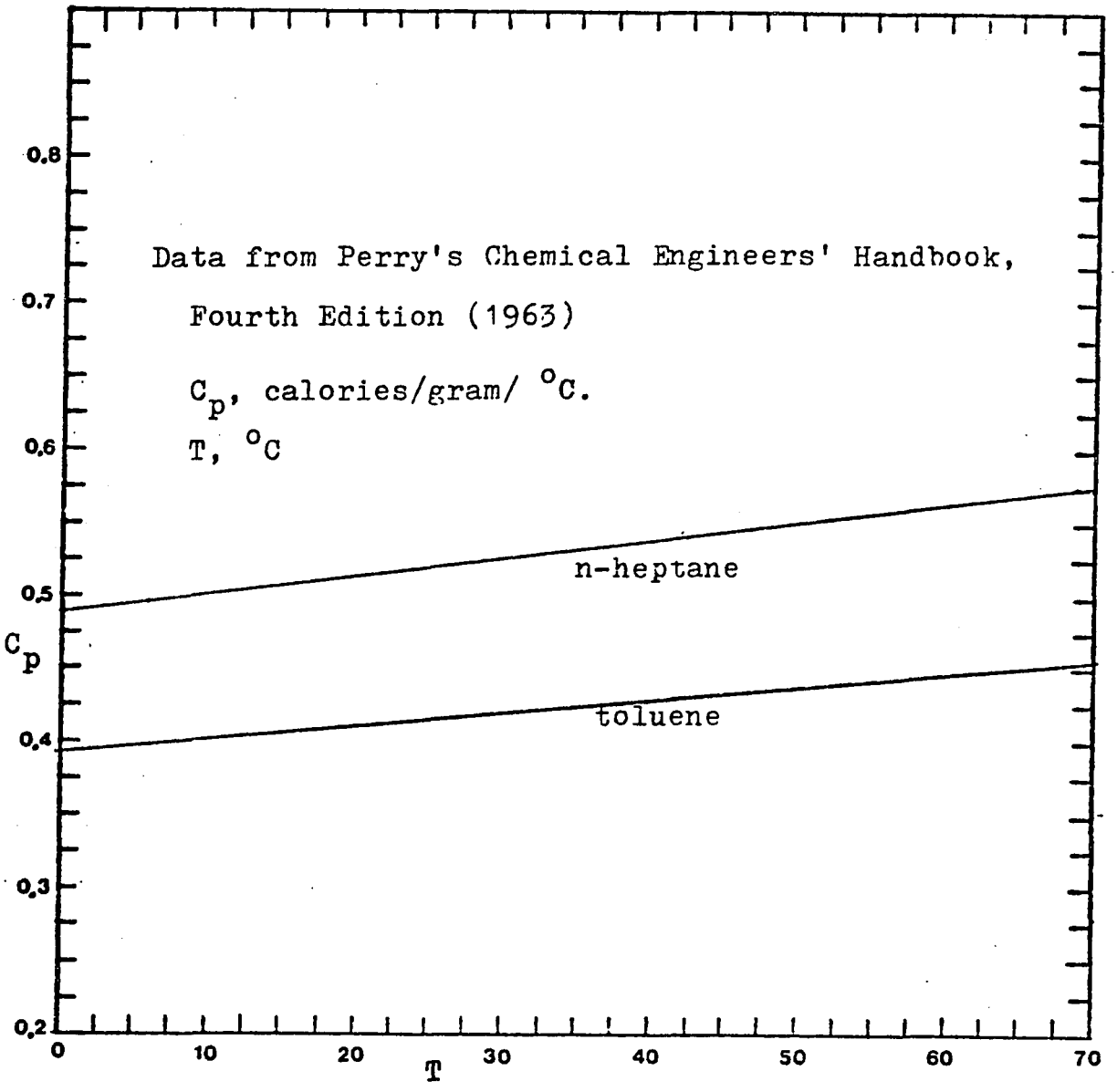

FIGURE (34)

Specific Heats of Toluene, n-Heptane

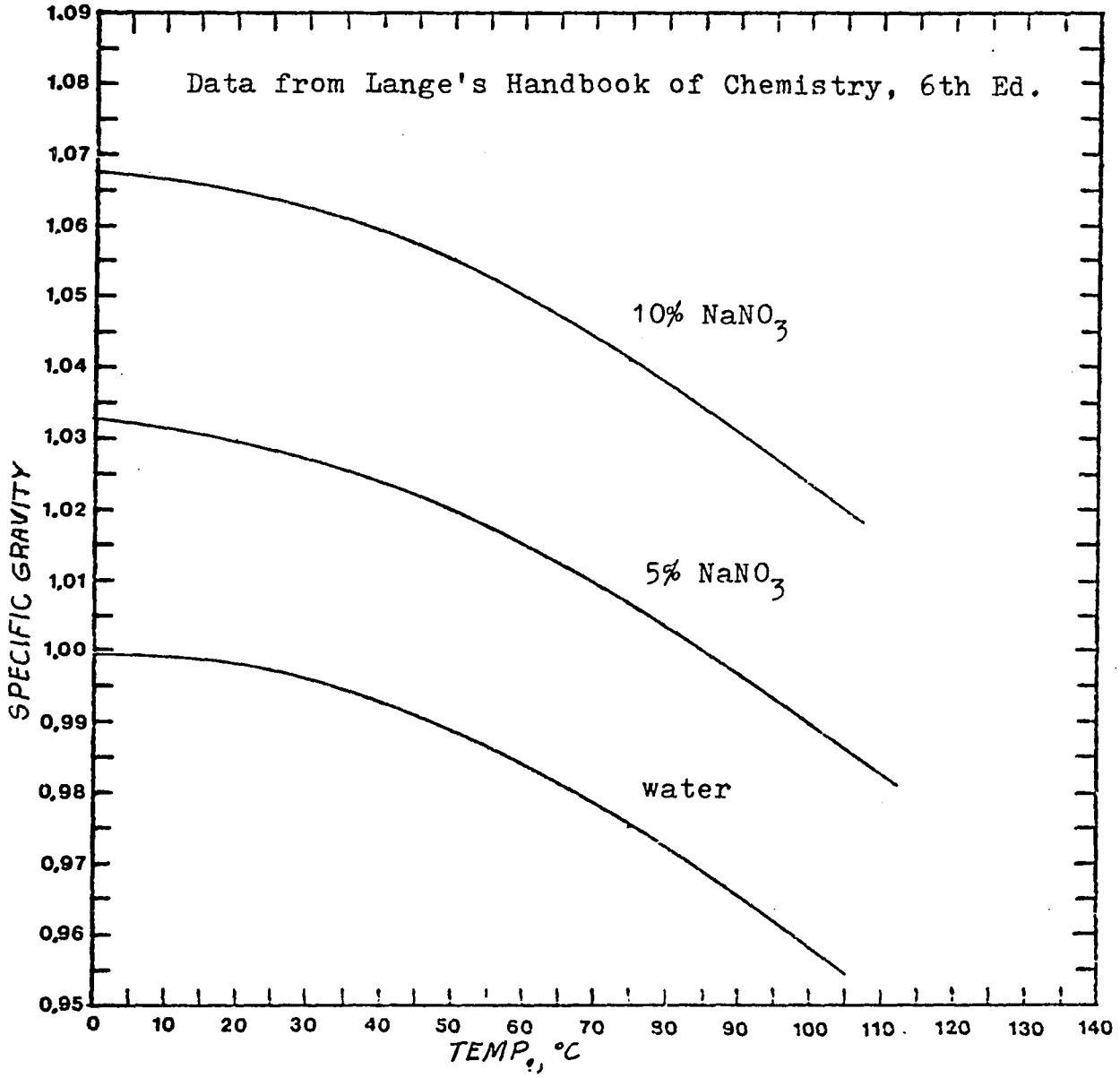

FIGURE (35)

Specific Gravities of Aqueous $NaNO_3$ Solutions

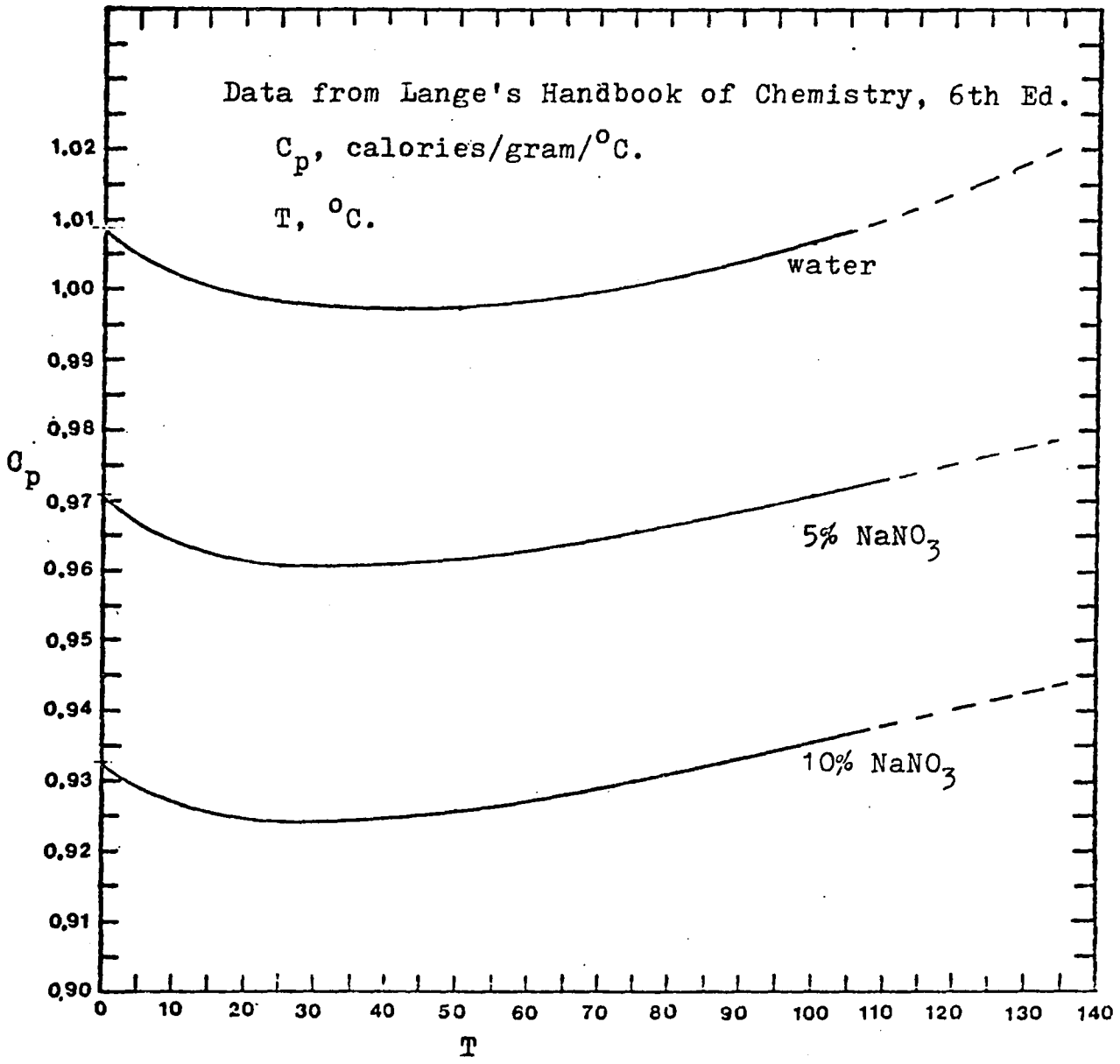

FIGURE (36)

Specific Heats of Aqueous N_aNO_3 Solutions

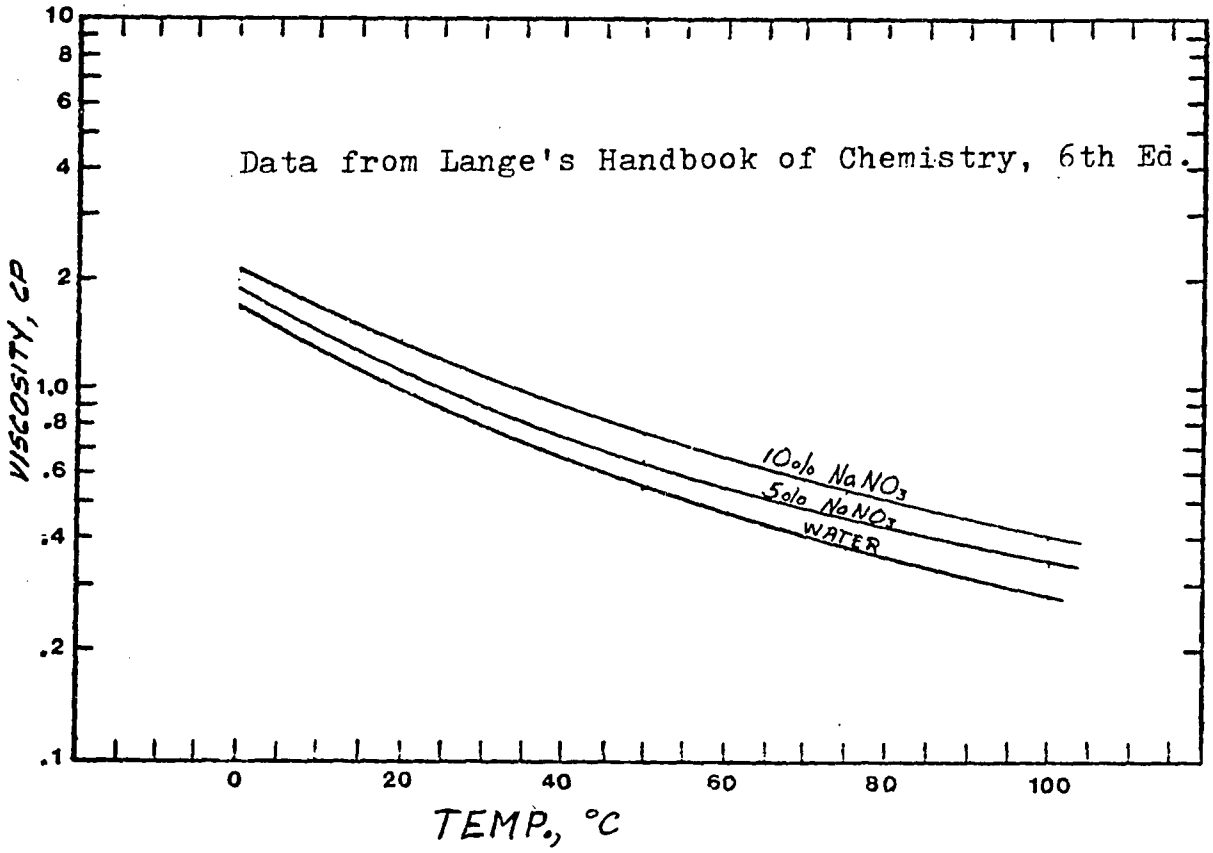

FIGURE (37)

Viscosity of Aqueous $NaNO_3$ Solutions

APPENDIX V

DESIGN EXAMPLE: SALT-WATER-RESIN SYSTEM

The design is based on multiple tubes, each of which is similar in size to the packed columns used in the laboratory. With tubes of these dimensions, the heat transfer through each tube would be similar to that measured by Sweed and Gregory (1971) who reported that the temperature inside the column reached 90% of its ultimate value in 1.5 min. + 0.5 min. lag time in between half cycles. This is a reasonably low fraction of a typical half cycle time of 20-30 minutes. It is essential that the temperature changes be instantaneous if the equilibrium theory equations of Chen and Hill (1971) and Chen et al. (1972) are to be incorporated into the design equations. Also, even in those cases where the equilibrium theory does not apply, the concept of instantaneous temperature change is usually a basic one.

For a practical design example, it is necessary to make certain basic assumptions regarding the mechanical components of the system, the fluid(s) used for heating and cooling, the column packing, and the fluid system undergoing separation. It should be pointed out that the assumptions in the first two categories could apply to practically all systems. For the last two categories, an ion exchange resin and a dilute aqueous salt solution

have been selected because of the availability of data and of the wide interest and applicability relating to dilute aqueous salt systems. The assumptions relating to the mechanical components are:

1. The parapump column assembly (heat exchanger) is a 3 ft. diameter unit with the full complement of 2226 0.5 inch o.d. 18 BWG tubes on an 11/16 inch triangular pitch with 6-inch baffle spacing. A tube length of 4 ft. (122 cm.) would be adequate to approximate the laboratory columns which are usually less then 100 cm. long. A typical flow rate would be 1 cc/min./tube or 2.65×10^{-4} GPM per tube.

2. The insulation is adequate to make the operation essentially adiabatic and to restrict the heating and cooling requirements to the process fluid, the adsorbent, and the tube walls.

3. The process reservoir pump lines are short and of sufficient diameter so that the line pressure drop between the tubes and the reservoirs is negligible.

4. The flow in the feed and product lines is laminar because of the low flow rate (less than 1 GPM).

5. All pumps operate at 50% efficiency for purposes of estimating power consumption.

6. Operation is continuous and is limited to 8,000 hours per year or 333 operating days, assuming automatic and trouble-free operation.

7. The equivalent length of the feed and product lines is arbitrarilly set at 100 ft. and the pipe diameter at 1 inch.

The assumptions relating to the column packing are:

1. The packing material may be assumed to be an ion retardation resin (Bio Rad AG 11 A8) with the properties (Appendix IV) listed as follows:

a. Void fraction $\varepsilon = 0.38$

b. Moisture = 36.8-40.3%

c. Particle size D_p = 149 microns = 4.89×10^{-4} ft.

d. Heat capacity $c_s = 0.65$ cal/gm/^{o}C.

2. The weight x specific heat of the packed column is easily calculated from the data in Appendix IV and includes a stainless steel tube, the packing, and the dilute aqueous solution saturating the packing. The value of $w_t c_t + w_s c_s + w_f c_f$ is determined as follows:

Tube is 0.5 in. o.d. 18 BWG, 0.402 in. i.d.

Internal volume per foot = $.785\ (.402)^2(12)(16.39) = 24.95\ cm^3$

Resin content = 0.475(24.95) = 11.85 gm. dry resin

Wet resin volume = $11.85/0.766 = 15.50\ cm^3$

Liquid volume = $(24.95 - 15.50)+(0.39/0.61)(11.85) = 17.026\ cm^3$

Volume of tubing = $(3.14/4)(0.5^2 - 0.402^2)12(16.39) = 13.62\ cm^3$

Weight of tubing = 13.62 (8.02) = 109.23 gm.

Weight x specific heat:

Resin:	11.85 x 0.65	= 7.70 cal/^{o}C
Water:	17.02 x 1.0	= 17.02 cal/^{o}C
Tubing:	109.23 x 0.12	= 13.11 cal/^{o}C
Total		= 37.83 cal/^{o}C = 0.150 BTU/^{o}K/ft.

The assumptions relating to the heating and cooling fluid are:

1. The fluid used is water which will be indirectly heated by steam and indirectly cooled by a brine refrigeration system.

2. The temperature range used will be assumed at 55^{o}C for the hot reservoir and 5^{o}C for the cold reservoir. It is assumed that the water must be kept just slightly above freezing.

3. The jacket water densities and specific heats may be assumed equal to 1 at the specified temperatures (Appendix IV). However, in Eq. (III-27), the viscosity is raised to the 0.2 power which effectively narrows the range to within engineering accuracy.

4. The minimum water rate may be taken as one shell-side volume displacement of 104.7 gallons over a 2-minute period or 52.35 GPM, assuming perfect displacement. As shown in the calculations, the rate corresponds to a jacket

water temperature rise of 76.4°F (42.4°C). This is a large temperature rise, but the controls could be arranged so as to dump the hot water into the hot reservoir and vice versa so as to minimize the effect on the reservoirs. Also, the reservoirs could be made large enough to minimize the overall temperature rise.

The assumptions relating to the process fluid are:

1. The fluid undergoing separation is a dilute sodium nitrate solution, the properties of which are shown in Appendix IV. The properties are measured over the range $T_1 = 55^{\circ}C$ and $T_2 = 5^{\circ}C$ and are shown below:

   a. $\rho_1 = \rho_2 = 62$ lb/ft^3

   b. $c_i = c_2 = 0.54$ BTU/lb/°K

   c. $\mu_1 = \mu_{TP} = \mu_F = 0.5$ cp $= 1.21$ lb$_m$/ft/hr

   d. $\mu_2 = \mu_{BP} = 1.5$ cp $= 3.629$ lb$_m$/ft/hr

2. The reservoir flow rate was assumed to be 2.65×10^{-4} GPM/tube x 2,226 tubes = 0.59 GPM or 4.73 ft^3/hr. One important constant relating to this rate and dependent on the particular system is the dimensionless (experimentally determined) separation parameter b. Most systems studied thus far have had values of b varying from 0.05 to 0.15.

   a. Assume a value of b of 0.1

   b. The ratio of the bottom product rate to the reservoir flow rate, $\emptyset_B$, must be less than b for good separation. Assume a value of $\emptyset_B$ of 0.05.

   c. A dimensionless feed rate, $\emptyset_B + \emptyset_T$, may be

assumed as typical, which means that the dimensionless top product rate is $\emptyset_T = 0.25$.

3. A typical half cycle time, π/ω, of 0.5 hr may be assumed, which means that the number, n, of cycles in 8,000 hours operating time is 8,000.

The process design for the parapump column assembly is:

$$\underline{\text{Flow rate in the columns}} = 2.65\text{x}10^{-4}\text{GPM/tube x 2226 tubes} = 0.59\ \text{GPM} = 4.73\ \text{ft}^3/\text{hr}.$$

$$\underline{\text{Crossflow area}} = (.402\ \text{in})^2\text{x}\ .785/144\ \text{x 2226 tubes} = 1.96\ \text{ft}^2$$

$$\underline{\text{Column (tube) velocity}} = 4.73/1.96 = 2.41\ \text{ft/hr}$$

$$\text{Column pressure drop} = \frac{150(1-\varepsilon)^2}{D_p^2\varepsilon^3 g_c}\,(u)(h)(v) \qquad \text{(III-20)}$$

$$= \frac{150\ (.62)^2}{(4.89\text{x}10^{-4})^2(.38)^3(4.17\text{x}10^8)}\,(2.42)(4)(2.41)$$

$$= (10.54)(2.42)(4)(2.41) = 245.8\ \text{lb/ft}^2 = 1.71\ \text{psi}$$

for a batch pump at 20°C. For a continuous pump operating at 55°C during hot upflow and 5°C during cold downflow and at a $\emptyset_B$ of 0.05, corrections must be made for viscosity and flow rate. From Appendix IV, the viscosities at the hot and cold temperatures are 0.5 and 1.5 cp, respectively.

For the hot upflow half cycle, the pressure drop is

$245.8 \times (0.5/1)(0.95/1) - 116.8 \text{ lb/ft}^2 = 0.81 \text{ psi}.$

For the cold downflow half cycle, the pressure drop is

$245.8 \times (1.5/1)(1.05/1) = 387.1 \text{ lb/ft}^2 = 2.7 \text{ psi}.$

Shellside Pressure Drop

$$\frac{1.525\times10^{-4}(w)^2(2h-1)}{(0.005732N^{0.9474}-0.00173N)^2} + \frac{2.756\times10^{-4}(w)^{1.8}(0.07117N^{.4737}-0.0417)(2h)}{(0.003293N^{0.4737}-0.01563)^{1.8}} \qquad \text{(III-33)}$$

Now since N = 2,226 tubes and h = 4 ft, the pressure drop is now equal to $4.95\times10^{-5}w^2 + 3.967\times10^{-3}w^{1.8}$. The minimum water rate was assumed to be 52.35 GPM or 7.281 lb/sec, and the corresponding pressure drop is equal to 0.144 psi.

The corresponding temperature rise of the water can be estimated from the data previously calculated. The mass x specific heat of the tubing and contents was estimated to be 0.150 BTU/^{o}K/ft of tubing. The duty is therefore 0.150 (4 ft) (2226) (50^{o}) = 66,780 BTU over the two-minute temperature changeover period. The temperature rise of the water is therefore equal to (66,780/2)(1/52.35)(1/8.35)($1/c_w$) = 76.4^{o}F = 42.4^{o}C. This temperature rise is high by a factor of at least five. Therefore, assume the temperature

rise is only 15.2°F. The resulting water rate would be 261.8 GPM and the new shellside pressure drop would be 2.63 psi. All the flow rates discussed are shown to be in the turbulent range according to the Reynolds number

$$Re = DG_c/u = (.5/12)(7.28/.46)(1/.000672) = 981$$

which is well above the transition range of 42-225 given by Donohue (1955).

Heat transfer during hot upflow = q_i =

$$\left[(w_t c_t + w_s c_s + w_f c_f)(N)(h) + Q(1-\phi_B)(\rho_1)(c_1)(\pi/\omega)\right](T_1 - T_2(n)$$

$$= \left[(0.150)(2226)(4) + 4.73(0.95)(62)(0.54)(0.5)\right](50)(n)$$

$$- (1335.6+75.2)(50)(n) = 7059\ln = 70{,}591 \text{ BTU/cycle}$$

Note that the heat required to change the temperature of the tubes (columns) required 94.7% of the total and that this occurred during the first two minutes at a rate of 2,003,400 BTU/hr as compared with 8057 BTU/hr for the remaining 28 minutes of the 0.5 hr half cycle.

Heat transfer during cold downflow = q_2 =

$$(w_t c_t + w_s c_s + w_f c_f(N)(h)(T_1 - T_2)n$$

$$+ Q(1+\phi_B)(\rho_2 c_2)(\pi/\omega)(T_{2H} - T_2)n$$

(III-18)

If it is assumed that the incoming feed is at temperature T_1, then $T_1 = T_{2H}$ and $\rho_1 = \rho_2$; $c_1 = c_2$.

$$q_2 = \left[(.150)(2226)(4)+(4.73)(1.05)(62)(.54)(.5)\right] (50)n$$

$$= (1335.6+83.1)(50)n = 70,935n = 70,935 \text{ BTU/cycle.}$$

REFERENCES

Alexis,R.W.,Chemical Engineering Progress,63,69 (1967).

Andrews,M.A.,PhD Thesis, Princeton University, N.J. (1967).

Acrivos,A.,Industrial and Engineering Chemistry,48,703 (1956).

Apostolopoulos,G.P.,Industrial and Engineering Chemistry, 14, (1975).

Aris,R.,Industrial and Engineering Chemistry Fundamentals, 8,603,(1969).

Bird,R.B.,Stewart,W.E., and Lightfoot,E.N., Transport Phenomena, Wiley (New York, 1960).

Bringhurst,F.R., B.S.E. Thesis, Princeton University, Princeton, N.J.(1970).

Butts,T.J., Gupta,R., and Sweed,N.J., Chemical Engineering Science, 27, 855 (1972).

Butts, T.J., Sweed, N.H., and Camero, A.A., Industrial and Engineering Chemistry Fundamentals, 12, 467 (1973).

Carslaw, H.S., and Jaeger, J.C., Conduction of Heat in Solids, Oxford University Press, 2nd Ed. (1959).

Chen, H.T., and Hill, F.B., Separation Science, 6, 411 (1971).

Chen, H.T., Jaferi, J., and Stokes, J.D., Paper 9e, 73rd National AIChE Meeting, Minneapolis (1972a).

Chen,H.T., Rak,J.L., Stokes,J.D., and F.B. Hill, AIChE Journal, 18, 356 (1972).

Chen, H.T., Reiss, E.H., Stokes, J.D., and F.B. Hill, AIChE Journal, 19, 589 (1973).

Chen, H.T.,Lin, W.W., Stokes, J.D., and W.R. Fabisiac, AIChE Journal, 20, 306 (1974).

Chen, H.T., and J.A. Manganaro, AIChE Journal, 20, 1020 (1974).

Chen, H.T., and V.J.D'Emido, AIChE Journal, 21 813 (1975).

Donohue, D.A., "Heat Exchanger Design" Series, Petroleum Refiner, (Aug., Oct., Nov., 1955).

Goldstein, R.J., B.S.E. Thesis, Princeton University, Princeton, N.J. (1969).

Gregory,R.A., and N.H. Sweed, Chemical Engineering Journal, 1, 207 (1970).

Gregory, R.A., and N.H. Sweed, Chemical Engineering Journal, 4, 139 (1972).

Gregory, R.A., AIChE Journal, 20, 294 (1974).

Jenczewski, T.J., and A.L. Myers, AIChE Journal, 14, 509 (1968).

Jenczewski, T.J., and A.L. Myers, Ind. Eng. Chem. Fundamentals 9, 216 (1970).

Kim, D.K., and H.M. Hulburt, Northwestern University, Paper presented at the AIChE Meeting in San Francisco, California (Dec. 1971).

Kim, C.Y., M.S. Thesis, N.J.I.T., Newark, N.J. (1976).

Kowler, D.E., and R.H. Kadlec, AIChE Journal, 18, 1207 (1972).

Kunin, R. "Ion Exchange Resins", 2nd Ed., John Wiley & Sons, New York (1958).

Lee, H. and D.E. Stahl, Paper 92e. Presented at 65th Annual AIChE Meeting, New York (Nov., 1972).

Lin, W., M.S. Thesis, Newark College of Engineering, Newark, N.J., (1974).

Patrick, R.R., Schrodt, J.T., and R.I. Kermode, Separation Science, 7, 331 (1972).

Perry, Chilton, Kirkpatrick, "Perry's Chemical Engineers' Handbook", 5th Ed. (1970).

Pigford, R.L., Baker, B., and D.E. Blum, Industrial and Engineering Chemistry Fundamentals, 8, 144 (1969).

Rolke, R.W., and R.H. Wilhelm, Industrial and Engineering Chemistry Fundamentals, 8, 235 (1969).

Sabadell, J.E., and N.H. Sweed, Separation Science, 5, 171 (1970).

Schroeder, H.G. and C.E. Hamrin Jr., AIChE Journal, 21, 807 (1975).

Shendalman, L.H. and J.E. Mitchell, Chemical Engineering Science, 27, 1449 (1972).

Skarstrom, C.W., Annals New York Academy of Sciences, 72, 751 (1959).

Sweed, N.H., PhD Dissertation, Princeton University, Princeton, N.J. (1969).

Sweed, N.H. and R.H. Wilhelm, Industrial and Engineering Chemistry Fundamentals, 8, 221 (1969).

Sweed, N.H. and R.A. Gregory, AIChE Journal, 17, 171, (1971).

Sweed, N.H. and J.M. Rigaudeau, Paper 18c. Presented at the 66th Annual AIChE Meeting, Philadelphia (Nov. 1973).

Turnock, P.H. and R.H. Kadlec, AIChE Journal, 17, 335, (1971).

Wakao, N., Matsumoto, H., Suzuki, K., and A. Kawahara, Kagaku Kogaku, 32, 169 (1968).

Wankat, P.C., Industrial and Engineering Chemistry, 12, 372 (1973).

Wankat, P.C., Separation Science, 9, 85 (1974).

Wilhelm, R.H., Rice, A.W., and A.R. Bendelium, Industrial and Engineering Chemistry, 5, 141 (1966).

Wilhelm, R.H., Intracellular Transport, Academic Press, pp. 199-220, (New York, 1966).

Wilhelm, R.H., Rice, A.W., Rolke, R. W., and N.H. Sweed, Industrial and Engineering Chemistry Fundamentals, 7, 327 (1968).

Wilhelm, R.H., and N.H. Sweed, Science, 159, 522 (1968).

NOMENCLATURE

a	deviation of m from the mean of the values at T_1 and T_2
a_p	interfacial area of the sorbent particles per unit volume of packed bed
a_t	total cross section area of a packed tube
b	dimensionless equilibrium parameter defined by Equation (21)
b_1	largest value of b_1 in a multicomponent system
b_s	smallest value of b_i in a multicomponent system
b_k	value of b_i in a multicomponent system which is $\leq \phi_B$
b_k+1	value of b_i in a multicomponent system which is $\geq \phi_B$
B_s	shellside baffle spacing, ft.
c	heat capacity
c_f	heat capacity of process fluid
c_{HTF}	heat capacity of heat transfer fluid
c_s	heat capacity of solid adsorbent
c_t	heat capacity of tube wall
C_1	$V_T/(Q\pi/\omega)$, dimensionless
C_2	$V_B/(Q\pi/\omega)$, dimensionless
c_o	total utility costs, $/year
C_{BR}	brine refrigeration costs, $/ton-hr
C_{EL}	electricity costs, $/kw-hr
C_{ST}	steam costs, $/lb steam
d	i.d. of shell parapump assembly
d_1	i.d. of adsorbent packed column
$\mathcal{D}$	axial diffusivity
D_f	fluid diffusivity

D	o.d. of adsorbent packed column
D_i	i.d. of pipe or conduit
D_p	adsorbent particle diameter
E	pump efficiency, fraction
f	fanning friction factor
F_{N1}	shellside pressure drop factor related to resistance through baffle openings
F_{N2}	shellside pressure drop factor related to resistance to flow across tube banks
g_c	gravitational conversion factor, $(lb_m/hr^2/ft)(ft^2/lb_f) = 4.17 \times 10^8$
h	packed column height
Hp	hydraulic horsepower
k	thermal diffusivity
K	constants (defined locally)
k_f	fluid phase mass transfer coefficient, bed volume/interfacial area/ time
l	length of pipe or conduit, ft.
L	wavefront propagation distances defined by Equations (17, 18)
M	x_i/y_i
m	dimensionless equilibrium parameter defined by Equation (6)
n	number of cycles of pump operation
N	number of packed columns or tubes in the parapump assembly
p	defined by Equation (30)
p_B	bottom product flow rate
q	defined by Equation (30)
q_i	total heat required during hot upflow half-cycle (including switchover period)

q_2	total cooling required during cold downflow half cycle (including switchover period
q_t	heat required to change temperature of packed tubes from T_1 to T_2 (switchover period)
Q	reservoir displacement rate, $ft^3/hr.$
r	packed column radius
t	time
T	temperature, ^oK
ΔT_w	temperature change of heat transfer fluid
u	wavefront propagation velocity in packed column
v	velocity of process fluid in packed bed
v_o	interstitial velocity in the packed column at the mean of the upflow and downflow half-cycles
V_A	molar volume of a solute
V_S	volume of shellside fluid
V_T	top reservoir dead volume
V_B	bottom reservoir dead volume
w	mass flow rate of heat transfer fluid, lb/sec.
w_f	mass per unit length of process fluid
w_s	mass per unit length of solid adsorbent
w_t	mass per unit length of tube wall
x_i	concentration of solute in the solid phase, moles per unit weight of adsorbent
y_i	concentration of solute in the liquid phase, moles per unit volume of fluid
y_i^*	equilibrium concentration in fluid phase
z	axial distance along packed bed
$\hat{z}$	z/v

Greek

α	thermal diffusivity (local)
α_{ij}	constant separation factor of component i relative to component j
Ψ	association parameter used in Equation (66)
λ	mass transfer coefficient (cm^3/sec/gm. adsorbent)
δ	defined by Equation (50)
$\emptyset$	product volumetric flow rate/reservoir displacement rate, dimensionless
π/ω	duration of half cycle
ϵ	void fraction in packing, dimensionless
τ	switchover time
ρ	density
ρ_f	density of fluid
ρ_s	density of adsorbent
μ	viscosity

Subscripts

0	initial condition or condition at mean value of T_1 and T_2
1	upflow
2	downflow
B	stream from or to bottom of column
i	solute i
F	feed stream
HTF	heat transfer fluid
P	product stream
T	stream from or to top of the column
BP	bottom product
TP	top product

VITA

Candidate: John Daniel Stokes

Educational Background: B.S., Upsala College, East Orange, N.J., June, 1949; M.S., Newark College of Engineering, Newark, N.J., June, 1951; Dr. Engineering Science, New Jersey Institute of Technology, June, 1976.

Professional Background: Production Supervisor at Givaudan Corp., Clifton, N.J., 1951- 1955; Research Engineer at Hercules Powder Co., Parlin, N.J., 1955-1958; Process Design Engineer at Hoffmann La Roche, Inc., Nutley, N.J., 1958 to present.

N.J. State Professional Engineer's License No. 10256, obtained in 1959.

Dissertation Research: Performed in the laboratories of New Jersey Institute of Technology, Newark, N.J. from Sept. 1972 to May, 1976.